

**Development of a Base Model for Flood Forecasting Studies in the Humber River
Basin (NL) and Selection of an Appropriate Model Forcing Dataset**

by

© Faten Jasim

A Thesis submitted to the

School of Graduate Studies

in partial fulfillment of the requirements for the degree of

Master of Engineering

Faculty of Engineering and Applied Science

Memorial University of Newfoundland

May, 2014

St. John's

Newfoundland

ABSTRACT

The Humber River basin (7860 km²) in Newfoundland is the second largest watershed on the island portion of the province. Efforts are underway to establish a base model for a flow forecasting system within the basin for flood damage mitigation and hydroelectric power optimization. This study examines three model forcing datasets (temperature and precipitation) and attempts to identify the best option based on the simulated streamflow amounts. In past stochastic studies, difficulty has been encountered due to a lack of observed data and the complexity of the hydrologic system, especially during the snowmelt period. Strong topographic influences within the basin limit the representativeness of observations.

Given the strong topographic influences on orographic precipitation and temperature, the WATFLOOD gridded hydrologic model was selected, which permits the use of topographically adjusted gridded meteorological inputs as well as station data. Adjusted station data from APC2 (Second Generation Adjusted Precipitation for Canada), NARR (North American Regional Reanalysis) and CaPA (Canadian Precipitation Analysis) were used in the study. Based on 30-year run sequences, a base model able to translate weather and antecedent moisture to streamflow has been developed.

Generation of initial conditions for forecasting purposes cannot rely on APC2 data due to its production lag. Instead, the NARR and CaPA products were evaluated against gridded station observations. Results indicated that APC2 produces the best results in terms of streamflow followed by NARR and CaPA. For model initialization purposes, the NARR precipitation dataset is recommended over CaPA for the Humber River.

ACKNOWLEDGEMENTS

I acknowledge my sincere gratitude and indebtedness to my supervisor Dr. Ken Snelgrove, Associate Professor, Faculty of Engineering and Applied Science, Memorial University of Newfoundland, for his dynamic guidance, continuous assistance and effective encouragement during the course of this study. His dedication to this study is the main reason that I enjoyed the whole process of conducting the study and the realization of this dissertation.

I express my deep sense of gratitude to Makamum Mahmood for his encouragement, technical assistance and guidance. I highly appreciate Jonas Roberts for his advice, assistance and kindness in providing all possible help. I thank all my friends, especially Mashrura Musharraf and Milka Patricia Podder for always being there for me. Thanks to Saad Shaifan Ahmed for motivating me to complete my research.

I gratefully acknowledge my parents and family members for their loving concern, continuous encouragement and support, without which the work would not have been completed.

Finally and most importantly of all, I am grateful to the Almighty who has given me the opportunity and strength to complete this work.

Table of Contents

ABSTRACT	ii
ACKNOWLEDGEMENTS.....	iii
Table of Contents	iv
List of Tables	viii
List of Figures.....	ix
List of Abbreviations	xiv
List of Appendices	xvii
Chapter 1 Introduction	1
1.1 Background	1
1.2 Study Area.....	3
1.3 Study Objectives	7
1.4 Organization of Thesis.....	8
Chapter 2 Literature Review.....	9
2.1 Floods in Canada.....	9
2.2 Hydrological Modelling	10
2.3 Hydrological Modeling for Flood Forecasting	11
2.4 Flood Forecasting Models in Humber River Basin	12
2.4.1 Streamflow Synthesis and Reservoir Regulation Model (SSARR)	12

2.4.2 Dynamic Regression Model.....	15
2.4.3 Rainfall-Runoff Routing Model	20
2.4.4 Artificial Neural Network Model (ANN)	23
2.5 WATFLOOD Flood Forecasting Model	28
2.6 Precipitation Forcing for WATFLOOD Model	32
2.6.1 Second Generation Adjusted Precipitation Data (APC2)	32
2.6.2 North American Regional Reanalysis Data (NARR).....	36
2.6.3 Canadian Precipitation Analysis Data (CaPA)	39
Chapter 3 Data Collection and Preparation	43
3.1 Model Setup Data	43
3.1.1 Surface Elevation Data.....	44
3.1.2 Land Cover Data.....	46
3.2 Model Forcing Data	49
3.2.1 Precipitation Data	50
3.2.2 Temperature Data	58
3.2.3 Climate Normals.....	62
3.3 Calibration and Validation Data (Streamflow)	63
3.4 Water Level Data for Lake Routing	66
3.5 Bias Correction	68

3.5.1 Precipitation Bias Correction.....	70
3.5.2 Temperature Bias Correction.....	73
Chapter 4 Model Set up	75
4.1 Modeling Approach.....	75
4.2 Equations for Hydrological Processes.....	76
4.3 WATFLOOD File Structure and Executables	79
4.4 Event Files.....	81
4.5 Watershed Delineation	82
4.6 Land Use Map.....	84
4.7 Map File Generation.....	85
4.8 Basin file/ SHD file.....	88
4.9 Map File Correction.....	89
4.10 Model Calibration and Validation	92
4.11 Model Initialization	97
Chapter 5 Results and Discussion	98
5.1 Streamflow Simulation at Gauge Locations.....	98
5.2 Bias Correction for NARR Data.....	102
5.3 Model Calibration Results with APC2, NARR and CaPA	104
5.4 Model Validation Results with APC2, NARR and CaPA.....	110

5.5 Simulations for Entire Study Period	115
5.6 Comparison of Streamflow Results among Datasets.....	120
5.7 Model Initialization Results	125
Chapter 6 Conclusions and Recommendations	128
6.1 Conclusions	128
6.2 Recommendations.....	130
Bibliography	133
Appendix A: Parameter File for APC2.....	145
Appendix B: Parameter File for NARR.....	156
Appendix C: Parameter File for CaPA	167

List of Tables

Table 1.1: Long Term Climate Data for Humber River Basin.....	6
Table 3.1: APC2 Precipitation Station Information.....	50
Table 3.2: Monthly Maximum and Average Precipitation for Deer Lake	57
Table 3.3: Temperature Stations Information.....	58
Table 3.4: Statistics of Historical and NARR Temperature Data	61
Table 3.3: Streamflow Stations Information	64
Table 3.4: Reservoir Release Station Information	65
Table 3.5: Reservoir Level Station Information.....	66
Table 4.1: Map File Specifications	85
Table 4.2: Optimized Parameter Sets.....	96
Table 5.1: Comparison of Results Using Uncorrected and Corrected NARR Data	102
Table 5.3: Nash-Sutcliffe Values for Respective Validation Period.....	110
Table 5.3: Nash-Sutcliffe Values for Respective Timeframes.....	119
Table 5.4(a): Statistics for Streamflows with APC2 and NARR (1982-2011).....	120
Table 5.4(b): Statistics for Streamflows with CaPA (2002-2011).....	121
Table 5.5: Nash-Sutcliffe for Model Initialization with APC2, NARR and CaPA	127

List of Figures

Figure 1.1: Deer Lake Power Opened Three Gates at a Main Dam on May 17, 2013	1
Figure 1.2: Humber River Basin (Dept. of Environment and Conservation, NL, 2013).....	4
Figure 2.1: Hydrological Modeling (Mark Williams, 2004).....	11
Figure 2.2: SSARR Flow diagram (Picco, 1997).....	16
Figure 2.3: Dynamic Regression Model Building Cycle (Goodrich, 1989).....	17
Figure 2.4: Forms of Dynamic Regression Models Used in Humber River Basin.....	19
Figure 2.5: Architecture of a Standard Three Layer Neural Network Model (Cai, 2010)	24
Figure 2.6: Trends in Annual and Seasonal Rainfall for 1950–2009 (Mekis and Vincent, 2011).	35
Figure 2.7: Distribution of Surface Observations Assimilated in NARR (January 1988) (Mesinger <i>et al.</i> , 2006).....	38
Figure 2.8: CaPA Analysis Domain over North America (Mahfouf <i>et al.</i> , 2007).....	42
Figure 2.9: Operational Configuration of CaPA (Fortin, 2011).....	42
Figure 3.1: DEM for Humber River Basin	46
Figure 3.2: Land Cover Map (GeoTIFF) for Humber River Basin.....	49
Figure 3.3: Location of Precipitation Stations.....	51
Figure 3.4: Monthly Average APC2 over Study Period.....	52
Figure 3.5: Monthly Average NARR over Study Period.....	54
Figure 3.6: Precipitation Data Sources for CaPA	54
Figure 3.7: Monthly Average Precipitation at Deer Lake	56
Figure 3.8: Precipitation at Deer Lake for the year 2011	56

Figure 3.9: Cumulative Precipitation at Deer Lake (2011)	57
Figure 3.10: Temperature Station Locations	59
Figure 3.11: AHCCD and Gauge Temperature at Goose Bay	60
Figure 3.12: Daily Average Temperature in 2011	61
Figure 3.13: Stream Gauge Locations	65
Figure 3.14: Station Locations for Reservoir Release and Level Data.....	66
Figure 3.15: Storage Discharge Curve for Deer Lake	67
Figure 3.16: Monthly Average Precipitation Plot for Deer Lake.....	68
Figure 3.17: Monthly Average Temperature Plot for Deer Lake.....	68
Figure 3.18: NARR ‘a’ and ‘b’ Bias Correction Values.....	71
Figure 3.19: Daily Average Precipitation for Deer Lake (1982-201).....	72
Figure 3.20: Mean NARR Precipitation Normalized Bias	72
Figure 3.21: Monthly Average Temperature for Deer Lake (1982-2011).....	74
Figure 3.22: Mean NARR Temperature Normalized Bias	74
Figure 4.1: Grouped Response Unit and Runoff Routing Concept	76
Figure 4.2: Major Hydrological Processes of WATFLOOD Model (Stadnyk, 2004).....	77
Figure 4.3: DEM and Predefined Channels.....	83
Figure 4.4: Basin Boundary and Basin Network.....	84
Figure 4.5: Land Use Map Created Using ArcGIS	85
Figure 4.6: WATFLOOD Map File with Visible Drainage Direction.....	88
Figure 4.7: Checking Negative Slopes with Humber_shd.r2c and Humber.map File.....	89
Figure 4.8: Matching DA after FRAC Adjustment.....	90

Figure 4.9: Watershed Delineation Errors near Indian Brook Diversion (Google Earth, 2013)	91
Figure 4.10: Channel Network Connections for Watershed Delineation	91
Figure 4.11: Lake Areas Generated in WATFLOOD.....	92
Figure 4.12: Streamflow Simulations at Indian Brook for Validation Period.....	96
Figure 5.1(a): Streamflow Simulation at Reidville (2003-2007)	98
Figure 5.1(b): Streamflow Simulation at Humber River Village Bridge (2003-2007).....	98
Figure 5.1(c): Streamflow Simulation at Black Brook (2003-2007)	99
Figure 5.1(d): Streamflow Simulation at Lewasechjeech Brook (2003-2007).....	99
Figure 5.1(e): Streamflow Simulation at Sheffield Brook (2003-2007).....	99
Figure 5.1(f): Streamflow Simulation at Glide Brook (2003-2007)	100
Figure 5.1(g): Streamflow Simulation at Boot Brook (2003-2007).....	100
Figure 5.1(h): Streamflow Simulation at South Brook at Pasadena (2003-2007)	100
Figure 5.2(a): Streamflow Time Series at Pasadena without Smearing	104
Figure 5.2(b): Streamflow Time Series at Pasadena with Smearing	104
Figure 5.3(a): Streamflow Simulation at Reidville with APC2	106
Figure 5.3(b): Streamflow Simulation at Reidville with NARR.....	106
Figure 5.3(c): Streamflow Simulation at Reidville with CaPA.....	106
Figure 5.4(a): Daily Ensemble Plot at Reidville with APC2.....	108
Figure 5.4(b): Daily Ensemble Plot at Reidville with NARR.....	108
Figure 5.4(c): Daily Ensemble Plot at Reidville with CaPA.....	108
Figure 5.5(a): Monthly Ensemble Plot at Reidville with APC2.....	109

Figure 5.5(b): Monthly Ensemble Plot at Reidville with NARR.....	109
Figure 5.5(c): Monthly Ensemble Plot at Reidville with CaPA.....	109
Figure 5.6(a): Streamflow Simulation at Reidville with APC2	111
Figure 5.6(b): Streamflow Simulation at Reidville with NARR.....	112
Figure 5.6(c): Streamflow Simulation at Reidville with CaPA.....	112
Figure 5.7(a): Daily Ensemble Plot at Reidville with APC2.....	113
Figure 5.7(b): Daily Ensemble Plot at Reidville with NARR.....	113
Figure 5.7(c): Daily Ensemble Plot at Reidville with CaPA.....	114
Figure 5.8(a): Monthly Ensemble Plot at Reidville with APC2.....	114
Figure 5.8(b): Monthly Ensemble Plot at Reidville with NARR.....	115
Figure 5.8(c): Monthly Ensemble Plot at Reidville with CaPA.....	115
Figure 5.9(a): 30 Year Streamflow Simulation at Reidville with APC2	116
Figure 5.9(b): 30 Year Streamflow Simulation at Reidville with NARR	117
Figure 5.9(c): 10 year streamflow simulation at Reidville with CaPA.....	118
Figure 5.10: Daily Ensembles of Streamflow at Reidville Using APC2.....	119
Figure 5.11: Monthly Ensembles of Streamflow at Reidville Using APC2.....	120
Figure 5.12(a): Scatter Plot Streamflows Using APC2 for 2010	121
Figure 5.12(b): Scatter Plot Streamflows Using NARR for 2010.....	122
Figure 5.12(c): Scatter Plot Streamflows Using CaPA for 2010	122
Figure 5.13: Bar Plot of Monthly Ensemble Streamflows (2002-2010).....	123
Figure 5.14: Probability Distribution Functions.....	123
Figure 5.15: Comparison between Streamflows for 2011	124

Figure 5.16: Hydrographs from Continuous Run and Initialization Runs (2009-2011).. 125

Figure 5.17: Hydrographs from Continuous Run and Initialization Runs (2009) 126

Figure 5.18: Simulation and Observation Hydrograph Differences Using NARR and
CaPA 126

List of Abbreviations

AML	Arc Macro Language
ANN	Artificial Neural Network
AOGCM	Atmospheric-Ocean Coupled Global Model
APC1	First Generation Adjusted Precipitation for Canada
APC2	Second Generation Adjusted Precipitation for Canada
BOREAS	Boreal Ecosystem-Atmosphere Study
BPNN	Back Propagation Neural Network
CaLDAS	Canadian Land Data Assimilation System
CaPA	Canadian Precipitation Analysis
CDCD	Canadian Daily Climate Data
CGIAR	Consultative Group on International Agricultural Research
CMC	Canadian Meteorological Center
CSI	Consortium for Special Information
CV	Coefficient of Variation
DA	Drainage Area
DDS	Dynamically Dimensioned Search
DEM	Digital Elevation Model
EC	Environment Canada
ECMWF	European Center for Medium-Range Weather Forecast
FIFE	First ISLSCP Field Experiment
GEM	Global Environmental Multiscale

GR	Global Reanalysis
GRNN	General Regression Neural Network
GRU	Group Response Unit
HEC-HMS	Hydrologic Engineering Center Hydraulic Modeling System
ISLSCP	International Satellite Land Surface Climatology Project
MAP	Mesoscale Alpine Program
MSC	Meteorological Service of Canada
NARR	North American Regional Reanalysis
NASA	National Aeronautics and Space Administration
NCEP	National Centre for Environmental Prediction
NCER	National Centre for Atmospheric Research
NHN	National Hydro Network
NL	Newfoundland and Labrador
NNGR	NCEP-NCAR Global Reanalysis
NOAA	National Oceanic and Atmospheric Administration
NTDB	National Topographic Database
NTS	National Topographic System
OI	Optimum Interpolation
PS	Pattern Search
QPF	Quantitative Precipitation Forecast
RCM	Regional Climate Model
RMCQ	Réseau Météorologique Coopératif du Québec

SD	Standard Deviation
SRTM	Shuttle Radar Topographical Mission
SSARR	Streamflow Synthesis and Reservoir Regulation
SWAT	Soil and Water Assessment Tool
SWBD	Shoreline and Waterbodies Database
USGS	United States Geological Survey
UZS	Upper Zone Storage
WMO	World Meteorological Organization
WRMD	Water Resources Management Division
WSC	Water Survey of Canada
WSCSSDA	WSC Sub-Sub-Drainage Areas

List of Appendices

Appendix A: Parameter File for APC2.....	145
Appendix B: Parameter File for NARR.....	156
Appendix C: Parameter File for CaPA	167

Chapter 1 Introduction

1.1 Background

In recent years there have been a number of flood forecasting studies done for the communities along the Humber River due to the frequent flooding that has caused damage and hampered development of the area. Even though communities, such as Steady Brook and Deer Lake, experience minor flooding each year, the occurrence of two major floods in 1961 and 1981 have led to efforts to develop an advanced flood forecasting system to warn residents of future floods. There was a potential for major flooding in May this year (2013) as Deer Lake Power opened three gates at its main dam to prevent reservoir overflow due to the enormous rainfall (Figure 1.1) (<http://www.cbc.ca/news/canada/newfoundland-labrador/flooding-warning-issued-in-deer-lake-1.1371929>). There are two hydroelectric generating stations in the basin, one on Deer Lake and one on Hinds Lake. These stations need accurate flow forecast information to operate safely and efficiently.



Figure 1.1: Deer Lake Power Opened Three Gates at a Main Dam on May 17, 2013

Flood forecasting models used in recent studies of the Humber River basin include (i) a deterministic continuous simulation model named Streamflow Synthesis and Reservoir Regulation (SSARR) (Cockburn, 1984), (ii) a statistically based dynamic regression model (Picco, 1997), (iii) an in-house routing model developed by the Department of Environment and Conservation, Government of Newfoundland (Cai, 2010) and (iv) a statistically based Artificial Neural Network (ANN) model (Cai, 2010). The first three of these models were unable to account for snowmelt, while the ANN model could predict an accurate forecast only one day ahead of time (Cai, 2010).

Due to flood forecasting and operational hydropower production needs, it is necessary to develop a more advanced and detailed flow forecasting model that will be able to overcome the drawbacks in previous models. It is expected that a model such as WATFLOOD could be used in a flow forecasting system since it is a continuous (rather than event) model that simulates the entire annual hydrologic cycle including the snowmelt period. WATFLOOD is a physically based, distributed hydrological model first introduced by Dr. Nicholas Kouwen of the University of Waterloo in 1972. Since then it has grown and expanded to become one of the leading hydrological models in Canada (Carlaw, 2000).

Within hydrological models, it is impossible to measure and simulate each and every interaction between air, water and land due to the limitations of our knowledge and computing power. Models are estimations of real world processes based on information that is feasible to obtain. Accuracy of input data is vital as model predictions can only be as good as the input data. The current study builds a base model using WATFLOOD for

flow forecasting in the Humber River basin and identifies appropriate sets of data for model calibration and validation. Input data used for evaluation include three sets of precipitation data: (i) Second Generation Adjusted Precipitation for Canada (APC2) (Mekis and Vincent, 2011), (ii) North American Regional Reanalysis (NARR) (Messinger *et al.*, 2006), and (iii) Canadian Precipitation Analysis (CaPA) (Mahfouf *et al.*, 2007). The model will be calibrated with all three sets of precipitation data and those which obtain the best objective function evaluation value will be selected.

Generation of initial conditions for the model cannot rely on APC2 data because of its production lag (only data up to 2011 is available). Up to date data are necessary to generate useful forecast. In this study, the model is initialized to bring the result from the calibration and validation period with APC2/NARR/CaPA data (depending on whichever gives the best result) to the starting date of the forecast simulation. NARR and CaPA products are available at forecast time. Therefore these datasets were evaluated and the appropriate dataset was selected based on the objective function and the generated streamflow hydrographs.

1.2 Study Area

The Humber River basin is located near the west coast of the island of Newfoundland. The river has a reach of 153 km, originating from Gros Morne National Park and draining into the Bay of Islands. The total drainage area of the basin is 8760 km² (Dept. of Environment and Conservation, NL, 2013), making it the second largest river system on the island. The two main branches of the river are the Upper Humber River

with an area of 2110 km² and Grand Lake with an area of 5030 km². Figure 1.2 shows the Location of the Humber River basin.

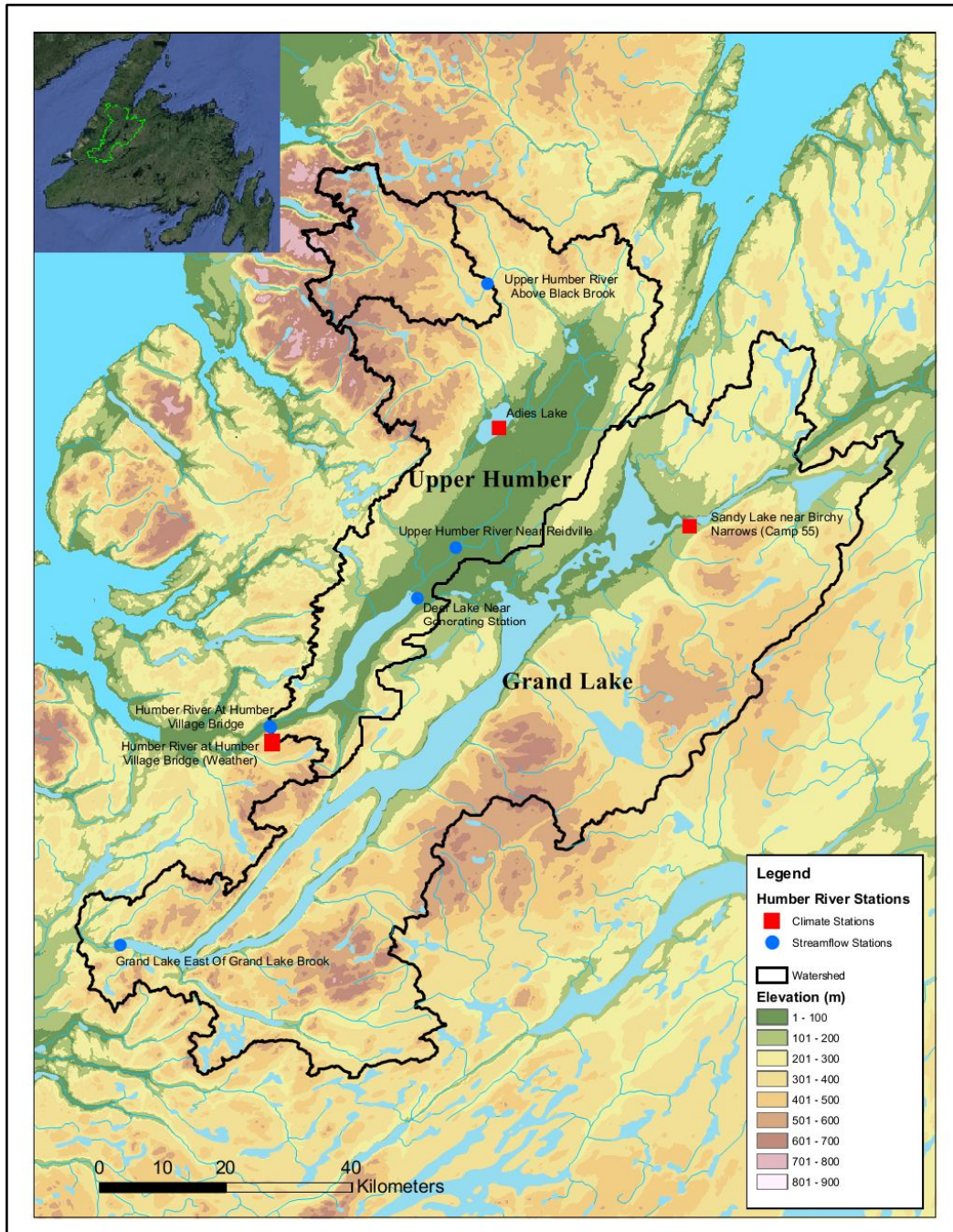


Figure 1.2: Humber River Basin (Dept. of Environment and Conservation, NL, 2013)

The Upper Humber River basin is in a relatively natural state and its flow is uncontrolled. Typically this region is covered by snow in the winter. This means the stream flow at Black Brook during spring is strongly influenced by snowmelt. The portion of the basin associated with Grand Lake has a controlled flow, regulated to produce hydroelectricity. The area contains of two large lakes; Grand Lake and Deer Lake, and other smaller lakes including Hinds Lake, Adies Lake, Birchy Lake and Sandy Lake. Grand Lake, Sandy Lake, Birchy Lake are all actually one lake that is connected due to regulation at Grand Lake water levels well above their natural level. The basin area extends from 58.18W to 56.4W and 49.8N to 48.48N.

The area has two hydroelectric generating stations, one each at Hinds Lake and Deer Lake. Hinds Lake Hydroelectric generating station, owned by Newfoundland and Labrador Hydro, is located on the eastern side of Grand Lake (49° 4' 58" N, 57° 12' 4" W). It uses the head difference of 220 m between Hinds Lake and Grand Lake (Global Energy Observatory, 2012). The plant operates under an average net head of 214 m. The average flow of 20.3 m³/s generates 75 MW electric power at peak. It has an average annual production of 352 GWh. A 7.79 km canal connects Hinds Lake to the powerhouse. The plant was commissioned in December 1980. (Global Energy Observatory, 2012). Deer Lake Hydroelectric generating station, owned by Kruger Energy, is located at Deer lake (49° 10' 11" N, 57° 26' 10" W). The plant has a total of 9 generators producing a peak output of 129 MW of electric power. An 11 km canal connects Grand Lake to the powerhouse. This plant has been operational since 1925 (Global Energy Observatory, 2012).

Most of the basin is situated in a physiographic region called the Newfoundland Highlands (Bostock, 1970). The area is further broken down into four sub-regions; (i) the Great Northern Highlands, (ii) Blow Me Down Mountains, (iii) Atlantic Uplands of Newfoundland and (iv) Grand Lake Lowlands. (Picco, 1997). The surficial geology of the basin consists of bed rock, glacial till, sand, gravel and organic soil, bedrock being the most common type. The basin has an elevation ranging from sea level to 700 m. This makes modeling the basin more difficult due to the influence of elevation on precipitation, snowmelt and evaporation.

The Humber River basin falls within the Boreal Forest Region of Canada, where the dominant tree species are White Spruce, Black Spruce, Balsam Fir, White Pine, Yellow Birch, White Birch, Trembling Aspen and Balsam Poplar (Picco, 1997). Table 1.1 shows the long term annual precipitation and annual daily temperature data for Humber River basin (Picco, 1997).

Table 1.1: Long Term Climate Data for Humber River Basin

Station	Elevation (m)	Annual Precipitation (mm) (1971-2000)	Annual Daily Temperature (°C) (1971-2000)	
			High	Low
Burgeo	11	1709	7	-2
Port-Aux-Basques	40	1570	7	1
Corner Brook	5	1271	9	1
Deer Lake	22	1079	9	-2
Gander	151	1202	8	-1
Grand Falls	60	1079	9	-1
Springdale	23	1000	9	-2
St. Anthony	33	1298	4	-3
Stephenville	26	1352	8	1

Over the years people gathered and built communities along the Humber River at Humber Village Bridge close to Deer Lake and Steady Brook. According to Statistics Canada, (2006) the population is over 25,000. A large number of homes have been built in the flood plains which face frequent floods during spring season. This calls for an accurate and early forecast of Humber River flows, so that the residents can be warned and preventive measures can be taken before any flood incident. Also the forecast information will be used for safe and efficient regulation of hydropower production.

1.3 Study Objectives

The main objective of this study is to create a base model which will be used for flood forecasting studies in Humber River basin and to select an appropriate model forcing dataset for the base model. Broadly these objectives are; (i) to create a base model for streamflow forecasting in the Humber River basin; (ii) to calibrate and validate the model with 3 sets of precipitation data, APC2, NARR and CaPA; (iii) to select the appropriate datasets for model calibration based on an objective function and statistical analysis, (iv) to perform bias correction on the NARR dataset, and recalibrate the model with the corrected dataset; and (v) to initialize and model flood forecasting simulations. The real time flood forecasting evaluation was not part of this thesis but is the natural extension of this research work. This research can be used by others for further flood forecasting studies as well as other hydrological studies in Humber River Basin.

1.4 Organization of Thesis

This thesis has six chapters including this introduction. The background of the study, study area and objectives of the study are presented in this chapter. Chapter 2 contains review of the previous literature related to the study. It includes a brief description of flood forecasting techniques, previous flood forecasting models used in Humber River basin, WATFLOOD as a modeling tool and APC2, NARR and CaPA datasets used for calibration of the model. Chapter 3 gives a detailed description of data collection, data preparation and linear and non-linear bias correction techniques. Chapter 4 describes the methodology including model setup, model calibration and validation and model initialization for forecast simulations. The results and discussion on hydrological simulations are given in chapter 5. Chapter 6 presents the conclusion and recommendations.

Chapter 2 Literature Review

2.1 Floods in Canada

Flooding (an overflow of water that submerges land normally not covered by water) is a major natural disaster in Canada and worldwide. This overflow may occur due to overflow of water from waterbodies when flow rate exceeds capacity or due to the accumulation of rainwater on saturated ground. The most devastating flood in Canadian history occurred on October, 1954 which was associated with Hurricane Hazel (Lawford *et al.*, 1995). The flood caused the deaths of 79 people and an estimated 133.3 million USD damage to buildings and infrastructure (Andrew, 1993).

Different regions of Canada are vulnerable to different types of floods, including those due to snowmelt, heavy summer rains or ice jams. Rapid melting of snow accumulated over the winter is common in most areas of Canada. Flooding due to summer rainfall occurs in places where a large percentage of the surface is impermeable, mostly urban areas. This also occurs in small watersheds where peak rainfall amounts have the greatest intensities. Due to the occurrence of snowmelt and ice cover on a large number of rivers in April, this is the most likely month of flooding. On the west coast of Canada, winter precipitation is high and temperature is close to 0 °C, leading to floods prior to April.

Large watersheds are most susceptible to snowmelt floods. Where the rate of excess precipitation is low, the area involved tends to be large. Approximately 36% of mean Canadian annual precipitation occurs as snow (Goodison, 1985). Snowmelt flood potential depends on the magnitude of snow accumulation and the snow melt rate

(Lawford *et al.*, 1995). Frozen soil and the relative infiltration potential also play important parts in snowmelt flooding. Snowmelt floods are most common in forested, central and eastern portions of southern Canada. Mid winter snow melt events produce rapid streamflow increases and can create a significant flood hazard then generated by a rain-on-snow event (Watt, 1989). The impact flooding has on Canadians created the demand of hydrological modeling for flood studies.

2.2 Hydrological Modelling

Hydrologic forecast information is important for water managers for preparation of responses to flooding events. These responses include warning people living in the flood plain, as well as efficient and safe operation of hydroelectric plants. Operational flood forecasting generally depends on hydrologic models with varying levels of complexity and completeness (Lawford *et al.*, 1995). The level of complexity of a model depends on what elements are selected to represent a particular process (Cai, 2010).

Generally the hydrologic cycle describes the movement of water in the atmosphere as well as on, above and below the earth's surface. Water moves from land and rivers to oceans, from oceans to atmosphere and then from the atmosphere to the land surface and then to rivers again. A hydrologic model conceptually presents vital processes in a simplified way. It aims to quantify and model all the processes that govern moisture movement through various systems. Among these processes, precipitation, runoff and evaporation are the principal processes. The rainfall-runoff relationship is one typical process of moisture movement and modeling of this relationship is valuable for many aspects of hydrologic studies (Singh, 1989). Rainfall-runoff models are developed based

on mathematical principles. These mathematically based models are called conceptual rainfall-runoff models.

2.3 Hydrological Modeling for Flood Forecasting

Flood forecasting is typically carried out using regression models or simulation models. Hydrologic models can be classified into index models, deterministic conceptual models, stochastic models and physically based models. Early hydrologic models used unit hydrographs for depicting basin response for given runoff depth, snowmelt and rainfall input. Two such models are the SSARR model and MUSKINGUM routing scheme.

Hydrologic forecasting has improved during the past decade due to the enhanced availability of remotely sensed data. Some recent widely used physically based models include HSPF (Johanson *et al.*, 1981), SLURP (Kite, 1992), SHE (Abbott *et al.*, 1986) and WATFLOOD (Kouwen, 1988) in addition to the many other statistically based models. Figure 2.1 shows the basic hydrological processes in a hydrologic model.

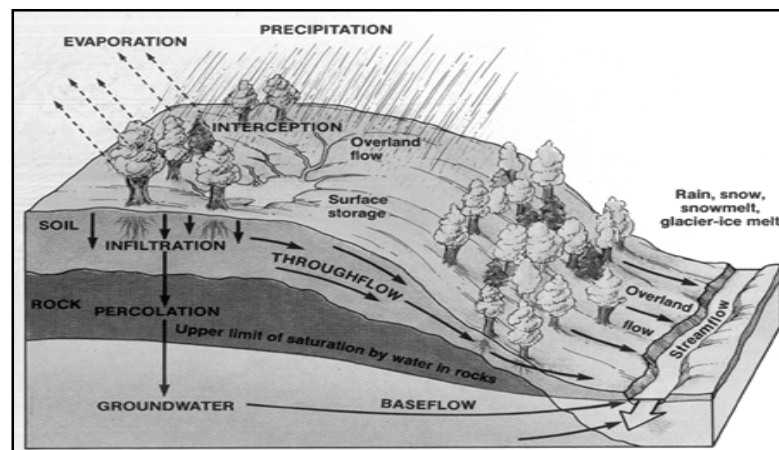


Figure 2.1: Hydrological Modeling (Mark Williams, 2004)

There are limitations in the measuring techniques of hydrological responses and the time period between measurements. For this reason, limited information can be extrapolated with the help of available modeling tools. Rainfall-runoff models are examples of tools that help extrapolate and predict hydrologic responses. These models depend mainly on rainfall records. They require two essential components: first, to determine the portion of rainfall that becomes part of a storm hydrograph, and then to describe the distribution of the runoff that forms the shape of the hydrograph (Cai, 2010). In addition to rainfall and runoff information, evaporation, interception, snowmelt and catchment physical characteristics are also important input variables. These determine the robustness of the model in time and separate models into event based and continuous models. In Canada, snowmelt is generally the most important source of annual maximum discharge, so the snow accumulation process and melt rate are also important.

2.4 Flood Forecasting Models in Humber River Basin

Since 1986 the Water Resources Management Division of the Department of Environment and Conservation has used several models for flood forecasting in Humber River basin. These are the SSARR model (Cockburn, 1985), Dynamic Regression model (Picco, 1997), Routing model and Artificial Neural Network model (Cai, 2010). These models are described below in brief.

2.4.1 Streamflow Synthesis and Reservoir Regulation Model (SSARR)

The SSARR model was first developed in 1956 by the US Corps of Engineers for planning, design and operation of water control works as well as to analyze and forecast

flows for controlled and natural reservoirs in the Pacific North West. The SSARR model was previously used in the Saint John River basin in New Brunswick in 1973 (Tang & Lockhart, 1983). It was selected for the Humber river basin due to its simple structure and the ability to use readily available data, its fast simulation, its excellent reservoir routing capability, the capability to account for the areal distribution of snowmelt and its widespread use in flood forecasting studies (Cockburn, 1984).

SSARR was developed to describe the main components of the hydrologic cycle (Picco, 1997). It has approximately 24 parameters that allow for an extremely flexible representation of the various hydrologic processes. Inputs in the older version of the model include daily rainfall, daily temperature, insolation and snowline elevation. The output is daily streamflow.

Like all other deterministic hydrological models, SSARR preserves some hydrologic principles in its hydrologic formulation, including the logical accounting of all basic hydrologic processes (rainfall, snowmelt, interception, soil moisture, interflow, groundwater recharge, evapotranspiration and the time delay processes). They are represented by objective functions that relate them to observed hydro-meteorological parameters. The ways of simulation processing depend on the level of complexity the model uses to represent a particular process.

Streamflow routing in SSARR uses a generalized system for solving the unsteady flow conditions in river channels where the streamflow and channel storage effects are related, either at a point or series of points along the channel system. The method involves a direct solution of a storage-flow relationship that uses a completely general

and flexible method for solving the flow routing equations. Application of these equations depends upon the type of available basic data and the river condition with respect to backwater effects from variable stage discharge effects (tidal or reservoir fluctuations).

SSARR was designed to include the effects of water control elements within the streamflow simulation process. Reservoirs can be described at any location in the river system and inflows are defined from single or multiple tributaries. The inflows can be derived from simulation of the upstream river basin. Specific flows as time series can be used as well as a combination of both.

Reservoir outflows are determined by specified operating conditions. In order to provide a once-through process for the system as a whole (including the natural effects and effects from human interventions) the basic hydrologic elements, channel storage effects and all the water control elements need to be considered sequentially in the basin simulation. A schematic representation of SSARR is presented in Figure 2.2.

Cockburn developed the model in 1984 and 1985 for the Humber River basin to assess the possibility of forecasting flows during the high flow events. They found that the data collection network needed to improve to allow the model to produce accurate flow forecasts. Additional stations for precipitation and temperature sensors and transmitters were then installed for near real time data acquisition (Cai, 2010).

Later, a new version of SSARR was developed and applied by the Water Resources Management Division (WRMD) which used only daily average temperature and total daily precipitation (Picco, 1997). The Humber River watershed was modeled using 11 sub-basins, two reservoirs and one lake. The meteorological data was weighted

by the user for each basin for each station. All stations were given equal weight initially (Picco, 1997) and later adjusted during the calibration period. The Snowmelt coefficient and routing coefficients were the additional parameters that required calibration. The precipitation and temperature weighting coefficients, snowmelt coefficients and routing coefficients are given in Picco (1997). The area-elevation relationship is input to allow adjustments for changes in temperature with changes in basin elevation relative to the climate stations.

In Picco study (1997), the SSARR model provided a reasonable estimation of peak discharge at the Reidville and Village Bridge sites which are important locations for flood forecasting. The model underestimated the runoff from rainfall/snowmelt events in December and overestimated the snowmelt in April. This indicated that the model did not predict enough melt of November/December snow. As the Upper Humber is mostly covered by snow during the winter, SSARR was not able to take into account the snowmelt effect from the Upper Humber River basin. Recently, there has been difficulty with the recalibration of the model. Additionally, the very steep learning curve and the lack of technical support for the software have caused the SSARR model to become obsolete.

2.4.2 Dynamic Regression Model

Dynamic regression models are single equation regression models that combine time series oriented dynamic features with the effects of explanatory variables (Goodrich, 1989). Time series data tend to be correlated through time rather than being independent.

In addition to the time series propagation, dynamic regression must also account for the influences of the explanatory variables (Picco, 1997).

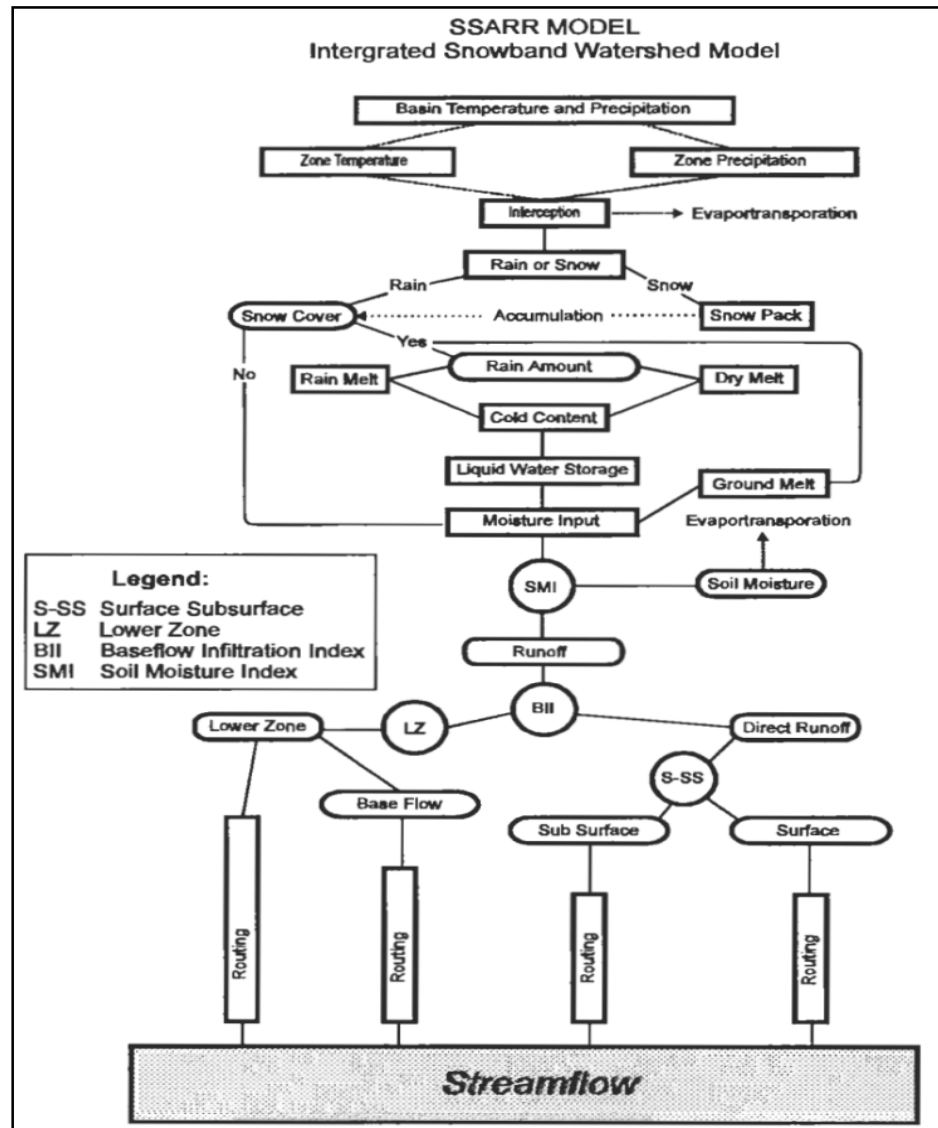


Figure 2.2: SSARR Flow diagram (Picco, 1997)

A Dynamic regression model can be used if long, stable datasets are available, as some time series exhibit inter-annual and intra-annual variation. For example, temperatures are high in summer and low in winter. Also, climate change trends must be

included. Hence, a long dataset is required to support a correlation based model. Additional explanatory variables, such as daily average temperature and daily total precipitation, should increase the performance of the model in a meaningful way. Otherwise a purely dynamic model would be sufficient. Figure 2.3 shows the procedure used to develop a dynamic regression model (Goodrich, 1989).

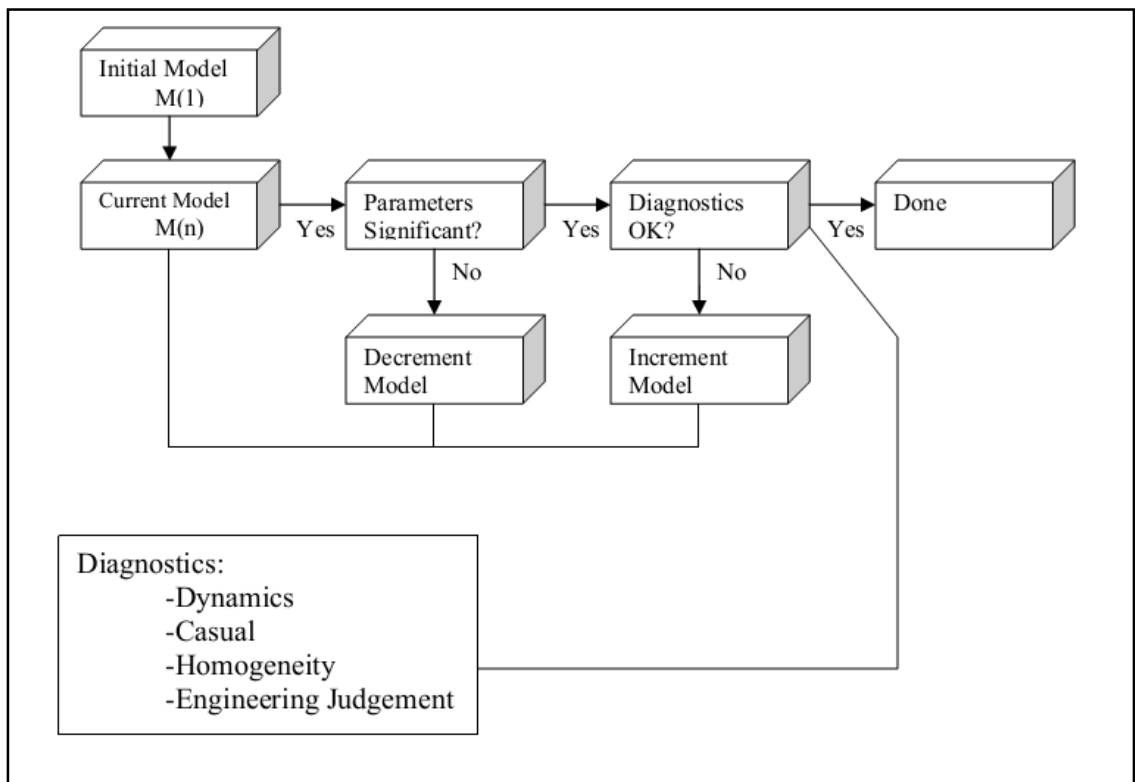


Figure 2.3: Dynamic Regression Model Building Cycle (Goodrich, 1989)

The model starts with a simple regression relationship and then builds on that relationship until the best fit to the data is obtained. The parameters' significance test was used by Picco (1997) to determine the importance of the model variables for the model. When all statistically significant variables were determined, diagnostic tests were run. Goodness of fit tests were also computed. The whole procedure continued until

satisfactory results were found. The ordinary least squares dynamic model takes the form shown in equation 2.1.

$$\Phi(b)Y_t = \beta Z_t + \epsilon_t \quad (2.1)$$

where $\Phi(b)$ = autoregressive polynomial

Y_t = dependent variable at time t

β = coefficient of i'th exogenous variable $Z_t^{(i)}$

Z_t = vector of exogeneous variables at time t

ϵ_t = errors where the errors are NID $(0, \sigma^2)$, i.e. normally and independently distributed with variance σ^2

Goodrich (1989) used a Cochrane-Orcutt model to improve the model dynamics.

He replaced Equation 2.1 with the following pair of equations:

$$\Phi(b)Y_t = \beta Z_t + \omega_t \quad (2.2)$$

$$R(b)\omega_t = \epsilon_t \quad (2.3)$$

where $R(b)$ = polynomial in the backward shift operator

ω_t = raw residual at time t

These two equations can be written into a single equation as:

$$R(b)(\Phi(b)Y_t - \beta Z_t) = \epsilon_t \quad (2.4)$$

In 1997, Picco used the dynamic regression model to develop forecasts for Humber River basin. The procedure was carried out using the Forecast Pro Software package. Hydrometric and climate data from each available gauging station were used. If local climate data was missing or unavailable, data closest to the gauge was used. Figure 2.4 shows the various dynamic regression equations developed by Picco (1997).

Sub-basin Name	Form of Dynamic Regression Equation
Lewaseechjeech Brook	$_CONST + a \text{ PREGLGI} + b \text{ FLOW}[-1] + c \text{ FLOW}[-2] + d \text{ FLOW}[-3]$; where: $_CONST = 0.149490$ $a = 0.244776$; $b = 1.664595$; $c = -1.046278$ $d = 0.336051$
Sheffield Brook	$_CONST + a \text{ PREINDI} + b \text{ FLOW}[-1] + c \text{ FLOW}[-2]$; where: $_CONST = 0.348126$ $a = 0.041432$; $b = 1.432156$ $c = -0.462627$
Indian Brook Diversion	$_CONST + a \text{ PRECINDI} + b \text{ FLOW}[-1] + c \text{ FLOW}[-2]$; where $_CONST = 0.448615$ $a = 0.118321$; $b = 1.297039$; $c = -0.362822$
Upper Humber River above Reidville	$_CONST + a \text{ PRESAND} + b \text{ FLOW}[-1] + c \text{ FLOW}[-2] + d \text{ FLOBLAC} + e \text{ _AUTO}[-1]$; where: $_CONST = 14.380586$ $a = -0.210896$; $b = 0.739059$; $c = -0.376750$ $d = 1.055177$; $e = 0.884608$
Upper Humber River above Black Brook	$_CONST + a \text{ PREBLAC} + b \text{ FLOW}[-1] + c \text{ FLOW}[-2]$; where: $_CONST = 1.254866$ $a = 0.558944$; $b = 1.238943$; $c = -0.315646$
Humber River at Humber Village Bridge	$_CONST + a \text{ PREBLAC} + b \text{ FLOW}[-1] + c \text{ FLOREID} + d \text{ FLOBLAC} + e \text{ _AUTO}[-1]$; where: $_CONST = 21.697851$ $a = 0.187210$; $b = 0.859492$; $c = 0.196181$ $d = -0.055710$; $e = 0.525336$

Figure 2.4: Forms of Dynamic Regression Models Used in Humber River Basin

Where, PREGLGI = Precipitation at Grand Lake at Glover Island

PREINDI = Precipitation at Indian Brook Diversion

PRESAND = Precipitation at Sandy Lake at Howley Road

PREBLAC = Precipitation at Upper Humber above Black Brook

FLOBLAC = Flow at Upper Humber above Black Brook

FLOWREID = Flow at Upper Humber River at Reidville

a, b, c, d and e are Dynamic regression coefficients.

The Dynamic Regression model provided better forecast results than SSARR. It required less data and effort in calibration. However it was not able to take into account snowmelt from the Upper Humber River basin. The model used was linear and hence it was unable to capture any non linear hydrologic effects.

2.4.3 Rainfall-Runoff Routing Model

The third model tried by WRMD was an in-house routing model developed by their own engineers. The model was based on a series of water balance equations organized into three EXCEL spreadsheets to simulate three different parts of the basin: the Upper Humber River at Black Brook, Reidville and Deer Lake (Cai, 2010).

The model used for the Upper Humber River at Black Brook deals with effective rainfall. Effective rainfall is the amount of rainfall that reaches the land surface. It can be calculated using equation 2.5:

$$\begin{aligned} ER &= OR - I \text{ (If Observed Rainfall} \geq \text{Interception)} \\ &= 0 \text{ (If Observed Rainfall} < \text{Interception)} \end{aligned} \quad (2.5)$$

where ER = Effective Rainfall

OR = Observed Rainfall

I = Interception

The daily net rainfall is calculated by multiplying the effective rainfall with the drainage area and converting it to the unit m³/d (Equation 2.6).

$$NR = \frac{ER * DA}{2.6 * 24} \quad (2.6)$$

where NR = Net Rainfall in m³/d,

ER = Effective Rainfall in mm/s

DA = Drainage area in km²

The flow at Black Brook is calculated in two ways: (i) when the observed flow 1 day previous is less than that of 2 days previous, equation 2.7 is used, and (ii) when the observed flow 1 day previous is greater or equal than that of 2 days previous, equation 2.8 is used.

$$F[t] = 1 + \frac{F[t-1]^2}{F[t-2]} + k1 * NR[t - 1] + k3 * \text{Net Rainfall}[t - 2] \quad (2.7)$$

$$F[t] = r * F[t - 1] + k1 * NR[t] + k2 * NR[t - 1] + k3 * NR[t - 2] \quad (2.8)$$

where [t-1] and [t-2] mean 1 day previous and 2 days previous respectively

F[t] denotes flow at time t

k1 is the rainfall runoff coefficient for t = 0.1

k2 is the rainfall runoff coefficient for rainfall t-1 = 0.6

k3 is the rainfall runoff coefficient for t-2 = 0

r is the recession coefficient for high flows = 0.5

The flow at Reidville was calculated by multiplying the flow at Black Brook by 2.5. Then the flows at Reidville, Indian Brook, Sheffield Brook, Lewaseechjeech Brook and outflows at Hinds Lake are all used to estimate the water level at Grand Lake. The net inflow of Grand Lake is calculated by the sum of the five sources multiplied with their coefficients minus the observed outflows (equation 2.9)

$$NI = 0.235 * F_R + 2 * F_I + 2 * F_S + 1 * O_H + 4 * F_L \quad (2.9)$$

where NI = Net Inflow

F_R = Flow at Reidville

F_I = Flow at Indian Brook

F_S = Flow at Sheffield Brook

O_H = Outflows of Hinds Brook and

F_L = Flow at Lewaseechjeech Brook

The water level and outflow of Deer Lake are also calculated. Deer Lake receives inflow from Reidville, local sources below Grand Lake, local inflow to Deer Lake and outflow of Grand Lake. The model calculated the water level of Deer Lake using equation 2.10 and 2.11:

$$NI[t-1] = F_R[t] + I_G[t] + I_D[t] + O_G[t] \quad (2.10)$$

where I_G = Local In low below Grand Lake = $\frac{199}{2108} * F_R$

$$I_D = \text{Local In low to Deer Lake} = \frac{640}{2108} * F_R$$

O_G = Outflow of Grand Lake

$$WL_D[t] = WL_D[t-1] + \frac{NI[t-1]}{\text{Lake Area}} \quad (2.11)$$

The flow at Village Bridge (outflow of Deer Lake) of day t is calculated based on the water level of Deer Lake at day t according to equation 2.12.

$$F_V [t] = 251.5 * WL_D[t] - 1092 \quad (2.12)$$

where F_V = Flow at Village Bridge

The mean absolute error is calculated comparing the computed and observed flows. The model was found to work well only for the downstream part of the Humber River basin, Deer Lake and Village Bridge. For the upstream portion, especially for Black Brook, it performed poorly because the model was not able to take into account the snowmelt effect from the upper part.

In addition to the inaccuracy in forecasting, the routing model also lacked a proper documentation of the model calibration process. Many of the parameters used were obtained subjectively. This is one of the reasons why WRMD abandoned this model (Cai, 2010).

2.4.4 Artificial Neural Network Model (ANN)

ANN is an advanced computation and simulation model which has been widely used in many areas of research and practical applications (Cai, 2010). In the last 20 years, ANN based models have been applied to the field of hydrological modeling. Examples include works by Li *et al.* (2008), Dawson *et al.* (2006), Campolo *et al.* (2003) and Danh *et al.* (1999). ANN is analogous to the human brain in the way it links the modeling inputs to outputs (Cai, 2010). It consists of neurons and connections similar to a simplified biological neural system. The models gather experiences that helps them do better in the future when they face a similar situation. The function of an ANN is to learn the relationship between inputs and outputs from a given set of data, so that it can predict future output values from a new set of input values (Cai, 2010). Figure 2.5 shows the architecture of a standard three layer neuron network.

Neurons and connections are two basic components of ANN architecture. The neurons receive input signals and output information with a weight assigned to the input paths of other neurons. Each neuron computes outputs using its output function and put the results through their neighbouring neurons for the next step of processing (Cai, 2010). For each neuron an intermediate value that comprises the weighted sum of all its inputs, $I = \sum W_{ij}X_{ij}$ is computed, where X is the input, W is the weight of each input and I is the

weighted sum, i is the number of input sources and j is the number of target neurons. I value is passed through a transfer function $f(I)$, which is typically logistic, linear, Gaussian or a hyperbolic tangent transfer function.

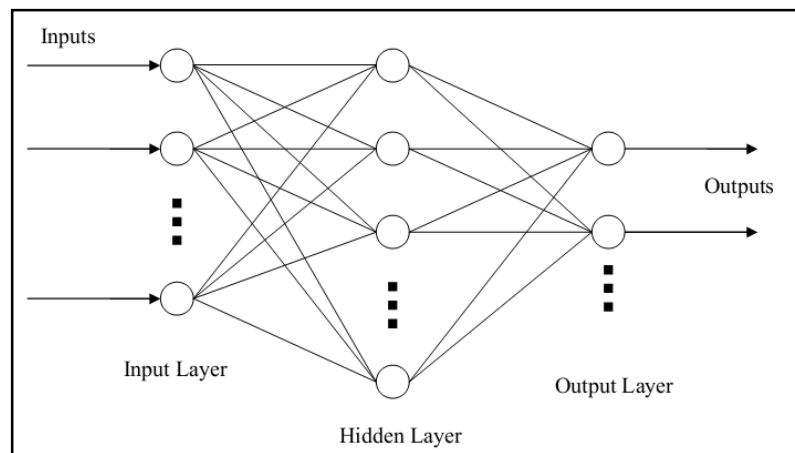


Figure 2.5: Architecture of a Standard Three Layer Neural Network Model (Cai, 2010)

ANNs have several advantages over regression models. One of them is that it can use field recorded data directly without any simplification. It can also simultaneously determine the effects of fixed and random input variables on the output variable. Insight into the interactions between the variables and the contribution of random variables to the response can be gained (Baxter *et al.* 2004). ANNs can do parallel computations and can simulate a non linear system (Cai, 2010). ANNs can perform quickly and efficiently for very complex problems and large datasets.

The disadvantages are computational time and the danger of overfitting. ANNs use a trial and error approach so one is never sure whether a unique optimal model has been obtained. The model can be over-trained with data and lose its power of generalizing to forecast future data. This happens when the training data is too long and there are too

many hidden neurons in the model. As the objective of ANN is to fit generalized data rather than a certain group of them, the selection of training patterns and configuration of the hidden neurons are crucial.

Network training (adjustment of the connection weights or network structure) enables the ANN to represent a set of data. Based on architectures and training algorithms, the ANN can be divided into different categories. Among them, the Back Propagation Neural Network (BPNN) and General Regression neural network (GRNN) are most commonly used for river flow forecasting (Cai, 2010) and are discussed below.

2.4.4.1 Back Propagation Neural Network

In BPNN, the given data are stored in the input neurons, which transmit these data to the hidden neurons across the links. Weights are used on each link to multiply the transmitted values. The weighted sum is then put through a transfer function to create a level of activity for the hidden neurons. Activation levels are transmitted to the output layer by the hidden neurons' transmission link. During the transmission they are weighted and summed again. Again the summed value is put through an activation function to get the activation level of the output neurons, which is the final solution of the network. The activation function used in BPNN is usually a logistic function:

$$f(I) = \frac{1}{1+e^{-I}} \quad (2.13)$$

where

$$I_i = \sum_{j=1}^n W_{ij} X_j \quad (2.14)$$

In BPNN, errors of the current layer are calculated based on the errors of the formal layer. This is an operation that propagates backward, hence “Back Propagation Neural Network”.

2.4.4.2 General Regression Neural Network

GRNNs are used for quick training on sparse datasets. They work by comparing patterns based on the distance of the connections from each other. They have the same three layer structure as BPNN. The output obtained from the network is proportional to the inputs in the training set (Gourrion, 2000). This proportion can be defined as (Savelieva, 2004):

$$W_{i(x,y)} = \frac{\exp(-\frac{d_i^2}{2\sigma^2})}{\sum_{j=1}^n \exp(-\frac{d_j^2}{2\sigma^2})} \quad (2.15)$$

where d_i is the computed distance,

σ is the spreading factor or smoothing factor of the transfer function.

A critical step in running GRNN is the calculation of the distance of new patterns from the training patterns. Two of the methods by which this calculation can be done are the Euclidean Distance and the City Block Distance Metric. Details of these methods can be found in the Ward System Group (2000). The well known ANN software developed by Ward Systems (2000) named Neuralshell2 has two options for calibrating a GRNN network: iterative and genetic adaptive. Iterative Calibration is used when all the input variables have the same contribution for predicting the output and a smoothing factor represents general impacts of inputs on outputs. In genetic adaptive calibration, each input

variable has its own smoothing factor. The larger the factor the more impact the variable has on the output. Therefore, this option is used when the input variables are of different types. Training by this option takes longer than using the iterative method. At the end of the training process, network performance is tested on independent test sets. The training and testing processes are carried out simultaneously to avoid the over-fitting of data, after which the network is tested on a validation dataset which is not used in the training.

In the ANN model developed by Cai (2010), a one day forecast model was developed for flow at three hydrometric stations; the Upper Humber River at Black Brook, the Humber River at Reidville and the Humber River at Humber River village bridge. To check the accuracy of the model, goodness of fit measures were used including Nash-Sutcliff efficiency, correlation coefficient r , mean squared error, mean absolute error and the percentage of outliers. The model gave better results than the in-house routing model developed by WRMD. Both GRNN and BPNN were only slightly better for some cases than the Dynamic Regression model developed by Picco (1997).

The results from all three stations were satisfactory, especially the two at the lower Humber. The Upper Humber station at Black Brook is highly influenced by snowmelt, which might not be taken into account accurately. The model could provide only a one day forecast with high accuracy. For two day forecasting two steps are needed: first a one day forecast is generated and then this forecast and other forecasted meteorological inputs are used to get two days forecast. Two step models do not usually perform very well, due to the associated errors with forecasted input factors from several sources. This is a drawback of the ANN model for the Humber River basin.

2.5 WATFLOOD Flood Forecasting Model

WATFLOOD is a physically based, fully distributed model of the hydrologic budget of a watershed (Carlaw, 2000). Fully distributed models operate using a square grid system for all input and output information in a given watershed. In these models the water balance calculations are made separately for each hydrologically significant land cover class. Its main purposes are flood forecasting and long term hydrologic simulations using gridded precipitation from rain gauges, radar or numerical weather models (Kouwen, 2011).

Like other hydrologic models, WATFLOOD represents only a small part of the overall physical processes occurring in nature and because the model is aimed at flood forecasting, the model incorporates only those physical processes with a prominent effect on runoff and streamflow (Carlaw, 2000). The physical processes include: interception, infiltration, evaporation, transpiration, snow accumulation and ablation, interflow, recharge, baseflow and overland flow, wetland and channel routing. WATFLOOD takes the grid data, initial conditions and input data and executes a series of internal calculations representing the physical processes of the water cycle. The vertical water budget is modeled with conceptual equations, while the routing from grid to grid is modeled with physically based equations (Bingeman *et al.*, 2006). The result is distributed output data which can be further evaluated using other sets of data.

WATFLOOD is a mesoscale, large domain distributed model. There are a large number of possible applications of WATFLOOD within research and operational communities. Some of these include augmenting flow records, dam safety studies,

confirmation for the atmospheric community, state variable estimation, environmental assessments, real time flow forecasting and non point source pollution modeling, among others.

WATFLOOD uses remotely sensed land cover images for the land cover information of the watershed. It classifies each pixel of the image into one of 16 different land cover classes (called Grouped Response Units, or GRUs), in addition to an impervious class. Each GRU has its own set of parameter values for representing its hydrologic characteristics. The model calculates and routes the response from each GRU to the channel based on its percentage contribution and user defined parameter values. In this approach, there is no need for the model grids to be homogeneous and the pixels of the GRUs need not be contiguous as the routing is not significantly affected by their position in the grid square (Kouwen *et al.*, 1993). One advantage of this method is that users can use similar parameter values for similar GRUs, and with change in land use over time, they only need to change the percentage of GRUs in each grid. WATFLOOD's main strengths are that it is fast and robust, and requires only temperature and precipitation as input data.

Evaluation of internal components for testing hydrologic models is crucial as different process descriptions often lead to very similar outflow hydrographs, without identifying specific problem sources in the simulations (Western *et al.*, 1999). Carlaw (2000) tested the ability of WATFLOOD to accurately estimate the soil moisture in the active upper zone in three different study regions during both short term (3 months) and long term (3 year) simulations. Soil moisture data were collected from three major

scientific projects: MAP (Mesoscale Alpine Program) in Europe, BOREAS (Boreal Ecosystem-Atmosphere Study) in Manitoba and Saskatchewan and FIFE (First ISLSCP (International Satellite Land Surface Climatology Project) Field Experiment) in Kansas. The evaluation was made by comparing the upper zone storage (UZS) calculated by WATFLOOD with the water content measured at various monitoring sites within the study regions. While WATFLOOD does not calculate soil moisture, it does calculate moisture in the upper layer of soil as a depth of water (UZS) by multiplying soil moisture content with porosity of soil layer. Modeled UZS calculated using MAP rain gauge precipitation data and radar data matched well with the measured water contents at all six measurement sites. The overall match was also good for the BOREAS data; however, the results obtained with FIFE were less than ideal. After investigating the relationship among recorded precipitation, soil moisture contents and streamflows, it was found that some fundamental problems existed in the dataset. This further showed that modeling is a useful tool to check datasets and possibly identify erroneous points (Carlaw, 2000).

Physically based models can predict the streamflow, yet model the hydrological processes incorrectly. For this reason, a standard split-sample streamflow calibration and validation are not enough for physically based models (Beven, 1989). There are several calibration-validation techniques given by authors which include validation of each of the hydrological processes of the water budget.

In a study made by Bingeman *et al.* (2006), explicit validations of several internal state variables (soil moisture, evaporation, snow accumulation and snowmelt, and groundwater flow) were presented. Data from BOREAS (1998) were used for validation

of the soil moisture and evaporation processes. Soil moisture was measured at 20 sites and at various depths. The data was then integrated to get cumulative soil moisture at each depth. These integrated values were compared with UZS modeled by WATFLOOD for each landcover and each grid. The evaporation data were obtained from eddy correlation flux measurement towers. Snow accumulation data from the Columbia River basin in British Columbia were used for the validation of snow accumulation and depletion algorithms in WATFLOOD. The validation of the model ensured that each of the major hydrological processes of WATFLOOD was operating with sufficient accuracy.

In another study by B.C Hydro in British Columbia, snow accumulation and depletion algorithms in WATFLOOD (Wong, 2005) were validated. Through the validation of hydrologic responses obtained in the study, modelers can have a greater confidence in applying the WATFLOOD model to domains where validation of internal processes is not feasible.

Cranmer *et al.* (2001) examined the effects of modeling the nonlinearities of hydrologic response to various storm intensities. Runoff hydrographs for three significant warm weather rainfall events occurring in 1995 were synthesized for this purpose. The observed and synthesized hydrographs were compared using the unit hydrograph method and the hydrographs matched extremely well in terms of shape, timing and peak flow magnitude. The results indicated that unlike Dynamic Regression models, WATFLOOD is capable of accurately modeling the nonlinear rainfall-runoff processes for increasing rainfall intensities with respect to peak flow, basin lag and time to peak flow.

2.6 Precipitation Forcing for WATFLOOD Model

In the current study a suitable precipitation dataset will be selected for the model calibration from three sets of data: (i) Second generation Adjusted Precipitation (APC2), (ii) North American Regional Reanalysis (NARR) and (iii) Canadian Precipitation analysis (CaPA). Though there have been a number of forecasting studies made using NARR data, the use of APC2 and CaPA is less widespread. An objective of this current study is to determine the applicability of these three datasets for forecasting studies in the Humber River basin. The following subsections give a brief description of these datasets and relevant studies.

2.6.1 Second Generation Adjusted Precipitation Data (APC2)

For hydrology and climate studies reliable climate datasets are crucial. The climate observations are recorded, transmitted, quality controlled and examined by experts of instruments, practice and climatology (Mekis and Vincent, 2011). These tasks are challenging due to relocation and closure of sites as well as changes in instruments and practices. These necessitate the adjustment of climate data to resolve these issues and ensure data continuity. Ding *et al.* (2007) noted that bias correction can change the magnitude and the direction of a trend. The gauge measured precipitation has a systematic bias mainly due to wind-induced under-catch, wetting losses and evaporation losses.

To address these problems, the first generation Adjusted Precipitation for Canada (APC1) was prepared in the mid -1990s (Mekis and Hogg, 1999). A second generation adjusted precipitation daily dataset (APC2) was prepared to make an improvement over the previous version (Mekis and Vincent, 2011). For each rain gauge type, corrections to

compensate for wind under-catch, evaporation, and gauge specific wetting losses were implemented (Devine and Mekis, 2008). For snowfall, density corrections based on coincident ruler and Nipher measurements were applied to all snow ruler measurements (Mekis and Brown, 2010). Daily rainfall and snowfall amounts were adjusted for 464 stations (Mekis and Vincent, 2011). The daily rainfall gauge and snowfall ruler data were extracted from the National Climate Data Archive of Environment Canada. All these measurements were made manually without the use of automatic measurement systems. Adjustments for rainfall from rain gauges were made by applying the following equation:

$$Ra = (Rm + Fc + Ec + Cc) \times (1 + Wc) \quad (2.16)$$

where

Ra = Adjusted daily rainfall (mm)

Rm = the measured daily rainfall (mm)

Fc = the container/receiver retention correction (mm) and

Wc = the wind correction factor (%) (Mekis and Vincent, 2011).

Ratios of corrected solid Nipher gauge precipitation measurements to snowfall ruler depth measurements, when both were operational, are calculated for snowfall adjustment from snow ruler measurements. The snow water equivalent adjustment factor ρ_{swe} map has been updated using 175 climatological stations with more than 20 years of concurrent observations (Mekis and Brown, 2010). Adjustments for flags for trace measurements are also made in APC2. Where the precipitation amounts are very low with significant number of trace events, the sum of those amounts becomes a significant portion of the total precipitation. The corresponding values of flag “T” which represent trace precipitation are assigned a value of zero. An additional amount of precipitation is

added to the observations when there is a trace flag. Flag “A” (accumulated precipitation), “C” (precipitation occurred) and “L” (precipitation may or may not have occurred) are replaced by the accumulated amount divided by the number of days affected to preserve the monthly total and minimize the impact on extreme values. For many locations, observations from nearby stations were merged to get a longer time series of rainfall and snowfall. Both the rainfall and snowfall precipitation amount were increased on the east coast. Figure 2.6 shows an increase of 30 % in trends in annual rainfall for the Humber River basin. In this Figure, the upward and downward pointing triangles indicate positive and negative trends, respectively. Filled triangles correspond to trends significant at the 5% level. The size of the triangle is proportional to the magnitude of the trend. The adjustments made for APC2 were found reasonable when annual, seasonal and monthly totals were analyzed.

Homogenized precipitation data were used in a number of climate trends studies including the trends in annual and seasonal temperature and precipitation in Canada (Zhang *et al.* 2000), changes in temperature and precipitation daily indices (Vincent and Mekis, 2006) and in global changes in daily and extreme temperature and precipitation (Mekis and Vincent, 2011).

For APC2, rain and snow were adjusted to provide more accurate amounts and to produce better estimates of trends. In a study by Roberts *et al.* (2012) for modeling the impacts of climate change on a sub-basin in the Lower-Churchill River watershed, APC2 data were used to compare with the Regional Climate Model (RCM) output. Bias corrections were made for RCM precipitation based on the APC2 data. APC2 was used in

a modeling study on the spatial and temporal variability of climate induced hydrological changes in the Fraser River, British Columbia, Canada (Shrestha *et al.*, 2012). The data was corrected for point precipitation biases. Based on the primary data, interpolated gridded data of 1/16 degree resolution were created that matched the resolution of the hydrologic model.

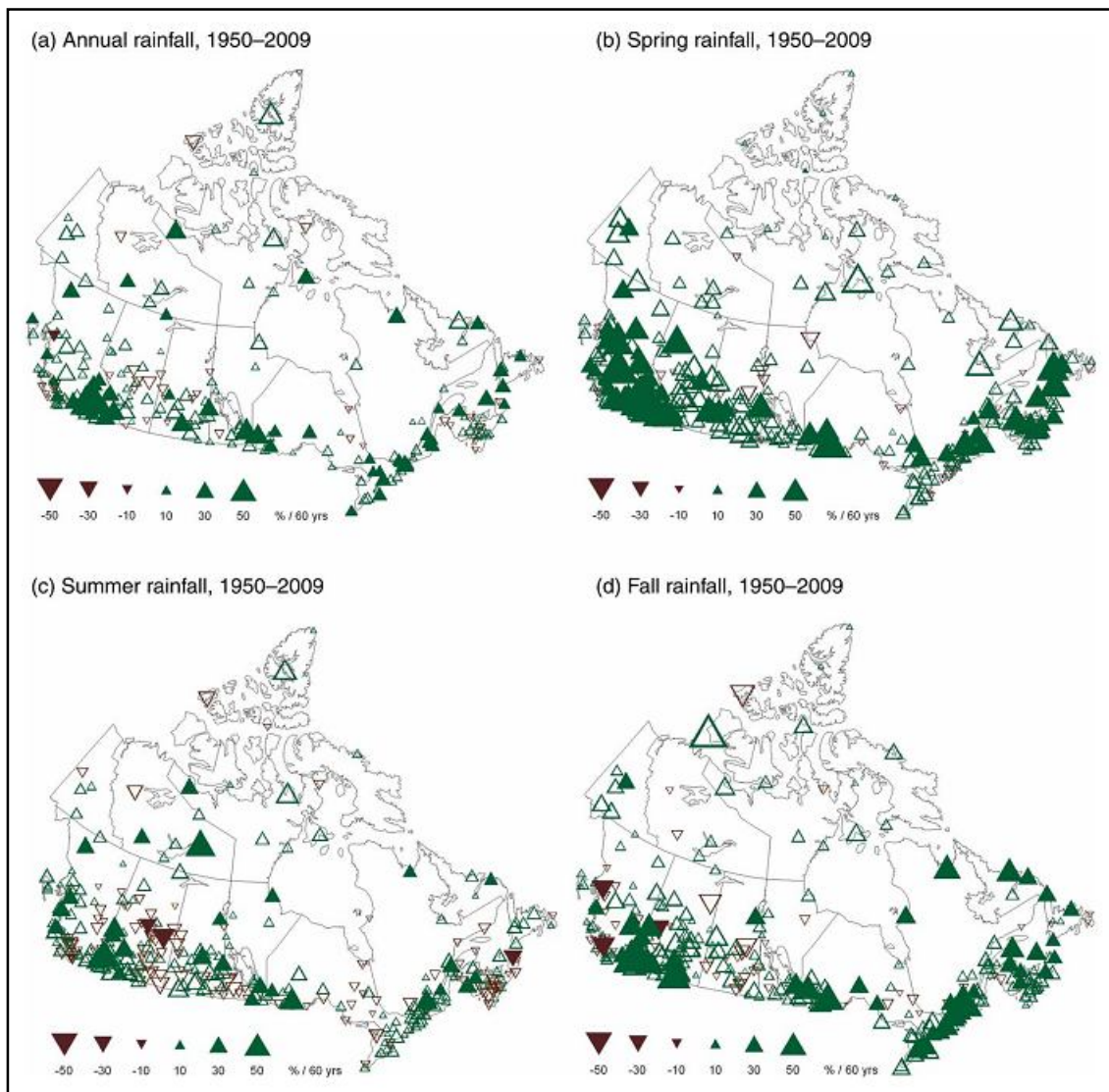


Figure 2.6: Trends in Annual and Seasonal Rainfall for 1950–2009 (Mekis and Vincent, 2011).

Shook and Pomeroy (2012) used APC2 to assess the change in the hydrological character of rainfall on the Canadian Prairies. According to these researchers, the APC2 dataset is the best quality historical data that can be obtained for Canada, and the data are as free from bias as possible because of the post processing procedures (Mekis and Vincent, 2011). From these above studies and others it is evident that APC2 can be successfully used for forcing hydrological models.

2.6.2 North American Regional Reanalysis Data (NARR)

Micro-scale analysis of river basins aids in the quantification of the global water cycle. This contributes to the knowledge of hydrologic processes and assists in the coupling of hydrologic and atmospheric models to investigate the effects of global climate change (Haberlandt and Kite, 1998). There are two limitations of point data obtained from weather stations: (i) they lack spatial coverage over an area of interest, especially in mountains and high latitude regions; and (ii) they are not continuous; periods of missing information are present. For these reasons point data from weather stations are limited for effective climate studies.

Gridded datasets such as those generated by Atmospheric-Ocean Coupled Global Models (AOGCMs) and RCMs, and reanalysis data such as those generated by the National Center for Environmental Prediction-National Center for Atmospheric Research (NCEP-NCAR) Global Reanalysis (NNGR) (Kalnay *et al.*, 1996) and North American Regional Reanalysis (NARR) (Messinger *et al.*, 2006) can be viable alternatives to alleviate these limitations of missing data and spatial biases resulting from uneven and

unrepresentative spatial modeling (Robeson and Ensor, 2006). These gridded datasets can be used to initialize climatic, ecological and hydrological models (Kittel *et al.*, 2004).

A reanalysis is an estimation of the state of the atmosphere, based on observations and a numerical weather forecast (Leander and Buishand, 2006). The NARR dataset (Messinger *et al.*, 2006) is a long term, dynamically consistent, high-resolution, high-frequency, atmospheric and land surface hydrology dataset for North America. This dataset is a major improvement over the NNGR dataset in both resolution and accuracy. NARR is an extension of NNGR and uses the high spatial resolution Eta model (0.3° X 0.3°; 32 km grid spacing, and 45 layers) with the Regional Data Assimilation System (RDAS). Most of the variables are collected at 3 hr intervals (eight times a day). NARR data is available from 1979 to the present.

The hallmarks of NARR are the incorporation of hourly assimilation of high quality precipitation observations, the inclusion of a recent version of the Noah Land surface model and the use of numerous other available datasets. All these improved NARR compared to the earlier Global Reanalysis products (Messinger *et al.*, 2006). NARR has been developed by assimilating high quality detailed precipitation observations in the atmospheric analysis which helps to improve analysis of land hydrology (Nigam and Ruiz-Barradas, 2006). However, NARR over Canada's regions has one significant weakness: the daily gauge-based data are sparse (1° grid) and may hamper for model performance. Also, the weather station data represent point information while NARR provides areal averages in a 32 X 32 km grid, within which there can be variations in climate. The latter limitation is a major drawback because in a hydrologic

model, areal representation of precipitation is more important than data for a single point (Choi *et al.*, 2009). Figure 2.7 shows the distribution of surface observations for the NARR data assimilation process.

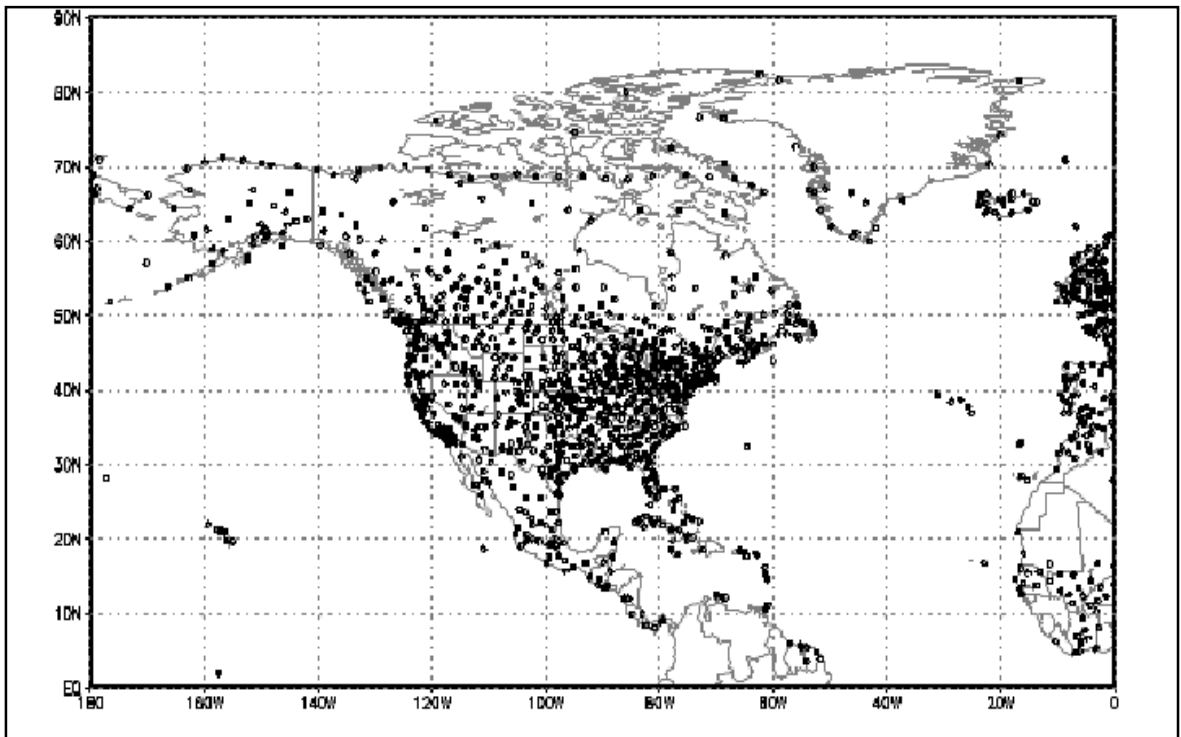


Figure 2.7: Distribution of Surface Observations Assimilated in NARR (January 1988)

(Mesinger *et al.*, 2006)

Nigam and Ruiz-Barradas (2006) compared ECMWF (European Center for Medium-Range Weather Forecast) and NARR to analyze hydroclimatic variability over the Eastern U.S. They found that NARR provided more realistic spatial variation of summer and winter precipitation. Woo and Thorne (2006) used temperature and precipitation data from ERA40, NNGR and NARR as input in a hydrological model and

estimated the snowmelt contribution to discharge from the Liard Basin in Subarctic Canada. They found that NARR provided a better representation of flow contribution.

Choi *et al.* (2007, 2009) evaluated monthly and daily NARR data and examined its potential as an alternative data source for hydrologic modeling in Manitoba. They got good results from temperature data but unsatisfactory results with precipitation, which showed negative bias in summer. That being said, NARR performed better than NNGR and the results indicated the suitability of the NARR data for hydrological modeling.

Solaiman *et al.* (2010) used NARR data for assessment of hydrologic impacts of climate change at a basin scale. Daily precipitation, maximum temperature and minimum temperature from NNGR and NARR were used as inputs into the semi-distributed Hydrologic Engineering Center Hydraulic Modeling System (HEC-HMS). The study found that NARR showed encouraging results in simulating summertime low flows with less variability and fewer errors. It was suggested that NARR can be used as an alternative data source for regions with scarce datasets.

Recently in many other studies, NARR had been used successfully for calibration and validation of hydrological models of river basins. One such study is by Shreshta *et al.* (2011). In that study, NARR precipitation, maximum and minimum air temperature, solar radiation, wind speed and relative humidity were used to force the SWAT (Soil Water Assessment Tool) model.

2.6.3 Canadian Precipitation Analysis Data (CaPA)

Spatial distribution of precipitation on short timescales is important for flood forecasting studies. Mahfouf *et al.* (2007) discussed the methodology used in the

Canadian Precipitation Analysis (CaPA) to convert the real time point measurements of precipitation into a gridded dataset. The project was initiated in November, 2003 through collaboration with the Meteorological Service of Canada (MSC), Meteorological Research Branch, Canadian Meteorological Center (CMC) and Quebec Region Service Weather National Laboratory. The objectives of this study were to combine different sources of information on precipitation into a single near real time analysis that produces 6 hr rainfall accumulation data at a resolution of 15 km over North America. The analysis is used to perform quantitative precipitation forecast verification (QPF), to provide input precipitation forcing to Environment Canada's land surface and hydrology modeling systems, including the Canadian Land Data Assimilation System (CaLDAS), to perform nowcasting of precipitation, for case study analysis and in climate and drought monitoring.

The information sources for precipitation come from direct and indirect measurements such as surface gauge networks, radar data, satellite imagery and short term forecasts from atmospheric models. These observations of precipitation are combined with a first guess (background field) to obtain the gridded precipitation analysis. The background field is a 6-hr precipitation forecast from the regional Global Environmental Multiscale Model (GEM), which has a resolution of 15 km. The Optimum Interpolation (OI) technique is used for CaPA construction. The OI technique performs the analysis on innovations (the difference between an observation and the corresponding background value). The OI technique requires the specification of error statistics

associated with each piece of information used to construct the analysis (i.e observation and background field) (Carrera & Fortin, 2008).

Surface stations plotted in Figure 2.8 correspond to three groups reporting 6-hr precipitation accumulations; the Synoptic Reports (SYNOP), the Meteorological Aerodrome Reports (METER) and Réseau Météorologique Coopératif du Québec (RMCQ) (Mahfouf *et al.*, 2007).

The examination of the resulting analysis from CaPA demonstrated that an improved product is obtained with more surface data. Carrera and Fortin (2008) performed a quantitative objective comparison study compared with global OI precipitation analysis. The result demonstrated that CaPA 6-hr analysis is not always better than the global precipitation product based on the GEM model, but it is superior for categorical scores for small precipitation quantities (where precipitation is less than 0.25 mm/day) and also for precipitation quantities of more than 1 mm/day. They also found that the bias in CaPA are smaller than the global OI product.

Vincent Fortin (2011) used CaPA data in collaboration with GEM and MESH to predict Great Lakes net basin supplies. Objectives of the project included building a gridded dataset covering a 5 year period (June 2004 – May 2009) describing the spatial and temporal evolution of the watershed and assessing whether it is possible to use GEM and MESH to forecast net basin supplies. The study concluded that CaPA is suitable for estimating overlake precipitation in real time. CaPA has been in operation since 2011. The operational Configuration of CaPA is shown in Figure: 2.9.

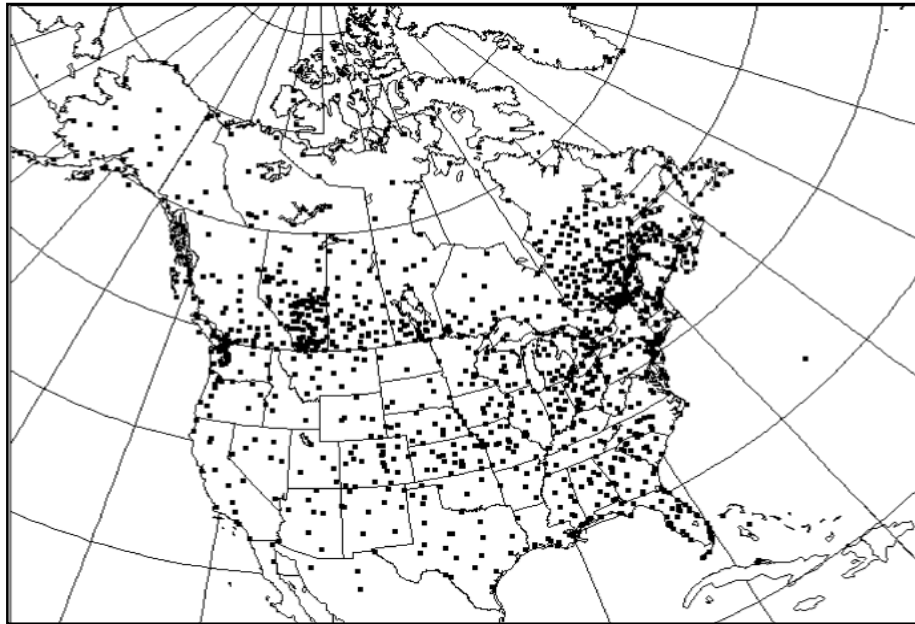


Figure 2.8: CaPA Analysis Domain over North America (Mahfouf *et al.*, 2007).

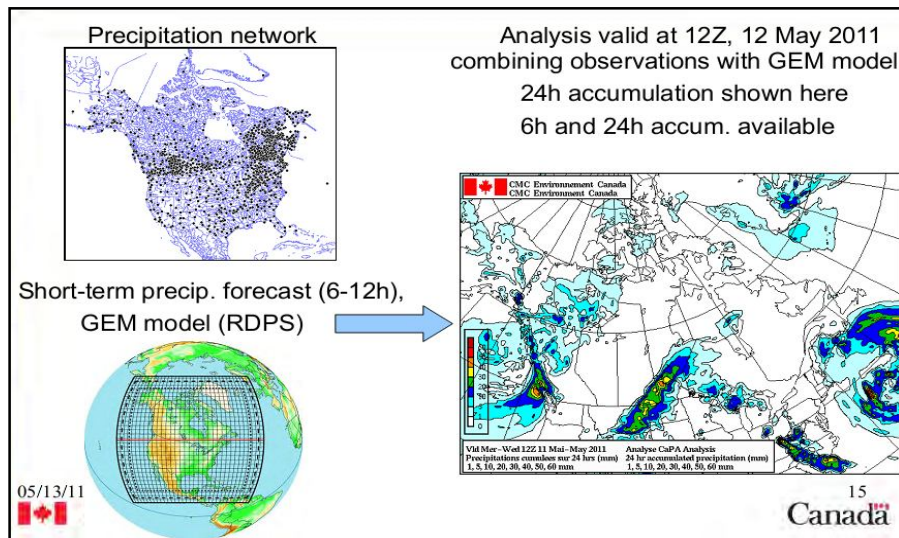


Figure 2.9: Operational Configuration of CaPA (Fortin, 2011)

Chapter 3 Data Collection and Preparation

This chapter contains details of the data collected for the study. The data includes those required for model set up (land surface characterization: land surface elevation and land cover), model forcing (precipitation, temperature and climate normals), calibration and validation (streamflow) and other associated data (water level for routing coefficients). The manipulation and preparation of all the final datasets are described as is the bias correction method applied over the forcing data.

3.1 Model Setup Data

Throughout history the landscape of the world has been changed by natural processes and by humans to meet their various needs. Due to economic, technological, institutional and cultural factors, globalization and agricultural expansion are the largest causes of land use change. Land cover changes affect local hydrology, which in turn has impacts on the environment and human society. Land surface characterization is crucial for the development of the hydrological model.

Land surface elevation and land cover information are used to generate the basin data required by WATFLOOD. Green Kenue, an Ensim application, is used to create a mapfile for WATFLOOD which converts it to the required basin file. A mapfile contains surface elevation data and the land cover data. Data used in this study are described in the next section.

3.1.1 Surface Elevation Data

Digital elevation models (DEMs) describe the land's topography and are widely used for simulating the surface hydrology of a basin (Moore *et al.*, 1991). In DEMs terrain is represented by a grid of squares. Each square is associated with a single elevation value. In this study, a DEM from the Canadian Daily Climate Data (CDCD) and DEM data provided by the National Aeronautic and Space Administration (NASA) from the February 2000 Shuttle Radar Topography Mission (SRTM) (Coltelli *et al.* 1996, Gamache 2004) were used. Unfortunately, both datasets have missing data problems.

Though SRTM has been one of the most widely used publicly available spatial datasets in recent years, the finished version of SRTM contains 3,339,913 data voids which total roughly 803,166 km² (Reuter *et al.*, 2007). These “no-data” holes typically occur over waterbodies, desert regions and mountains where heavy shadow prevents the quantification of elevation. These holes prevent the use of this dataset directly in many applications, especially in the field of hydrological modeling. Reuter *et al.* (2007) developed a method to fill voids using an interpolation algorithm in conjunction with other sources of elevation data. The Consultative Group on International Agricultural Research-Consortium for Special Information (CGIAR-CSI) followed this method and their GeoPortal is able to provide the processed SRTM 90m DEM (3 arc-second product) covering 60N to 54S. In this study the DEM data from CGIAR-CSI GeoPortal (Jarvis *et al.*, 2008) are used.

Filling of data voids involves the production of vector contours and points, as well as re-interpolation of these derived contours back into a raster DEM. The processing was

made using the Arc/Info Arc Macro Language (AML). The original SRTM DEM was used to produce the original point and contour data.

Canadian Digital Elevation Data (CDED) Level 1 derived from 1:50,000 and 1:250,000 topographic maps available from Geobase were used as auxiliary DEM data (<http://www.geobase.ca/geobase/en/data/aded1.html>) and the 30 second SRTM30 (Gamache 2004) was used as an auxiliary DEM when no other high resolution DEMs were available. Where high resolution auxiliary DEMs were available, the contours and points inside and surrounding the data holes were interpolated to produce a hydrologically sound DEM using TOPOGRID in Arc/Info (Jarvis *et al.*, 2008). This process interpolates through the data holes and produces a smooth elevation surface where no data was originally found.

For the areas lacking high resolution auxiliary DEMs, an appropriate interpolation technique was selected based on void size and landform topology and applied on the surrounding data. The best interpolation methods found were Kriging (McBratney *et al.*, 1986) and Inverse Distance Weighting Interpolation (Watson and Philip, 1985) for small and medium size voids in relatively flat low-lying areas; Spline Interpolation (Franke, 1982 and Mitas and Mitasova, 1988) was used for small and medium sized holes in high altitude and dissected terrain; Triangular Irregular Network or Inverse Distance Weighting interpolation was used for large voids in very flat areas; and an advanced Spline method (ANUDEM) was used for large voids in other terrains (Jarvis *et al.*, 2008). Interpolated DEMs for the no-data regions were then merged with the original DEM to create a continuous elevational surface without any data voids. The entire process of data

void filling was performed for each tile with large overlapping tiles. It created a seamless and smooth transition in topography in large void areas. The resultant seamless dataset was clipped along coastlines using the Shoreline and Waterbodies Database (CGIAR-CSI, 2004).

The SRTM 90m DEM has the resolution of 90m at the equator. The DEM tiles can be downloaded from the CGIAR-CSI site in mosaiced 5 degree x 5 degree tiles in either ASCII or GeoTiff format. In this study, the GeoTiff format was used. CGIAR uses WGS84 datum. The reported vertical error in elevation is less than 16m. The downloaded DEM data was cropped using ArcGIS in the required area for the study.

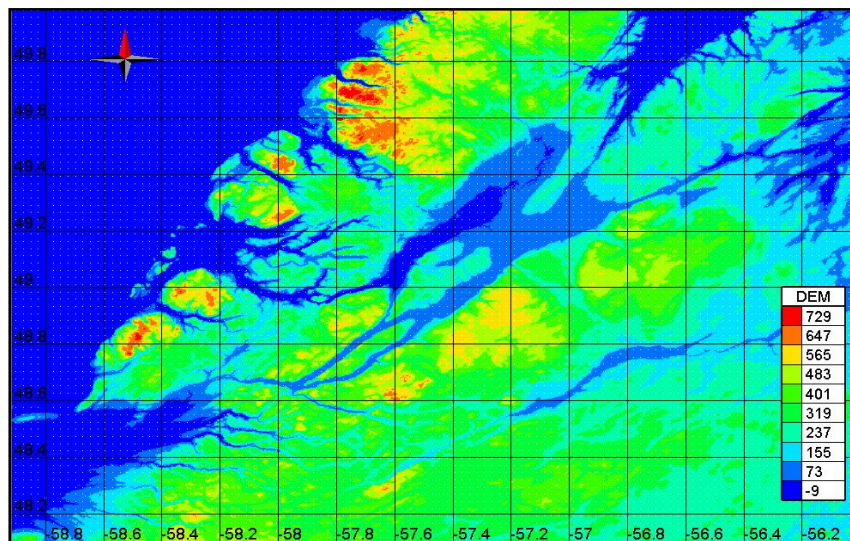


Figure 3.1: DEM for Humber River Basin

3.1.2 Land Cover Data

Land cover data are required for the WATFLOOD Model. They were collected from the National Topographic Data Base (NTDB) and the National Hydro Network (NHN).

NTDB comprises digital vector datasets that cover the entire Canadian landmass (Geogratis, Natural Resource Canada). The data are based on North American Datum 1983 (NAD83) and available at either the 1:250,000 or 1:50,000 scale. The data were downloaded in shape files after locating them with the National Topographic System (NTS) Map sheet (12A, 12B, 12G, 12H). The NTDB maps include features such as waterbodies, urban areas, vegetation, roads, railways etc. In the current study, only maps of vegetation and wetland areas are used.

NHN provides geospatial vector data describing hydrographic features such as lakes, reservoirs, rivers, streams, canals, islands, waterfalls and human constructions (eg. dams) as well as a linear drainage network. The data are based on a latitude-longitude coordinate system. It is difficult to specify the scale of these data as the NHN data are acquired by using several sources (provincial and federal data, NTDB data). According to the NHN product specification, the data used in the study are most likely to be in the scale of 1:250,000. In this study, NHN shape files of waterbodies and work units are used.

NHN datasets are produced and distributed per “NHN Work Unit” which is actually a drainage area defined by the Water Survey Canada (WSC) for stream gauge numbering. The limits of the work unit are not officially mapped boundaries for the watershed or drainage area. The work unit limits were created to define the extent of the NHN dataset and for referring to NHN data products. The work units are simple contiguous polygons and make up a complete territorial coverage without any discontinuity or overlap. There are 1150 work units or terrestrial divisions covering the entire Canadian landmass, from the Canada/USA international boundary up to the

Canadian territorial sea or to the NTS tile limits along the Canadian coastline. The original NHN Work Unit Limits were created based on the Water Survey of Canada (WSC) Sub-Sub-Drainage Areas (WSSDA) and Fundamental Drainage Areas (FDA) from the Atlas of Canada (Geobase, NHN Work Units). Provincial data were brought into the data production for modification and refinement of NHN work units. The product was introduced as a “phased” implementation and is expected to evolve over time as better sources (provincial data) are incorporated.

WATFLOOD requires land use data to be incorporated within its map file format. This input data is pre-processed by Green Kenue for WATFLOOD. Green Kenue provides tools to obtain pre-processed land use information. WATFLOOD permits a number of land uses described in its map file. Land use data can be added to the map file using closed polygons or using GeoTIFFs. In this study, land use data are obtained from GeoTIFFs (Figure 3.2).

Land use classes can be directly generated from one or more classified GeoTIFFs. The images are processed so that only required land use classes exist. In this study it was decided to map land use data from a single GeoTIFF image. The number of land cover types is arbitrary. However, selection of a large number of cover types requires the definition of more and more hydrologic parameters. Owing to the limited number of stream gauges available in this study, only four land cover classes (vegetation, wetland, water and impervious) were selected for the study. Correct stream gauge density provides greater amounts of calibration data that would support splitting of land cover classes (e.g., forest class into coniferous and deciduous). The shape files of waterbodies, wetlands and

vegetation are defined in the GeoTIFF using ArcGIS. The remaining regions are classified as impervious. NTDB polygons were first converted to raster data and then reformatted as a GeoTIFF image.

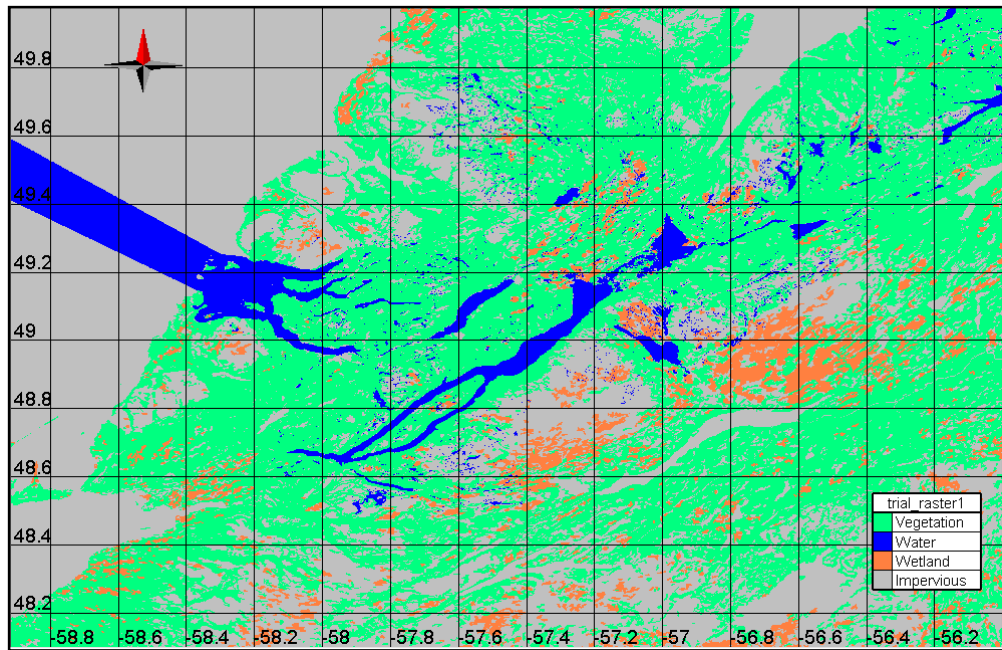


Figure 3.2: Land Cover Map (GeoTIFF) for Humber River Basin

3.2 Model Forcing Data

The climate stations from Environment Canada record a range of climate variables used in this study. Temperature and precipitation were most important in this study as WATFLOOD requires at least temperature and precipitation data for simulating streamflow. Data for a 30-year period from 1982 to 2011 were sought for the study. It should be noted that not all the stations selected for the study contain the entire 30 year dataset. A brief description of the selected meteorological stations and the datasets is given below.

3.2.1 Precipitation Data

Three sets of precipitation data were chosen as model forcing: (i) APC2, (ii) NARR and (iii) CaPA. General descriptions and other uses of these datasets can be found in Chapter 2.

3.2.1.1 APC2

APC2 (Mekis and Vincent, 2011) was obtained directly from Environment Canada (Mekis, 2013). Among the 23 stations in Newfoundland, 14 stations that are within or close to the Humber River basin were selected. Table 3.1 summarizes the rainfall stations with their ID, location, elevation and period of available data.

Table 3.1: APC2 Precipitation Station Information

Station ID	Station Name	Longitude	Latitude	Elevation (m)	Data Period
840C401	St. Anthony	-56.1	51.4	33	1983-2009
8400413	Bay D'espoir	-55.8	48.0	23	1982-2011
8400798	Burgeo	-57.6	47.6	11	1982-1995
8401300	Corner Brook	-58.0	49.0	5	1982-2011
8401400	Daniel's Harbour	-57.6	50.2	19	1982-2010
8401501	Deer Lake	-57.4	49.2	22	1982-2011
8401550	Exploits Dam	-56.6	48.8	154	1982-2009
8401700	Gander	-54.6	49.0	151	1982-2011
8402050	Grand Falls	-55.7	48.9	60	1982-2007
5402450	Isle Aux Morts	-59.0	47.6	5	1982-2004
8402958	Plum Point	-56.9	51.1	6	1982-2011
8403700	Springdale	-56.1	49.5	23	1982-1993
8403800	Stephenville	-58.6	48.5	26	1982-2011
8404201	Westbrook St. Lawrence	-55.4	47.0	31	1982-1995

Figure 3.3 shows the location of the precipitation stations selected for the study superimposed on a background map of the Humber River basin. In the Figure, Y axis X axis shows the Latitude and Longitude of the mapped area respectively. Each data file collected from EC contains all the daily adjusted precipitation data available for a station. These data are then combined, formatted and written in the format required by WATFLOOD (_rag.tb0).

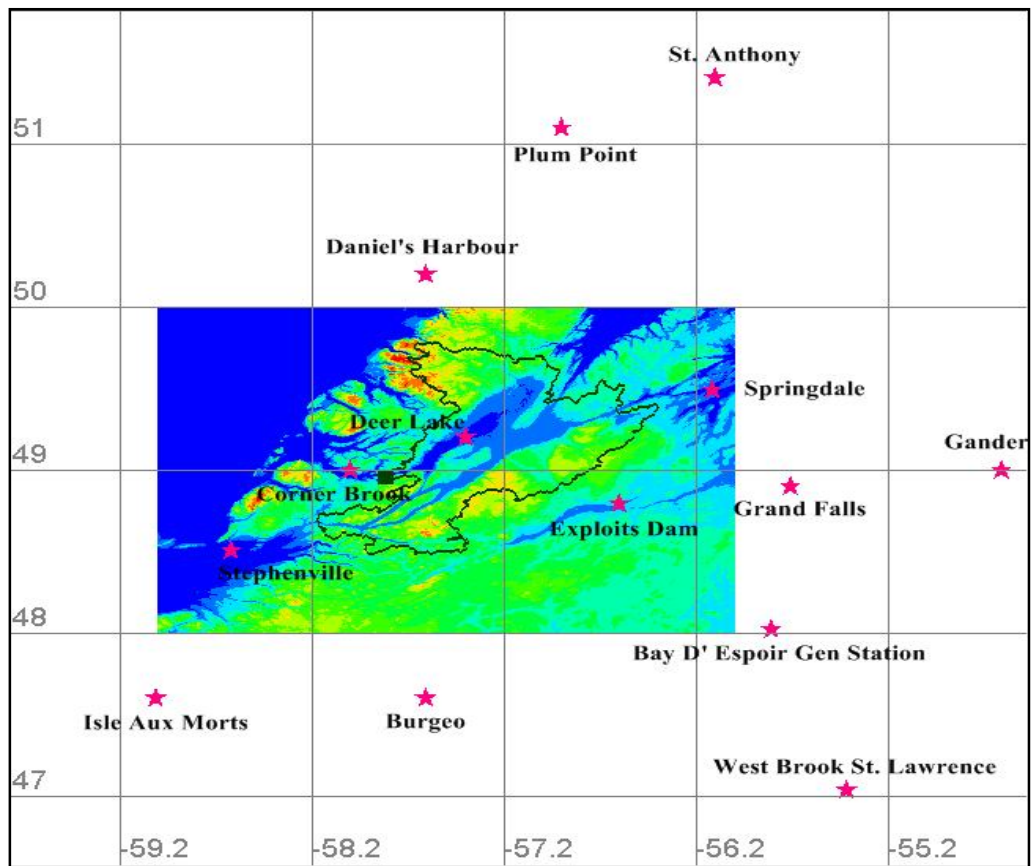


Figure 3.3: Location of Precipitation Stations

Figure 3.4 shows the precipitation variation in APC2 among six locations (Corner Brook, Daniel's Harbour, Deer Lake, Exploits Dam, Grand Falls and Stephenville), which are

located within or close to the basin, for the study period (1982-2011). Among these six stations, Stephenville experiences the overall highest precipitation and Grand Falls experiences the overall lowest precipitation.

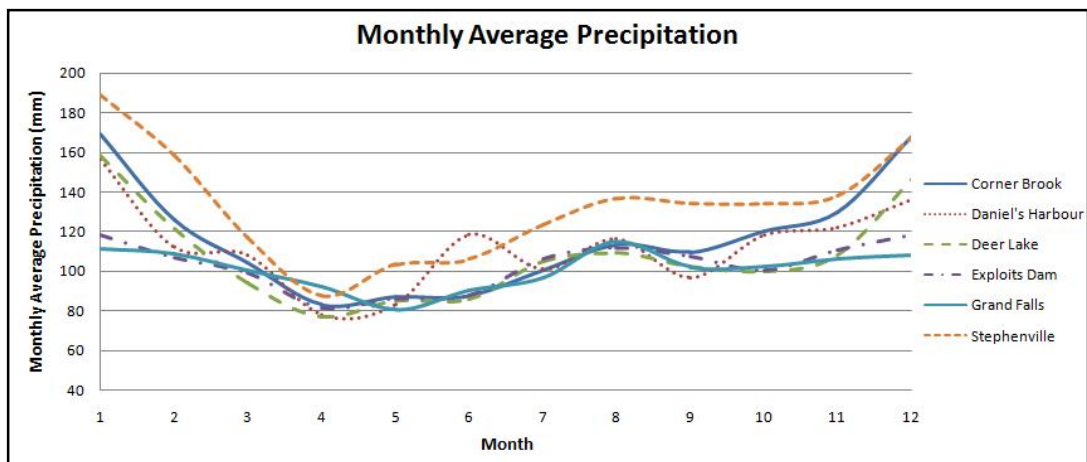


Figure 3.4: Monthly Average APC2 over Study Period

3.2.1.2 NARR Precipitation Data

The hallmarks of NARR are: (i) incorporation of hourly precipitation accumulation, (ii) use of the recent version of the Noah land surface model and (iii) use of other datasets that are improved compared to Global Reanalysis (GR). The assimilation system is fully cycled, meaning that it uses the prognostic land states with a 3hr forecast from the previous cycle which serves as the first guess for the next cycle (Mesinger *et al.*, 2004). Assimilation of observed precipitation ensures that the model precipitation is close to observations. This is accomplished by adjusting atmospheric moisture to best match observed precipitation. This result produces a more realistic hydrological cycle compared to one that would be generated if the model were free to forecast precipitation without observation. The precipitation analyses are disaggregated into hourly analysis in NARR's

computational grid. Over Canada the hourly precipitation analyses are obtained by disaggregating the 24 hour analysis of rain gauge data using a Cressman successive-scan analysis technique. A detailed discussion of the NARR data processing can be found in Shafran *et al.* (2004).

Joon (2012) compared NARR precipitation data with observed precipitation data to check the reliability of NARR precipitation as a proxy dataset. In his study, based on six reference sites in central Canada (Brandon, Churchill, Dauphin, The Pas, Thompson and Winnipeg), he found that the annual average precipitation is approximately 6% less than the overall observed precipitation.

NARR data was downloaded from the National Oceanic and Atmospheric Administration (NOAA) for the period of January 1979 to June 2013 (<http://nomads.ncdc.noaa.gov/thredds/catalog/narr/catalog.html>). The NARR precipitation data are 3-hr accumulation of precipitation. The data are then formatted and written in the format required by WATFLOOD (_met.r2c).

Figure 3.5 shows the precipitation variation in NARR among six locations (Corner Brook, Daniel's Harbour, Deer Lake, Exploits Dam, Grand Falls and Stephenville) for the study period (1982-2011). Among the six stations, Stephenville experiences the overall highest precipitation. All the stations show decreased precipitation compared to measured values, particularly in winter months (December, January and February).

3.2.1.3 CaPA

CaPA produces 6 hr rainfall accumulation data at a resolution of 15 km over North America in near real time. CaPA combines a variety of sources of information on

precipitation into a single, near real time analysis. Figure 3.6 shows the many sources of precipitation data used in CaPA analysis (Carrera and Fortin, 2008).

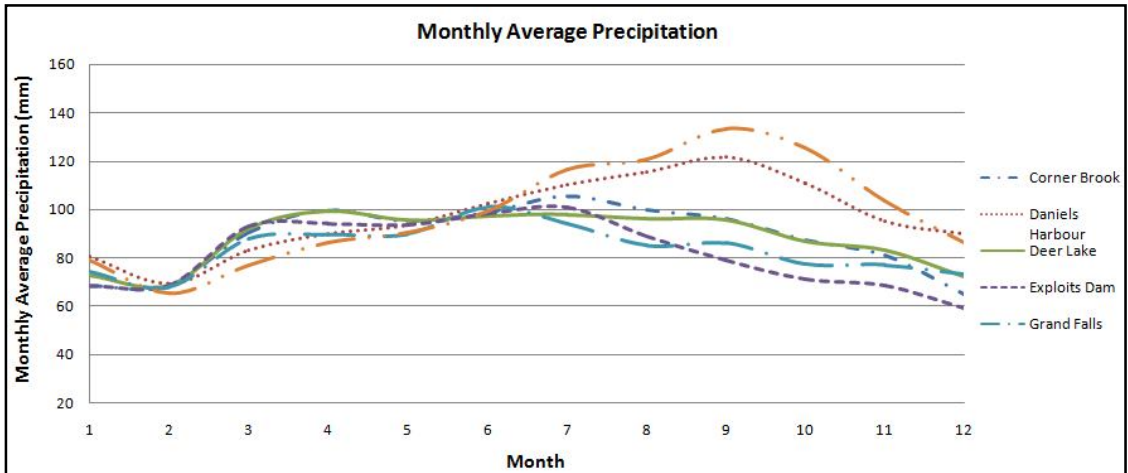


Figure 3.5: Monthly Average NARR over Study Period

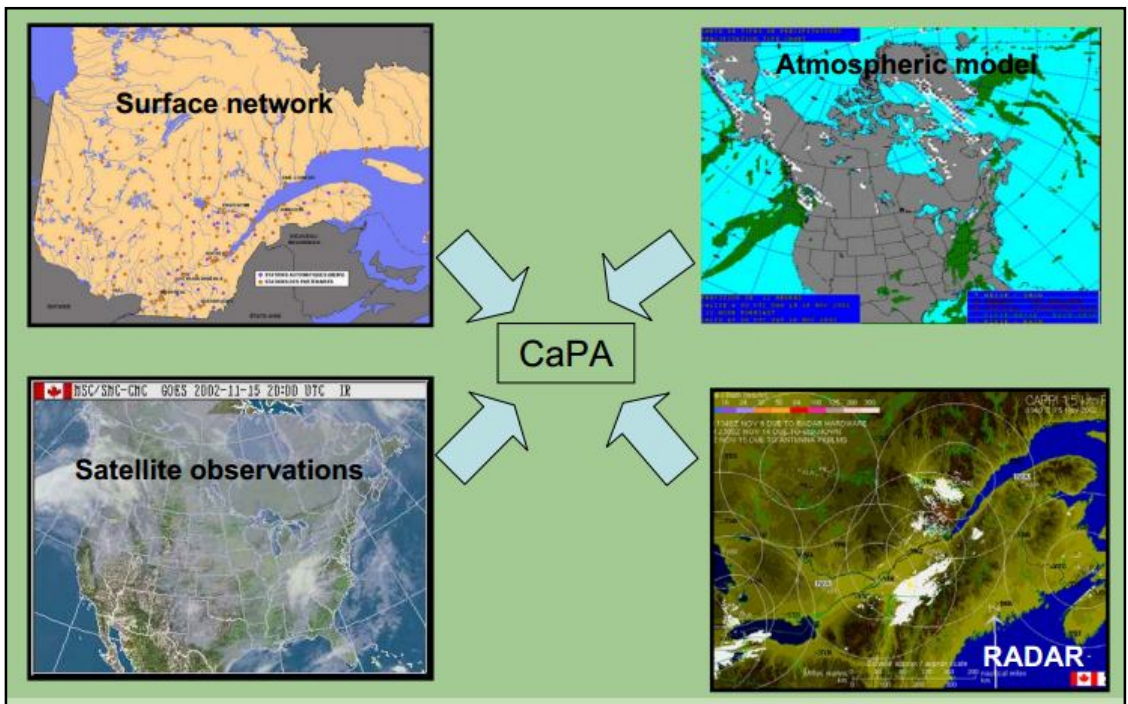


Figure 3.6: Precipitation Data Sources for CaPA

A statistical interpolation technique (SI) (also known as Optimum Interpolation) has been chosen for the production of precipitation analysis (Brasnett, 1997, 1999). For a set of N precipitation observations y_o^i , and a background field x_b^j available on a grid (M points), the statistical interpolation provides an analysis x_a^j at the model grid point j , as

$$x_a^j = x_b^j + \sum_{i=0}^N W^{ij} (y_o^i - y_b^i) \quad (3.1)$$

where y_b^i = background field spatially interpolated to the observation point i

The analysis is performed on a transformed variable, which must be normally distributed:

$$x = \ln(p + \alpha) \quad (3.2)$$

where p = 6 hr accumulated precipitation in mm

α = an arbitrary constant = 1 mm

α is chosen to be 1 mm so that zero precipitation corresponds to $x = 0$.

A detailed description and preliminary result of the CaPA project can be found in Mahfouf *et al*, (2010). CaPA Data was obtained from Bruce Davison (Davison, 2013) for the period of January 2002 to June 2013. The data was then formatted and written in the format required by WATFLOOD (_met.r2c).

Figure 3.7 presents the monthly average precipitation at Deer Lake from APC2, NARR and CaPA. There is a significant difference in NARR precipitation from APC2 and CaPA. NARR seems to fall especially short in winter precipitation. It also shows higher precipitation in spring. Figure 3.8 represents the precipitation variation in three datasets for the year 2011 at Deer Lake.

Figure 3.9 shows the cumulative precipitation for Deer Lake in 2011. It shows that NARR and CaPA both underestimate the total precipitation. CaPA underestimates the

precipitation by 34%. Table 3.2 shows a significant difference between the three precipitation datasets (APC2, NARR and CaPA) in terms of monthly maximum and monthly average precipitation for Deer Lake.

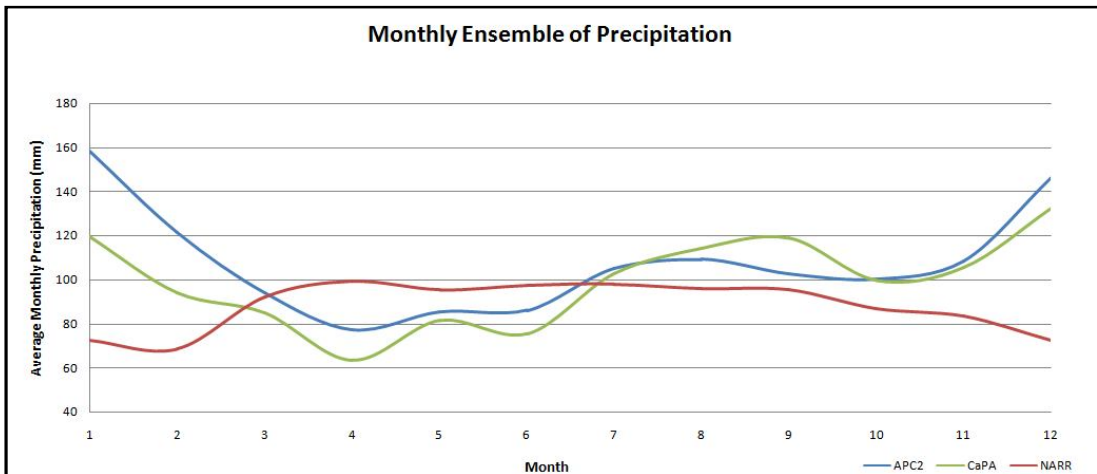


Figure 3.7: Monthly Average Precipitation at Deer Lake

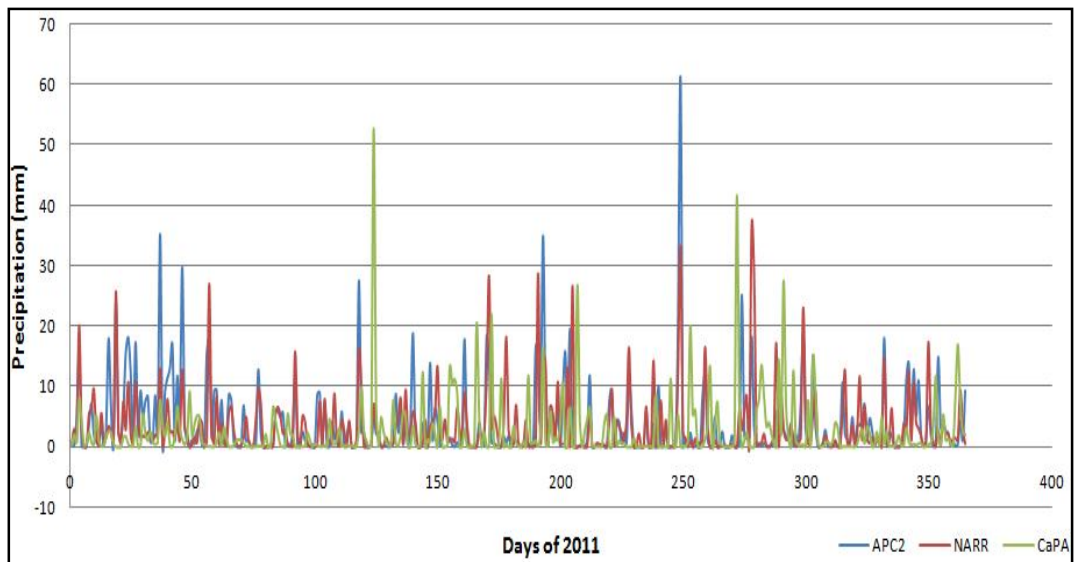


Figure 3.8: Precipitation at Deer Lake for the year 2011

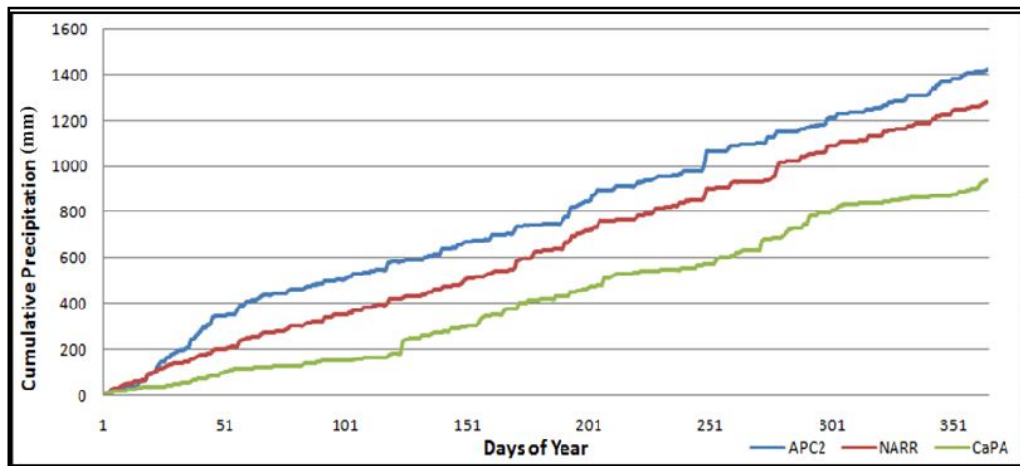


Figure 3.9: Cumulative Precipitation at Deer Lake (2011)

Table 3.2: Monthly Maximum and Average Precipitation for Deer Lake

Month	APC2 (1982-2011)		NARR (1982-2011)		CaPA (2002-2011)	
	Max (mm)	Average (mm)	Max (mm)	Average (mm)	Max (mm)	Average (mm)
Jan	40.08	150.23	45.02	81	28.07	108.44
Feb	42.24	119.53	32.81	71.67	28.21	86.34
Mar	53.28	97.47	27.11	66.93	34.75	77.58
Apr	32.88	76.47	30.21	67.09	28.46	58.03
May	50.4	76.82	47.72	74.66	52.67	74.46
Jun	68.88	84.54	44.41	86.87	34.26	69.25
Jul	59.52	86.46	57.1	96.69	44.6	93.95
Aug	53.52	103.83	46.87	93.88	41.25	104.52
Sep	61.2	107.89	50.51	91.77	83.11	108.78
Oct	39.36	103.9	39.86	94.37	31.63	91.47
Nov	50.64	105.28	35.43	91.25	35.63	96.87
Dec	44.88	111.01	36.19	91.56	29.62	121.54

3.2.2 Temperature Data

Two sets of temperature data were used in this study: (i) historical temperature data (station observations) from National Climate Data and Information Archive (EC), and (ii) NARR temperature data.

3.2.2.1 Historical Temperature Data

Six temperature stations are selected around the basin boundary. In this study, data were sought for the period of 1982 to 2011. Table 3.3 summarizes the gauges with their location, elevation and period of data collected. Each data file contains hourly temperature data for a month. These data are then combined, formatted and written in the format required by WATFLOOD (_tag.tb0). Figure 3.10 shows the location of the weather stations. Table 3.3 shows the elevation variations among the stations used.

Table 3.3: Temperature Stations Information

Station Name	Longitude	Latitude	Elevation (m)	Data Period
Badger	-56.07	48.96	102.7	1987-2011
Corner Brook	-57.92	48.93	151.8	1994-2011
Daniel's Harbour	-57.58	50.24	19.0	1982-2011
Deer Lake	-57.40	49.22	21.9	1982-2011
Port Aux Basques	-59.15	47.57	39.7	1982-2011
Stephenville	-58.55	48.53	24.7	1982-2011

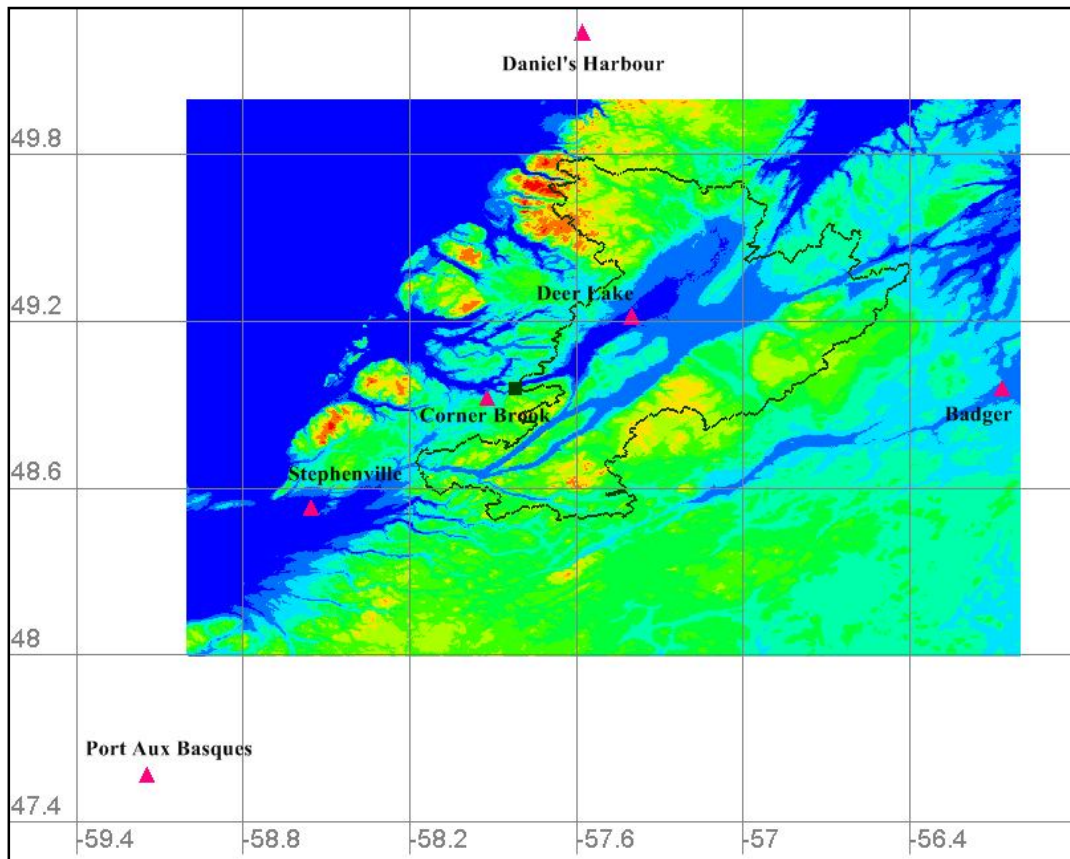


Figure 3.10: Temperature Station Locations

APC2 was not used for temperature. Previous studies (Pryse-Phillips, 2010) have showed that the adjusted temperature data are almost the same as the observed temperature data. As such, APC2 temperature data were not used in this study. Figure 3.11 illustrates the comparison between adjusted and observed mean monthly temperatures for the period of 1953-2008 at Goose-Bay (Pryse-Phillips, 2010). It clearly shows that the adjusted mean monthly temperatures matches very well with observed mean monthly temperature for the mentioned period.

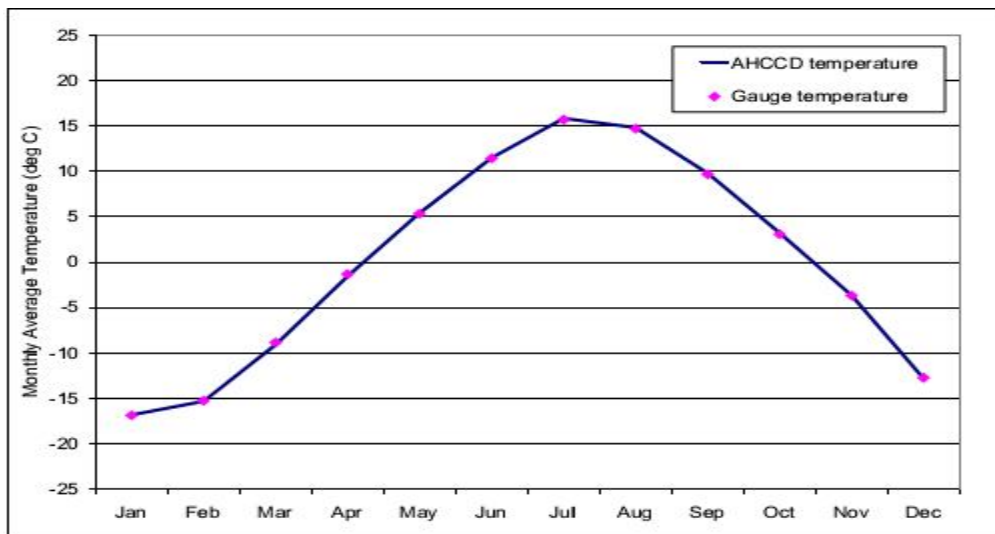


Figure 3.11: AHCCD and Gauge Temperature at Goose Bay

3.2.2.2 NARR Temperature Data

NARR temperature data has been less widely used compared to the precipitation data. Joon (2012) compared the NARR data with the weather station data to assess the reliability of NARR as a proxy for observed climate data at the station scale. It was expected that NARR would show good agreement with observation on a regional scale due to its high spatial resolution and general reliability. Comparing the data from six weather stations, Joon found that NARR temperature was approximately 1 °C higher than the observed temperature.

NARR data were downloaded from the National Oceanic and Atmospheric Administration (NOAA) for the period of January 1979 to June 2013 in .grb format (<http://nomads.ncdc.noaa.gov/thredds/catalog/narr/catalog.html>). NARR temperature data are 3 hr average temperature data. The data are then formatted and written in the format required by WATFLOOD (_tem.r2c).

Table 3.4 lists the monthly maximum, minimum and average historical and NARR temperature for a 30 year study period (1982-2011). It shows that, NARR represents a cooler winter and warmer summer and fall. A comparative plot of daily average historical and NARR temperature is plotted in Figure 3.12 for the year 2011..

Table 3.4: Statistics of Historical and NARR Temperature Data

Month	Historical Temperature (°C)			NARR Temperature (°C)		
	Min	Max	Average	Min	max	average
Jan	-29.8	12.7	-7.7	-31.4	5.5	-11.1
Feb	-31.1	12.0	-8.4	-31.3	8.6	-10.4
Mar	-28.4	9.6	-4.8	-24.3	12.3	-4.4
Apr	-15.9	13.1	0.5	-13.6	21.7	4.0
May	-5.1	16.6	5.1	0.4	27.1	12.7
Jun	-0.9	22.0	10.3	2.4	28.4	17.0
Jul	2.4	23.2	14.5	7.7	28.1	20.1
Aug	3.3	23.0	14.4	4.3	26.6	18.7
Sep	-1.3	23.7	10.5	3.0	24.4	13.0
Oct	-6.0	21.1	5.3	-5.8	20.5	5.1
Nov	-19.0	18.8	1.2	-16.6	14.5	-5.1
Dec	-24.5	13.7	-3.8	-24.7	7.0	-6.5

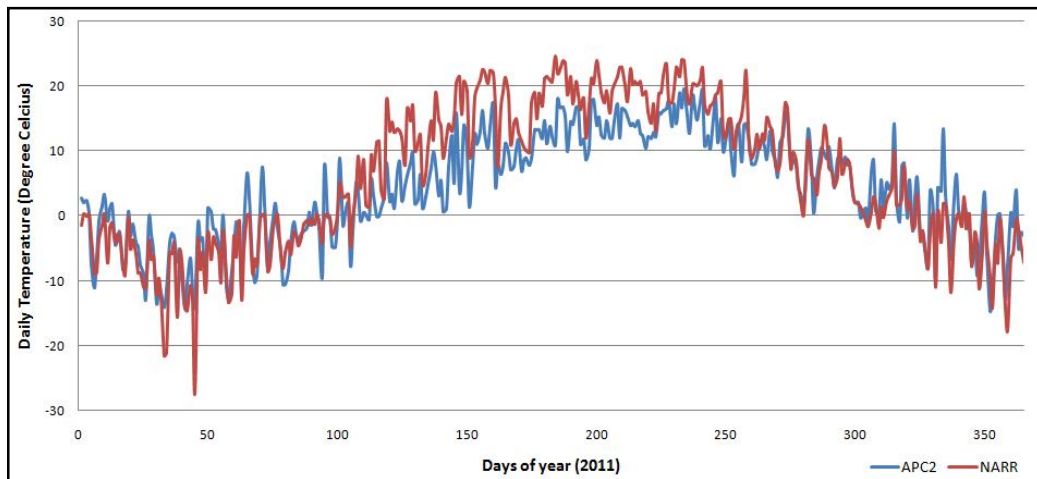


Figure 3.12: Daily Average Temperature in 2011

3.2.3 Climate Normals

Climate normals are the mean or total of monthly climate values for a given location over a specific period of time. Climate normals can be used to classify the climate of a particular area which helps in making decisions for a wide variety of purposes including basic habitability, agriculture, transportation and tourism. They are used as a reference for seasonal monitoring of temperature and precipitation, which can be used in climate studies. The World Meteorological Organization (WMO) recommends that countries prepare climate normals for the official 30-year normals periods ending in 1930, 1960 and 1990, for which the WMO World Climate Normals are published.

According to WMO, 30 years is sufficient to encapsulate the year to year variability. Environment Canada computes climate normals over a 30 year period of consecutive records, starting January 1st and ending December 31st. The normals are arithmetic means calculated for each month of the year from daily data with a limited number of allowable missing data. Normals can be averages (temperature) or totals (precipitation). For normals representing averages, a month is not used in calculation of normals if three consecutive days or a total of five days are missing from that month. This rule is called the “3 and 5 rule” established by the WMO.

For normals representing totals, an individual month can be used in normals calculation only if the month is 100 % complete. The average or total as appropriate for an element is first calculated for all individual months for all locations. Then the normals are calculated as the mean of each month from all the individual months in that period which fulfills the requirement of completeness described above.

Environment Canada updates its climate normals for as many locations and as many climatic characteristics as possible at the completion of each decade. Climate normals are calculated based on Canadian climate stations that have at least 15 years of data in a 30-year period.

In this study the climate normals used are computed for the period 1981 to 2010. Environment Canada has Climate Normals for different stations within the basin boundary. It was decided that normals for Deer Lake would be used in the study. The climate normals used in the study for WATFLOOD input are: (i) mxmn - Difference between daily maximum and minimum temperature (Degree Celsius), (ii) humid – average relative humidity (%) and (iii) press – average station pressure (kPa).

3.3 Calibration and Validation Data (Streamflow)

For model calibration and validation observed hydrometric data (streamflow) are used. The calibration is done based on an objective function which is calculated using the observed and simulated streamflow values. Streamflow data were collected from archived hydrometric data from HYDAT, of WSC. HYDAT is the archival database which contains all water information collected through the National Hydrometric Program. The information includes daily and monthly mean flow, water level and sediment concentration. Data are collected from 2500 active and 5500 discontinued hydrometric monitoring stations across Canada (<http://www.ec.gc.ca/rhc-wsc/default.asp?lang=En&n=EDA84EDA-1>)

Nine stream gauges were selected for the study within the basin boundary. Eight were used for calibration and one station (Indian Brook) was added later for validation

and further study. In this study, data were sought for the period of 1982 to 2011. Table 3.3 summarizes the gauges with their ID, location, area and period of data collected. Each data file contains daily streamflow values for a year. These data are then combined, formatted and written in the specific format required by WATFLOOD (_str.tb0). Figure 3.13 shows the location of the streamflow gauges.

Table 3.3: Streamflow Stations Information

Station	Station Name	Longitude	Latitude	Area (km ²)	Data Period
02YL001	Upper Humber River near Reidville	-57.36	49.24	2110	1982-2011
02YL003	Humber River at Humber Village Bridge	-57.76	48.98	7860	1982-2011
02YL008	Upper Humber River Above Black Brook	-57.29	49.62	471	1988-2011
02YK002	Lewaseechjeech Brook at Little Grand Lake	-57.93	48.62	470	1982-2011
02YK005	Sheffield Brook near Trans Canada Highway	-56.67	49.33	391	1982-2011
02YK007	Glide Brook Below Glide Lake	-57.37	49.11	112	1984-1997
02YK008	Boot Brook at Trans Canada Highway	-57.10	49.27	20	1985-2011
02YL004	South Brook at Pasadena	-57.61	49.01	58.5	1983-2011
02YM004	Indian Brook Diversion above Birchy Lake	-56.62	49.37	238	1990-2011

Reservoir release data were also collected from archived hydrometric data of WSC. For release data, two stream gauges on the reservoirs are selected. Table 3.4 summarizes the gauges with their ID, location and period of data collected. Each data file contains daily release data for a year. These data are then combined, formatted and written in the specific format required by WATFLOOD (_rel.tb0).

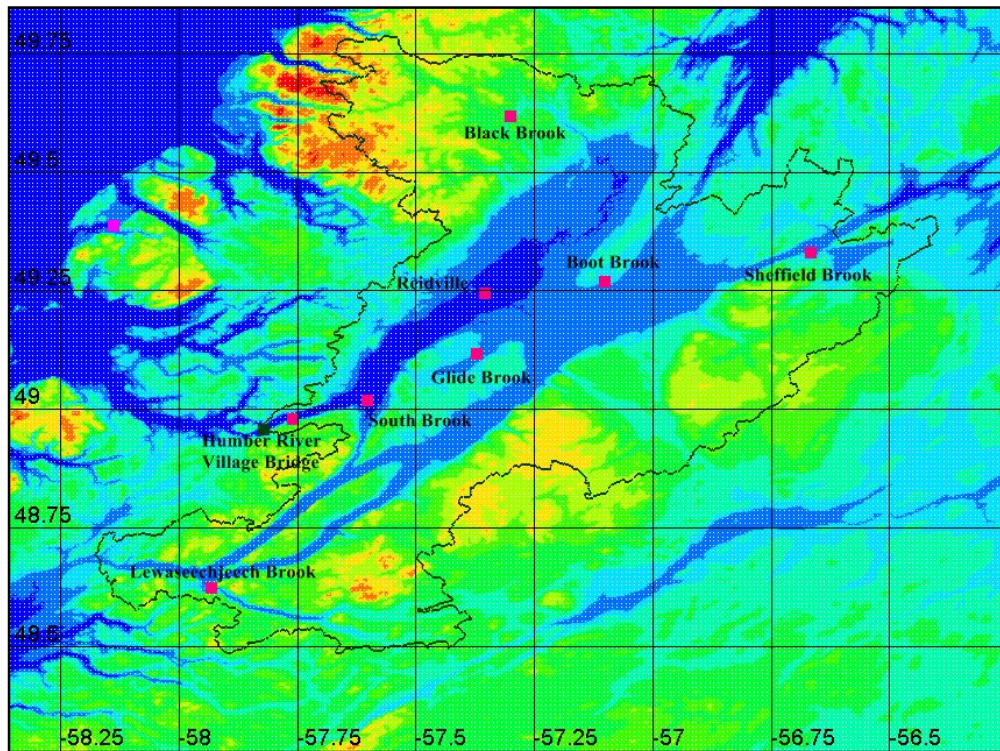


Figure 3.13: Stream Gauge Locations

Table 3.4: Reservoir Release Station Information

Station ID	Station Name	Longitude	Latitude	Data Period
02YK001	Humber River at Grand Lake Outlet	-57.42	49.16	1982-2010
02YL007	Hinds Brook at Hinds Brook Power House	-57.20	49.08	1982-2010

3.4 Water Level Data for Lake Routing

Reservoir Level data were collected from archived hydrometric data of WSC. For level data, two stream gauges on the reservoirs were selected. Figure 3.14 shows the locations of the stations for level and release data.

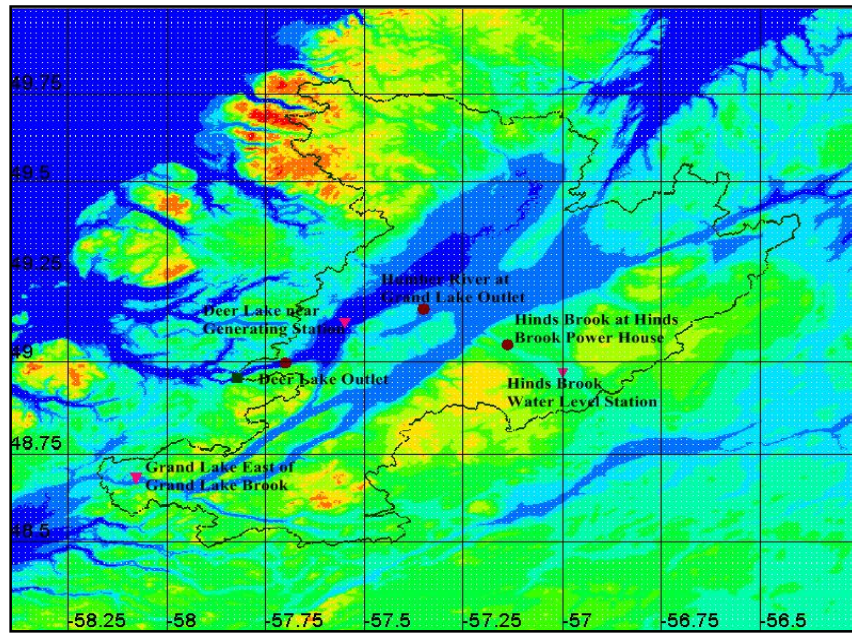


Figure 3.14: Station Locations for Reservoir Release and Level Data

Table 3.5 summarizes the gauges with their ID, locations and period of data collected. Data are downloaded in .CSV format. Each data file contains daily level data for a year. These data are then combined, formatted and written in the specific format (_lvl.tb0) required by WATFLOOD.

Table 3.5: Reservoir Level Station Information

Station ID	Station Name	Longitude	Latitude	Data Period
02YK010	Grand Lake east of Grand Lake Brook	-58.08	48.67	1988-2011
02YL007	Deer Lake near Generating Station	-57.44	49.17	1987-2011

In the model Deer Lake was defined as a lake. In WATFLOOD, water is routed through a lake using a user specified function, either a power function or a polynomial. In the current study the following function was used:

$$\text{Outflow} = b_1 * \text{Storage}^{b_2} \quad (3.3)$$

A power function was fitted to the storage discharge curve of Deer Lake to get the values of b_1 and b_2 . Storage was calculated from the following equation

$$\text{Storage} = \text{Area} * \text{Level} \quad (3.4)$$

The area of Deer Lake was used from the stat.txt file generated from the SPL run. From the basin setup, the area of Deer Lake was found to be 67.7 km^2 . For level data, the station used was Deer Lake near Pasadena (02YL006) and for discharge data, the station used was Humber River at Village Bridge (02YL003). For the storage discharge curve, data from 1989 was used. Figure 3.15 illustrates the rule curve for lake routing in Deer Lake. From this rule curve, values of b_1 and b_2 are obtained to be $2\text{E-}37$ and 4.564 respectively. These values are necessary parameters used in the streamflow files for lake routing.

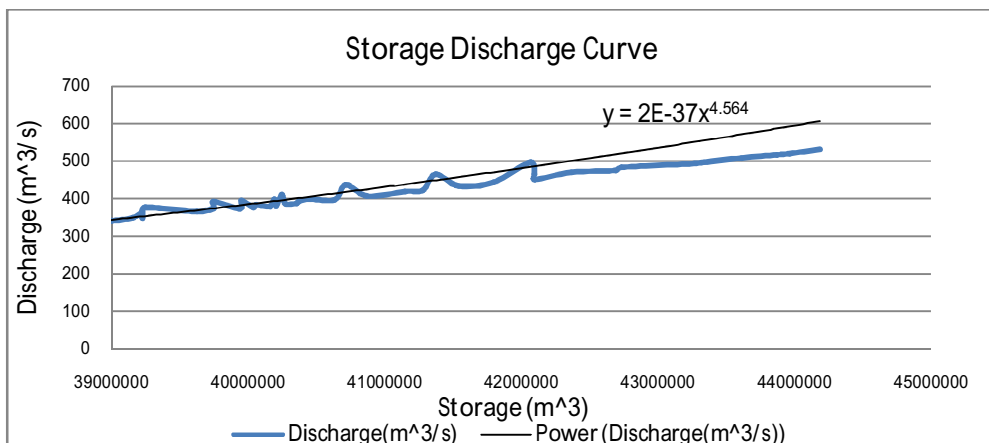


Figure 3.15: Storage Discharge Curve for Deer Lake

3.5 Bias Correction

The daily average plots of APC2 and NARR precipitation data for Deer Lake for the period 1982-2011 are illustrated in Figure 3.16. Figure 3.17 shows the monthly average observations and NARR temperature plots for the same time period.

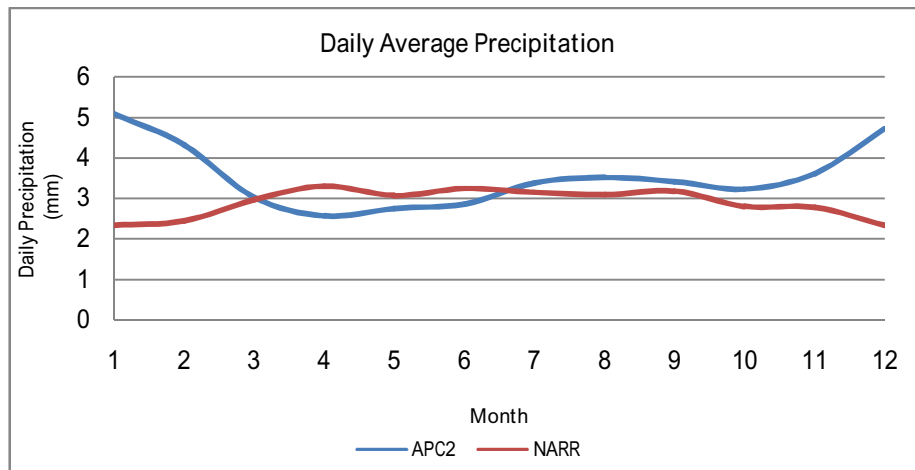


Figure 3.16: Monthly Average Precipitation Plot for Deer Lake

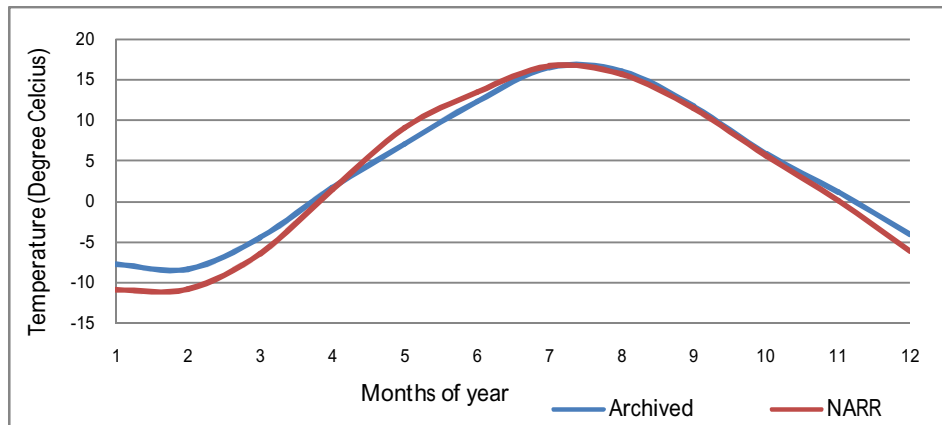


Figure 3.17: Monthly Average Temperature Plot for Deer Lake

Figure 3.16 and 3.17 show that, NARR data underestimated the APC2 for precipitation, but the differences in temperature were insignificant. The bias in the data necessitates a correction methodology to be applied to the NARR dataset.

At first, a simple linear correction was made to precipitation to check the improvement in the model if calibrated with corrected data based on APC2. The following equation was used to correct precipitation:

$$P^* = P(1 + \%error) \quad (3.5)$$

$$\%error = \frac{(P_{APC2} - P_{NARR})}{P_{NARR}} \quad (3.6)$$

where P^* is the bias corrected NARR precipitation,

P is the uncorrected NARR precipitation.

P_{APC2} and P_{NARR} are the monthly averages.

Monthly averages were used to reduce the sampling variability and to capture the seasonality. The model was re-calibrated with the corrected dataset but the results were not satisfactory. The linear scaling correction has the disadvantage of leaving standard deviation unchanged.

Leander and Buishand (2006) found a relatively simple nonlinear correction adjusting both the biases in the mean and coefficient of variation (CV), which performs better than the commonly used linear scaling correction to reproduce observed precipitation amounts. CV is equivalent to standard deviation (SD) divided by mean. This procedure was used in this study to correct the NARR precipitation data. Though it was suggested by Leander and Buishand (2006) that basin averages should be used if there are more than one climate station, the bias correction was made based on the APC2 data at

Deer Lake only. The reasons behind selecting Deer Lake for bias correction are: (i) its location, which is almost in the centre of the basin and (ii) its most up-to-date and complete data years.

3.5.1 Precipitation Bias Correction

Linear correction adjusts the mean precipitation, but leaves the CV unaffected, because both mean and SD are multiplied by the same factor. The applied correction methodology (Leander and Buishand, 2006) uses a power transformation which corrects both mean and CV. In this non linear correction, each daily precipitation amount is transformed to a corrected amount using Equation 3.5:

$$P^* = aP^b \quad (3.5)$$

where P^* is the bias corrected NARR precipitation,
 P is the uncorrected NARR precipitation,
 a is correction parameter corresponding to mean
 b is correction parameter corresponding to CV

To reduce the sampling variability the two factors a and b will be determined for each 5 day period of the year, including data from 30 days before and after this 5 day period, thus creating a 65 day window. All the data will be averaged over the calibration period (1982-2011). Terink *et al.* (2009) and Roberts *et al.* (2012) used the same method for bias correction of precipitation. First, b was calculated such that the CV of the corrected daily precipitation matched that of the APC2 data. This was done iteratively using a root-finding algorithm, the Secant method. Then the factor a (which depends on the value of b) was determined such that the mean of the corrected daily precipitation

matched that of the observed daily precipitation. Figure 3.18 gives all 73 values of ‘a’ and ‘b’ used here. Figure 3.19 compares the daily mean precipitation among APC2, uncorrected and non-linear bias corrected NARR datasets for Deer Lake.

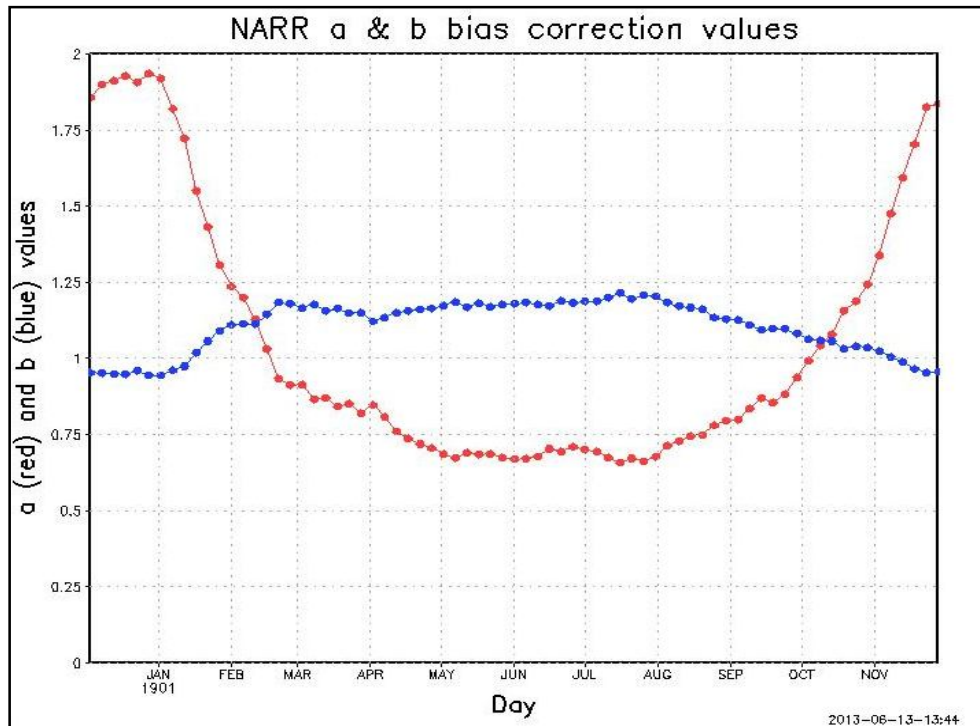


Figure 3.18: NARR ‘a’ and ‘b’ Bias Correction Values

Normalized precipitation bias is the bias as a percentage of the original precipitation value. Percentage Normalized bias for Precipitation can be calculated using equation 3.7.

$$B_N = \frac{(P^* - P)}{P} \quad 3.7$$

where P^* is corrected Precipitation

P is uncorrected Precipitation

A value of zero would indicate no bias. Figure 3.20 illustrates the Normalized bias for mean NARR precipitation.

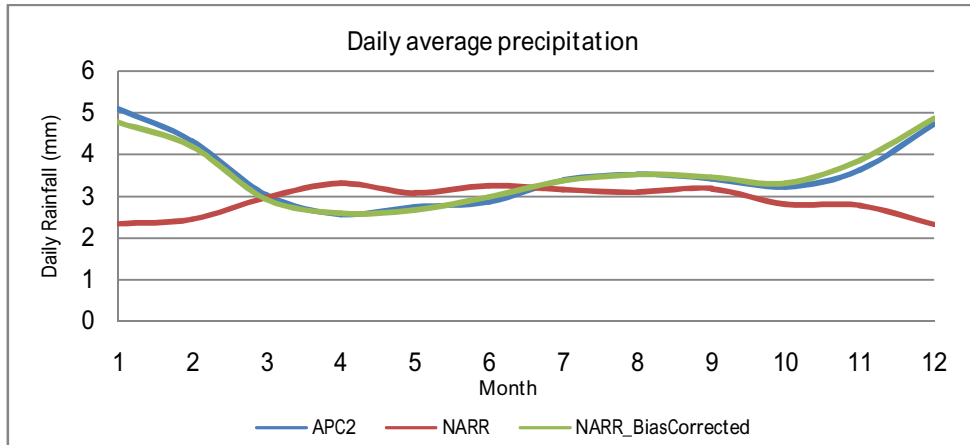


Figure 3.19: Daily Average Precipitation for Deer Lake (1982-201)

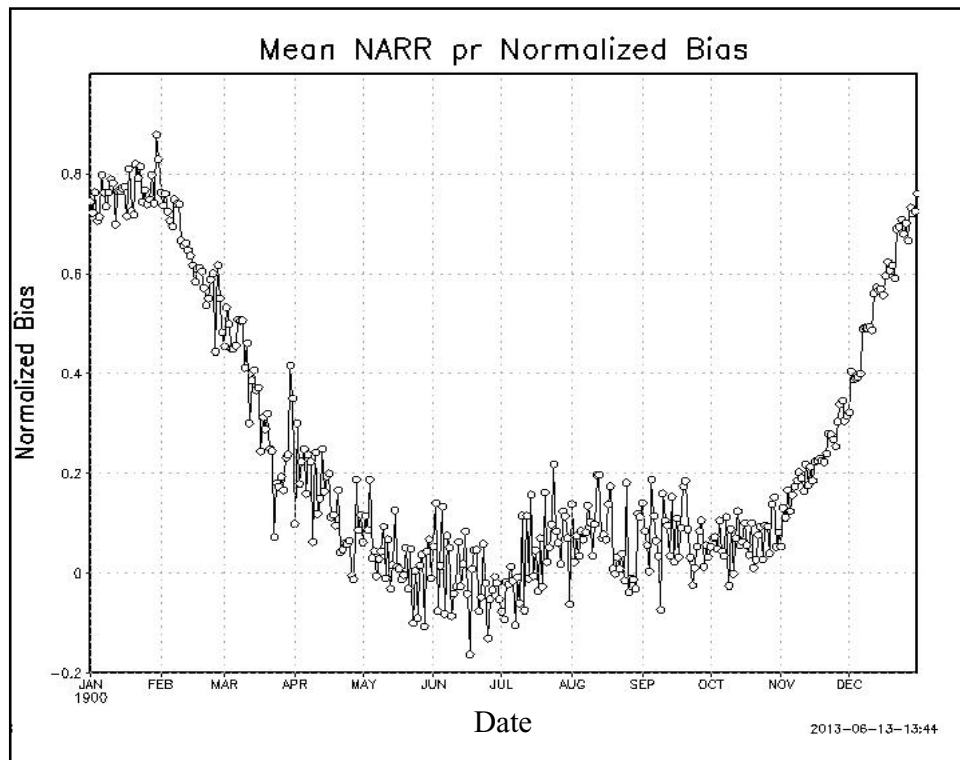


Figure 3.20: Mean NARR Precipitation Normalized Bias

3.5.2 Temperature Bias Correction

A different technique was used for correcting the temperature bias. The method is more straightforward than that of precipitation. It involves shifting and scaling to adjust the mean and variance (Leander and Buishand, 2006). The corrected temperature was obtained using equation 3.8:

$$T^* = \bar{T} + (T - \bar{T}) \frac{\sigma(T_{APC2})}{\sigma(T_{NARR})} + (\bar{T}_{APC2} - \bar{T}_{NARR}) \quad (3.8)$$

where T^* is the bias-corrected NARR temperature,

T is the uncorrected NARR temperature,

\bar{T} indicates 30-year average, and

σ is the standard deviation.

To reduce the sampling variability, the same 65 day window was used here. Terink *et al.* (2009) and Roberts *et al.* (2012) used the same method for bias correction of temperature.

Figure 3.21 compares the average temperature from historical climate data, uncorrected and bias corrected NARR datasets for Deer Lake. It shows that the corrected NARR temperature is higher in winter months compared to the observed temperature. Figure 3.23 illustrates the Normalized bias for mean NARR temperature.

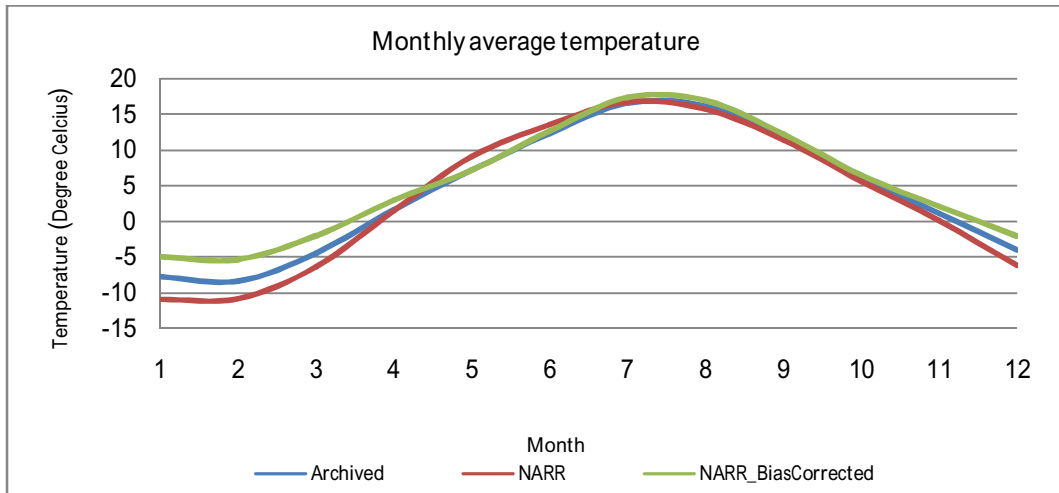


Figure 3.21: Monthly Average Temperature for Deer Lake (1982-2011)

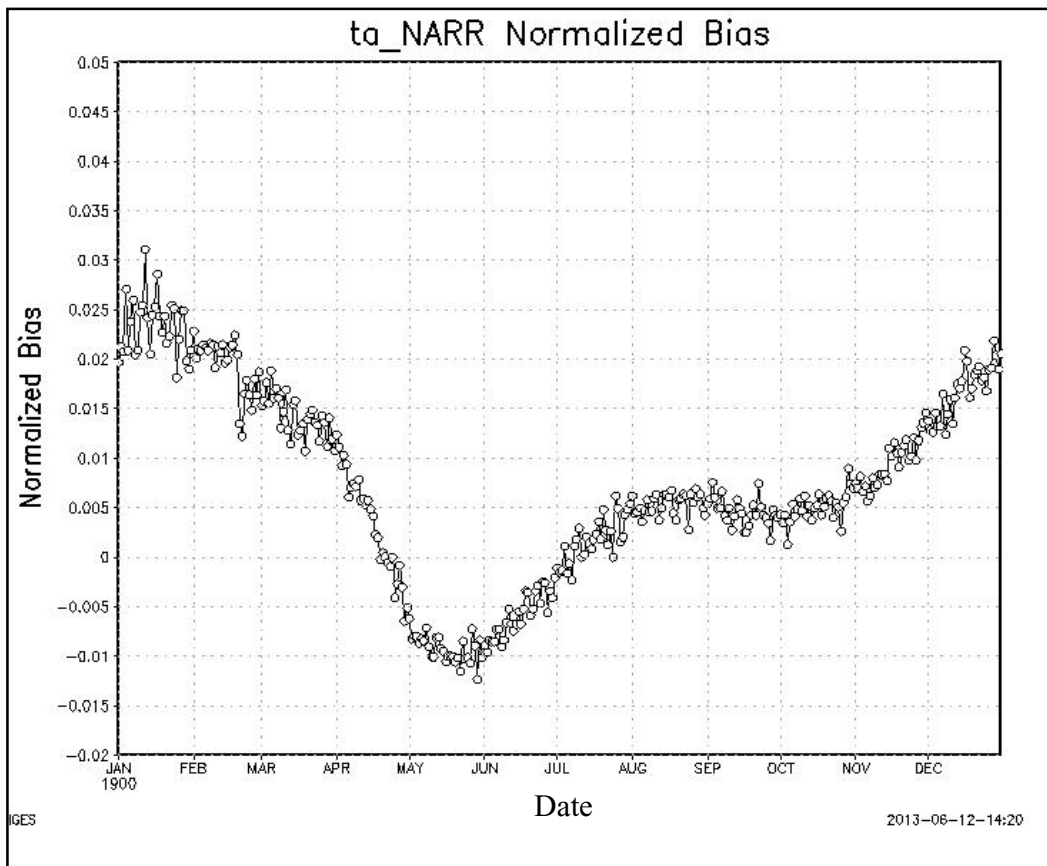


Figure 3.22: Mean NARR Temperature Normalized Bias

Chapter 4 Model Set up

WATFLOOD is a combination of a physically based routing model and a conceptual hydrological simulation model of a watershed. It models physical processes including interception, infiltration, evaporation, transpiration, snow accumulation and ablation, interflow, recharge, baseflow and overland, wetland and channel routing. It is operated in DOS using a set of FORTRAN programs. WATFLOOD can be used both for short-term flood forecasting and long term simulation for climate change studies. This chapter contains a description of the modeling approach and the mathematical equations used for the hydrological processes modeled in WATFLOOD. It also describes the WATFLOOD file structure, executables and complete set-up of the model for this study, including its calibration and validation procedure.

4.1 Modeling Approach

Distributed hydrological models do not require the averaging of watershed parameters, which may lead to inaccurate runoff estimates. The grid squares are divided into several land cover classes and each class has its own parameter set. Defining the smallest area that WATFLOOD can model depends on the resolution of available meteorological data and the size of the smallest watershed that has to be modeled.

WATFLOOD is based on grouped hydrological units. The pixels of land cover data are classified into a number of land cover classes and their ratios in the grids are determined. WATFLOOD combines all the pixels in one group for computation. The runoff from each hydrologically significant sub-group in each grid is calculated and

routed downstream in two steps: from overland flow to the channel system and from channel flow to the next grid. This approach is called grouped response unit (GRU). Figure 4.1 shows the GRU and runoff routing concept schematically (Donald, 1992). In this figure, A, B, C and D each represent a hydrologically significant group.

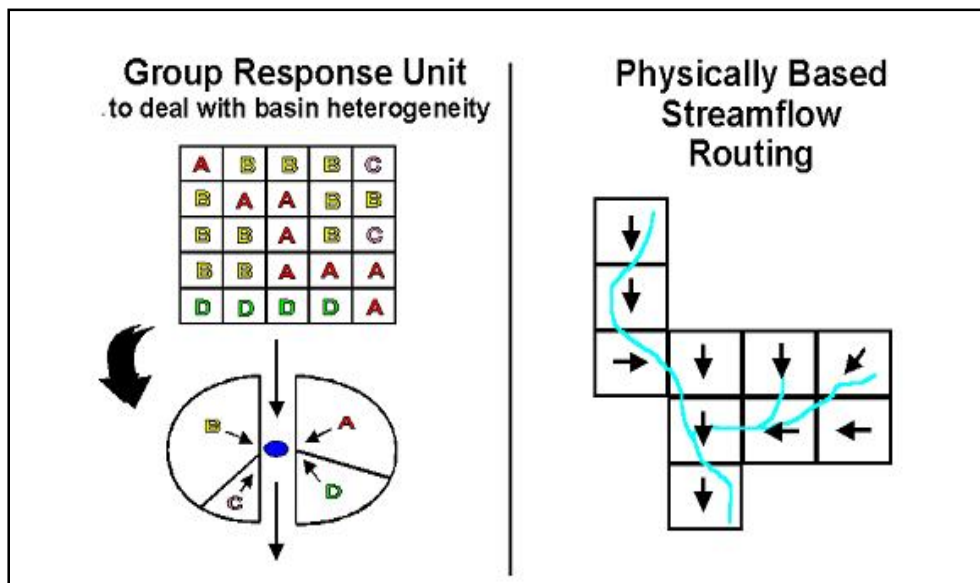


Figure 4.1: Grouped Response Unit and Runoff Routing Concept

4.2 Equations for Hydrological Processes

Using the grid data, the initial conditions and input data, WATFLOOD executes a series of internal calculations for determining the hydrological processes of the water cycle represented by mathematical equations. The results obtained are a distributed representation of output data. Figure 4.2 presents the major hydrological processes in the WATFLOOD model (Stadnyk, 2004).

Surface storage is calculated using equation 4.1. It is assumed that the limiting value of depression storage D_s is reached exponentially (Linsley *et al.*, 1994).

$$D_s = S_d (1 - e^{-kP}) \quad (4.1)$$

where D_s = depression storage,
 S_d = maximum depression storage
 k = constant for depression storage and
 P = accumulated rainfall excess.

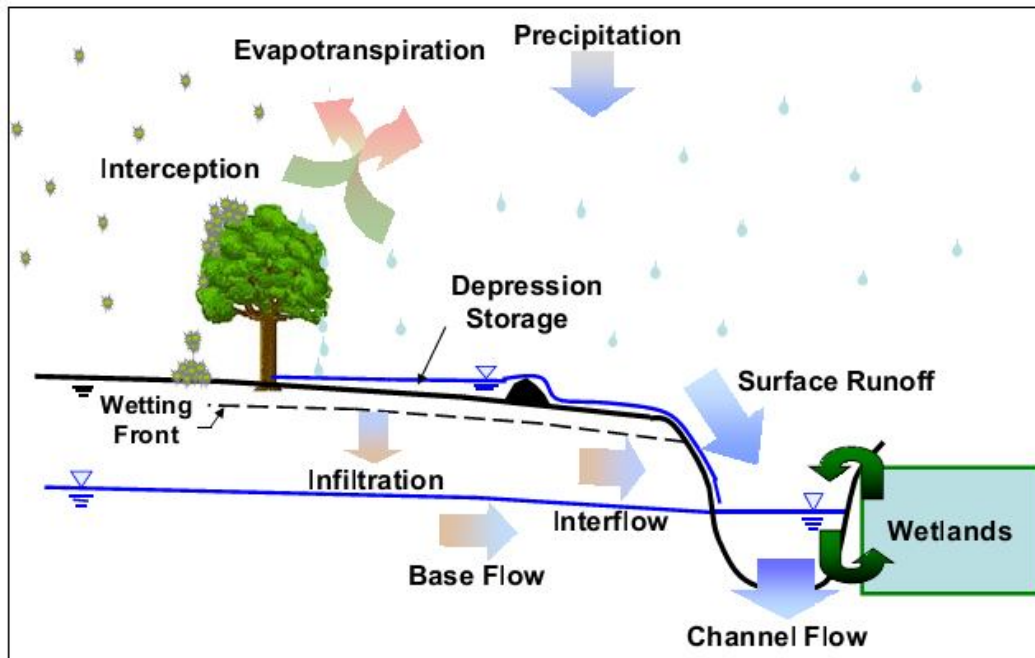


Figure 4.2: Major Hydrological Processes of WATFLOOD Model (Stadnyk, 2004)

Infiltration capacity is an important and highly variable quantity. Quantification of infiltration requires a great deal of attention. The Philip formula (Philip, 1954) is used to represent the important physical aspects of the infiltration process (Equation 4.2).

$$\frac{dF}{dt} = K \left[1 + \frac{(m-m_0) + (P^* + H)}{F} \right] \quad (4.2)$$

where F = total depth of infiltrated water (mm)
 t = time (hours)

K = hydraulic conductivity (mm/hour)

m = average moisture content of soil to the depth of wetting front

m_o = initial soil moisture content

P^* = capillary potential at the wetting front (mm)

D = depth of water on the soil surface.

Hargreaves equation (Hargreaves and Samani, 1982) is used to calculate the potential evapotranspiration (Equation 4.3). This equation is empirical in nature.

$$PET = 0.0075R_a * C_t * \delta_t^{1/2} * T_{avg} \quad (4.3)$$

where

PET = potential evapotranspiration rate (mm/day)

R_a = total incoming solar radiation (mm)

C_t = temperature reduction coefficient

δ_t = difference between mean monthly maximum and mean monthly minimum temperature

T_{avg} = Mean temperature ($^{\circ}F$)

Actual evapotranspiration is calculated from PET by applying three coefficients, (i) Upper Zone Storage Indicator (UZSI), (ii) soil temperature coefficient (FPET2), and (iii) forest vegetation coefficient (FTALL).

Upper zone storage (UZS) after percolating downward or exfiltrating to nearby water courses is called interflow. It is represented by a simple storage-discharge relation (Equation 4.4) (Kouwen, 2011).

$$DUZ = REC * (UZS-RETN) * S_i \quad (4.4)$$

where

DUZ = depth of upper zone storage released as interflow (mm),

REC = a dimensionless coefficient found by optimization,

$RETN$ = retention

S_i = land surface slope

Surface runoff (also known as overland flow) is calculated based on the Manning formula and represented by Equation 4.5 (Kouwen, 2011).

$$Q_r = (D_1 - D_s)^{1.67} * S_i^{0.5} * A * R_3 \quad (4.5)$$

where Q_r = channel inflow (m^3/s)
 D_1 = surface storage (mm)
 D_s = depression storage capacity (mm)
 A = the area of the basin (m^2)
 R_3 = combined channel roughness and channel length parameter.

Base flow is initially calculated from a measured hydrograph at the basin outlet.

Total runoff is obtained by adding the surface runoff, the interflow and the base flow.

A simple storage routing relation is used to account for the routing of water through the channel system. This relation (Equation 4.6) is based on the Continuity equation (Kouwen, 2011).

$$\frac{I_1 + I_2}{2} - \frac{O_1 + O_2}{2} = \frac{S_1 + S_2}{\Delta t} \quad (4.6)$$

where $I_{1,2}$ = inflow to the reach (m^3/s),
 $O_{1,2}$ = outflow from reach (m^3/s),
 $S_{1,2}$ = storage in reach (m^3),
 Δt = time step of routing (s)
 Subscript 1 and 2 indicate the beginning and end of a time step.

4.3 WATFLOOD File Structure and Executables

WATFLOOD is operated in DOS mode by the WINDOWS operating system. The entire system is installed under the \SPL directory which has to be in the root directory. The following tree structure shows the file structure of WATFLOOD maintained in this study:

C:\SPL-

|--- All Executables

|--- HUMBER - some batch files

 |--- BASIN- watershed files, parameter files

 |--- DDS – DDS working directory

 |--- EVENT - event files

 |--- LEVEL – reservoir level files

 |--- MOIST –initial soil moisture files

 |--- RADCL - adjusted radar or rain gauge files

 |--- RAING – rain gauge data files

 |--- RESL – reservoir release files

 |--- RESULTS - all model output

 |--- RESRL - reservoir release files

 |--- SNOW1 - snow course and climate data

 |--- STRFW - streamflow or river stage files

 |--- TEMPG - point temperature files

 |--- TEMPR - gridded temperature files

WATFLOOD is comprised of a set of executables written in FORTRAN. The following is a list of WATFLOOD executables used in the study:

- BSN -> Creates shd.r2c from Map file to be used by SPL
- MAKE_EVT -> Creates events for WATFLOOD simulation
- RAGMET -> Converts gauge rain data (rag.tb0) to gridded rain data (met.r2c)
- TMP -> Converts gauge temperature data (tag.tb0) to gridded temperature data (tem.r2c)
- SNW -> Converts gauge snow data (crs.pt2) to gridded snow data (swe.r2c)

- MOIST-> Converts gauge soil moisture data (psm.pt2) to gridded soil moisture data (gsm.r2c)
- SPLX-> Main model compiled for maximum speed
- SPLD -> Main model compiled for maximum debugging

The following files are the essential files required for this study before WATFLOOD/SPLX can be run.

Humber\BASIN\Humber_shd.r2c
 Humber\BASIN\Humber_par.csv
 Humber\BASIN\Humber.pdl
 Humber\BASIN\Humber.SDC
 Humber\BASIN\monthly_climate_normals.txt
 Humber\EVENT\event.evt
 Humber\RADCL_met.r2c
 Humber\SNOW1_swe.r2c
 Humber\TEMPR_tem.r2c
 Humber\STRFW_str.tb0

Additional data files for the reservoir and lake are:

Humber\LEVEL_lvl.tb0
 Humber\RESRL_rel.tb0

4.4 Event Files

The event file contains a list of all the data files, related to the specific event, required for the SPLX run. Other than BSN.EXE, all the WATFLOOD executables refer to this event file to determine which files are active for a particular job. An event file is created by running MAKE_EVT.EXE in the working directory. In the present study, lengths of events are selected to be either one month or one year. All the years from 1982 to 2011 have yearly events (19820101.evt, 19830101.evt, etc.). As it is suggested by Kouwen (2011) to start the simulation from October, monthly events for the month of

October, November and December are created for three different years (1982, 1988, 1997), spanning the simulation period. While creating event files, initial soil moisture was set to 0.25 and wetland coupling was used. The first event was copied to a file named event.evt. Successive events were then sequentially linked at the end of this file to run a continuous simulation. The flags in the event files control whether a process will take place (y) or not (n).

4.5 Watershed Delineation

Green Kenue is an advanced data preparation, analysis and visualization tool that creates a watershed file from DEM and land use data. The Watershed file is vital for WATFLOOD as it contains all the necessary geographical and geophysical data. Topography and land use are the most important physiographic features that affect the outcome of the model (Bingeman, 2006).

In Green Kenue, a watershed object is created from the SRTM DEM (discussed in section 3.1.1). There are two algorithms for watershed delineation: AT_Search and the Depressionless DEM algorithm. AT_Search algorithm is a tree search algorithm. It does not modify the DEM and as such allows for more genuine channel delineation. The algorithm is iterative and does not have to deal with recursion and the subsequent memory problems which occur with large DEMs. The depressionless DEM algorithm is implemented recursively, which may lead to memory problems with large DEMs.

For the purpose of delineating the watershed, in this study the AT_Search algorithm was selected. The “Predefined Channels” option is used to include the information about the actual paths of existing channels while creating the channel

network and basin boundary. The channel network was then checked to match the predefined channels.

In addition to the flow paths, the channel object can also display watershed outlet nodes. A basin outlet is selected, from which the basin is partially defined. The basin boundary is an isoline that completes the watershed definition. It contains all the nodes of the DEM that drain towards the selected basin outlet. The basin boundary is checked to match with NHN work units. A basin network is then extracted using the watershed tool and checked to match the existing channel network.

Figure 4.3 shows the locations of the predefined channels (the polygons in black boundary) and Figure 4.4 shows the basin boundary and basin network after watershed delineation.

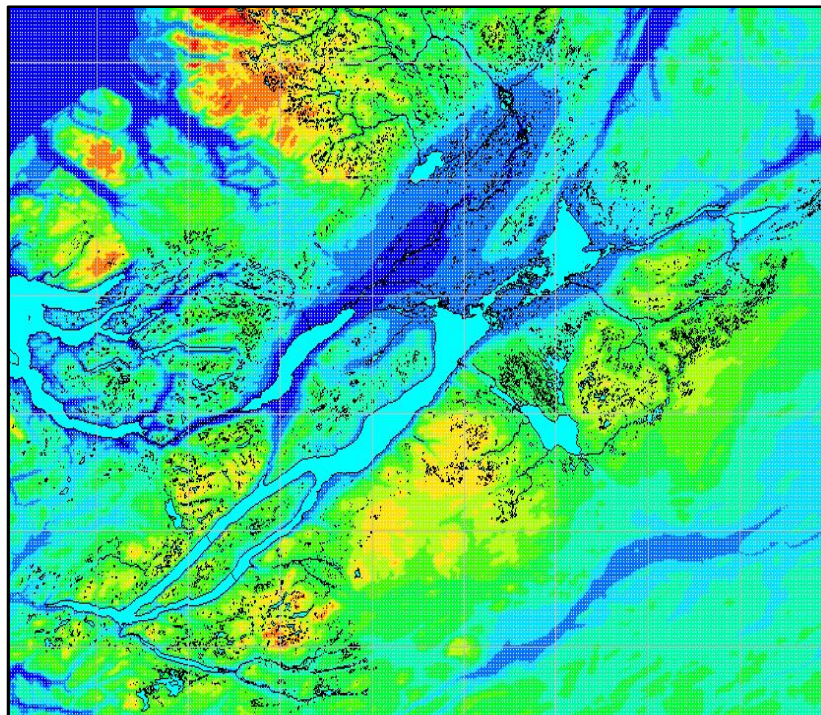


Figure 4.3: DEM and Predefined Channels

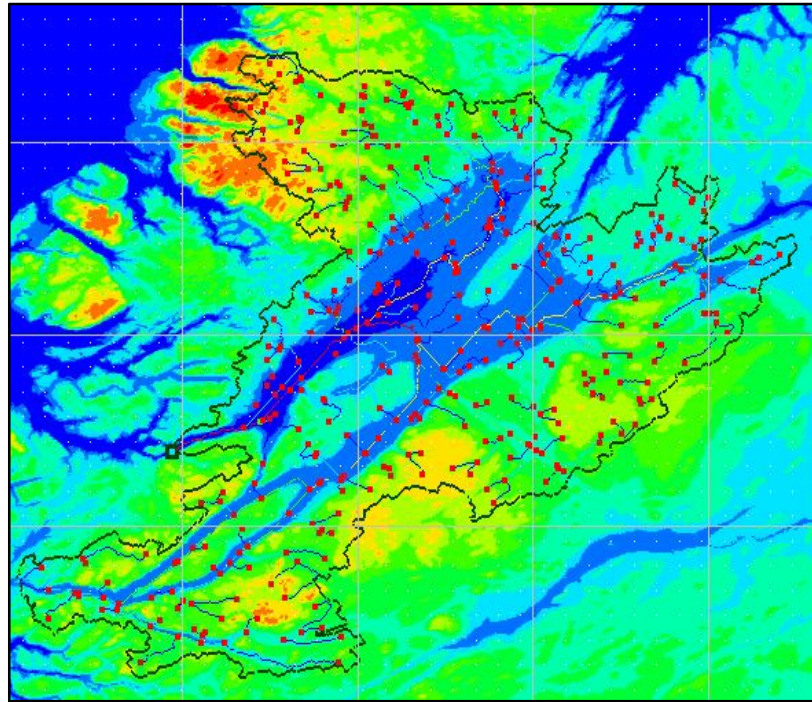


Figure 4.4: Basin Boundary and Basin Network

4.6 Land Use Map

WATFLOOD requires land use data to be incorporated with the Map File. Land use data attributes cannot be calculated from the DEM so GreenKenue provides tools to obtain land use information. The number of land uses described in the map file should correspond to the number described in the parameter file. Land use data can be added to the map file using closed polygons or using GeoTIFFs. In this study land use data was obtained from GeoTIFFs.

Land use classes are directly generated from one or more classified GeoTIFF. The images are processed so that only required land use classes exist. In this study it was decided to map land use data from a single GeoTIFF image. For this, the shape files of waterbodies, wetlands and vegetation are combined using ArcGIS. First they were

converted to raster data and then from raster to the GeoTIFF image. Figure 4.5 shows the land cover map used for mapping land use data.

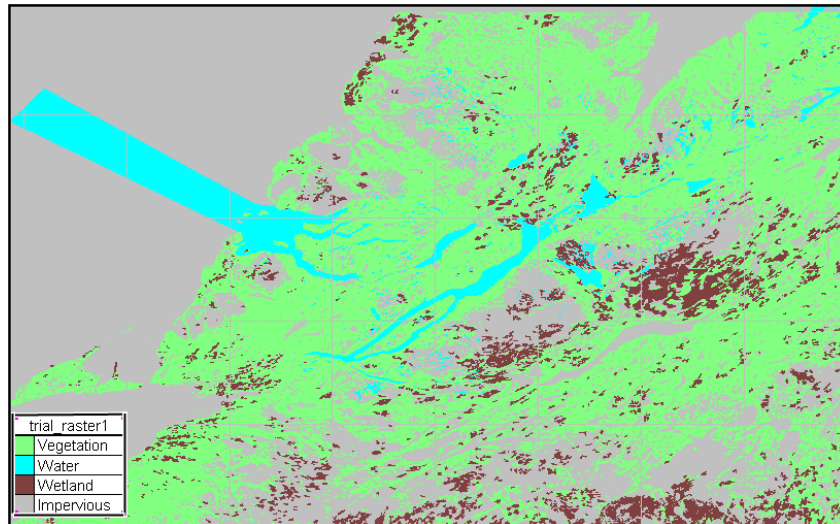


Figure 4.5: Land Use Map Created Using ArcGIS

4.7 Map File Generation

The map file is a required input file for WATFLOOD. The map object uses information in the watershed object to calculate most of the data attributes for the grid cells. Land use data attributes are calculated using other tools (here mapping with GeoTIFF). The map file is created in GreenKenue and specifications can be set manually or automatically. Setting the specifications manually requires that a watershed be associated with the map file. The specifications are set as specified in Table 4.1.

Table 4.1: Map File Specifications

	X	Y
Origin	-58.4	48.3923
Count	34	36
Delta	0.0625	0.041675

Delta is the distance between two adjacent nodes. It was selected such that the grid size of the map file is roughly around 5 km. Count is the number of grid points along the row and column. After setting the specification, the entire watershed data contained within the WATFLOOD specification were collected and applied to the WATFLOOD Map object. The “Calculate FRAC from Contributing Areas” option was enabled so that the effective area of each cell was adjusted based on the amount of inflow from neighbouring cells. The WATFLOOD map follows the WATFLOOD grid rules below:

- The watershed outlet is a square outside the watershed
- There is a border of blank grid squares around the sides of the watershed boundary
- The grid size is below 99 cells by 99 cells.

It was also ensured that the GeoTIFF used for mapping land use data covers the full spatial extent of the basin. The GeoTIFF file was examined and a list of land use classes was created in the Map file. A pixel mask was created for each cell. The numbers of pixels of each land use class falling within the cell were counted and the integer percentages were assigned to map land use classes. Then, the land use classes were rearranged in the specific order required by WATFLOOD to operate (Vegetation, Wetland, Water and Impervious).

The WATFLOOD Map data attribute “Contour Density” (IROUGH) is an indication of the number of contours in a cell. The default contour elevation interval is 1. The value of contour crossing in a cell should be between 1 and 99. Therefore, the contour elevation interval was increased to ensure that IROUGH was appropriately described.

Another map attribute, Routing Reach Number (IREACH) has a default value of zero assigned to all cells. Values greater than zero, will produce channel inflows at those cells. It is important to specify IREACH for lakes and reservoirs. In the Map file, reach numbers were given to the grids which are all or part of Deer Lake, Grand Lake and Hinds Lake except if a streamflow station is located near the lake within the grid or if the grid is part of a gauged watershed. “The program will not produce a hydrograph if a station is in a lake grid and the watershed area will be incorrect if the grid is part of the lake.” (Kouwen, 2011)

Drainage direction (S) is another important data attribute to check. This value indicates the direction of flow out of the cell. Possible directions are North, South, East, West, North East, South East, North West, South West and N/A (Not applicable). N/A is applied only to the cell containing the watershed outlet. The drainage direction is displayed by an arrow when the “Directions Visible” check box is checked and also by selecting the attribute as the current attribute.

It is very important to check and ensure that the drainage directions are following the existing channels within the boundary and that no direction is indicating flow towards outside the basin boundary. When necessary, the drainage directions were edited manually, ensuring that flow direction was from higher to lower elevation. After checking and adjusting the data attributes, the map file was saved in .map format. Figure 4.6 shows the mapfile with drainage direction.

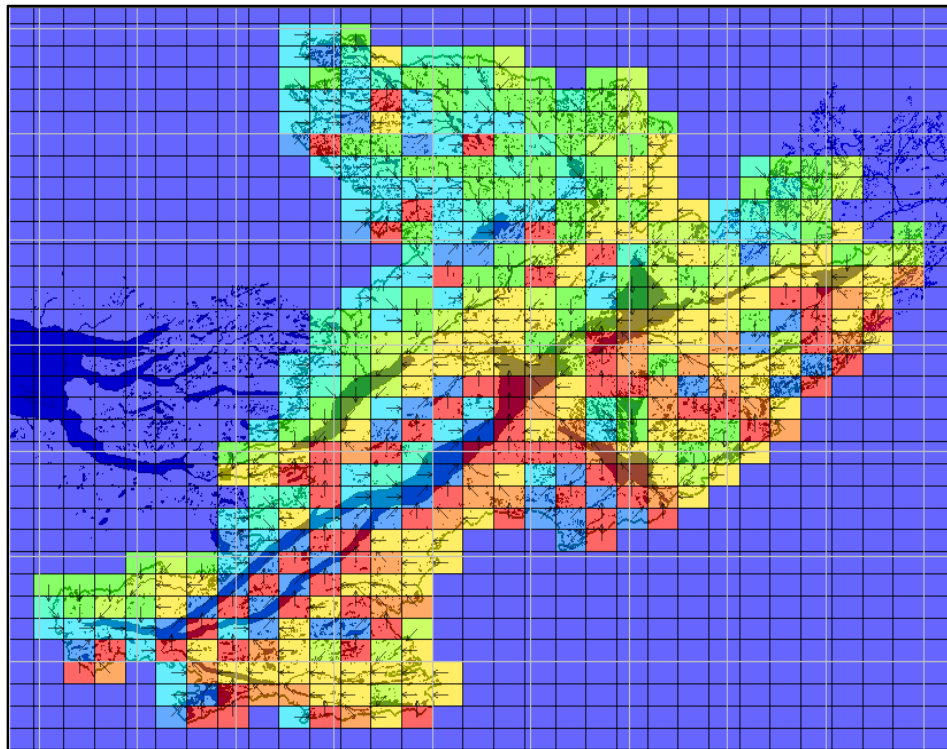


Figure 4.6: WATFLOOD Map File with Visible Drainage Direction

4.8 Basin file/ SHD file

Watershed data is read by SPLX from the Humber_shd.r2c file. This file is created by running BSN.EXE, which reads information from map files created by GreenKenue. After running the executable, a file named new_shd.r2c was created which was then renamed to Humber_shd.r2c. While creating the file, negative slopes were calculated due to the wrong drainage direction. This problem is fixed in GreenKenue by loading the Humber.map file with drainage directions and elevation shown, and importing Humber_shd.r2c to show the negative slopes coloured to a specific colour. Grids with black dots in Figure 4.7 show the negative slopes. As such, the grids with negative slopes were easily identified. Then data attributes (Elevation and Drainage Direction) were

checked and edited in the Map file. BSN.EXE was run again and a new Humber_shd.r2c was created and checked for negative slopes again.

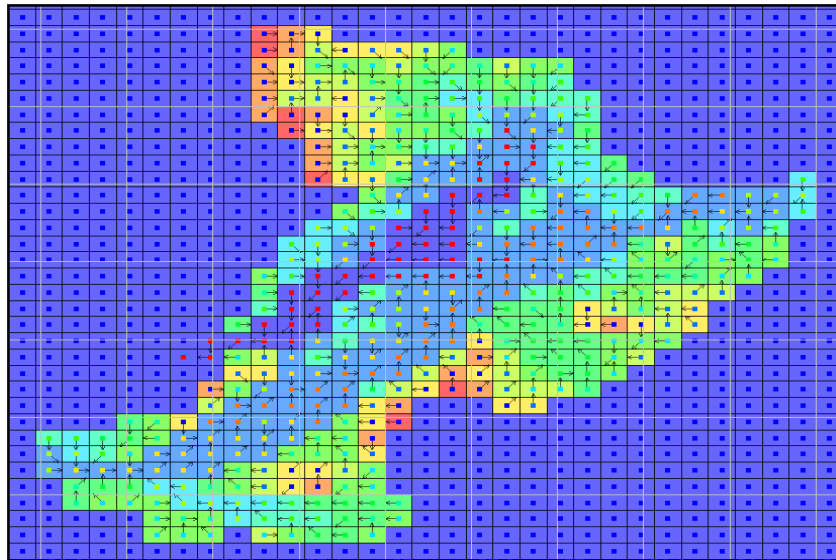


Figure 4.7: Checking Negative Slopes with Humber_shd.r2c and Humber.map File

4.9 Map File Correction

After running all the executables and preparing gridded datasets for WATFLOOD, SPLX.EXE was run. The file Humber\Basin\flow_station_info.txt was created with the stream gauge station name, y and x coordinates and the published drainage area in km². Upon reading this file SPLX created a file called area_check.xyz in the working directory. This file writes the simulated “Drainage Area” (DA) and percentage difference from the published areas. Using this file the drainage areas can be checked easily for any run. To make the modeled drainage areas equal to the published drainage area, the ‘FRAC’ was adjusted with neighbouring grids. FRAC is the percentage of the area of a grid cell within the watershed boundary that flows in the indicated

drainage direction. Each time FRAC was adjusted, BSN.EXE and SPLX.EXE were run and areas were checked. It is a trial and error process and adjustments are made until the areas found are satisfactory.

Figure 4.8 shows that except for one gauge (Indian Brook) all the other gauges have DA within 1% error. This is because Indian Brook was added later for validation. When all the adjustments were made and model calibrated, Indian Brook station was not used.

longitude	latitude	#	station	actual	model	% difference
-57.360	49.240	1	Reidville	2110.	2113.	0. %
-57.760	48.980	2	Humbervilleg	7860.	7823.	0. %
-57.290	49.610	3	Blackbrook	471.	471.	0. %
-57.930	48.620	4	LewaseechB	470.	472.	0. %
-56.670	49.330	5	SheffieldB	391.	393.	0. %
-57.370	49.110	6	GlideBrook	112.	112.	0. %
-57.100	49.270	7	BootBrook	20.	20.	0. %
-57.610	49.010	8	SouthBrPasad	58.	58.	-1. %
-56.620	49.370	9	IndianBrook	238.	223.	-6. %

Figure 4.8: Matching DA after FRAC Adjustment

While delineating the basin, Green Kenue excluded some of the lakes at the north-eastern side of the basin due to the lower precision of DEM. This included Gillard Lake, another large lake upstream of it (Figure 4.9), and also some portion of Hinds Lake. To overcome this problem, a new artificial channel was created in Green Kenue so that it connects the channel network within the boundary with the water bodies outside the boundary. This artificial channel was then used as a predefined channel. As such, the AT_Search algorithm was able to create the actual boundary including those water bodies. Figure 4.10 shows the joining of the channel networks over Hinds Lake to the channel network near the power house.

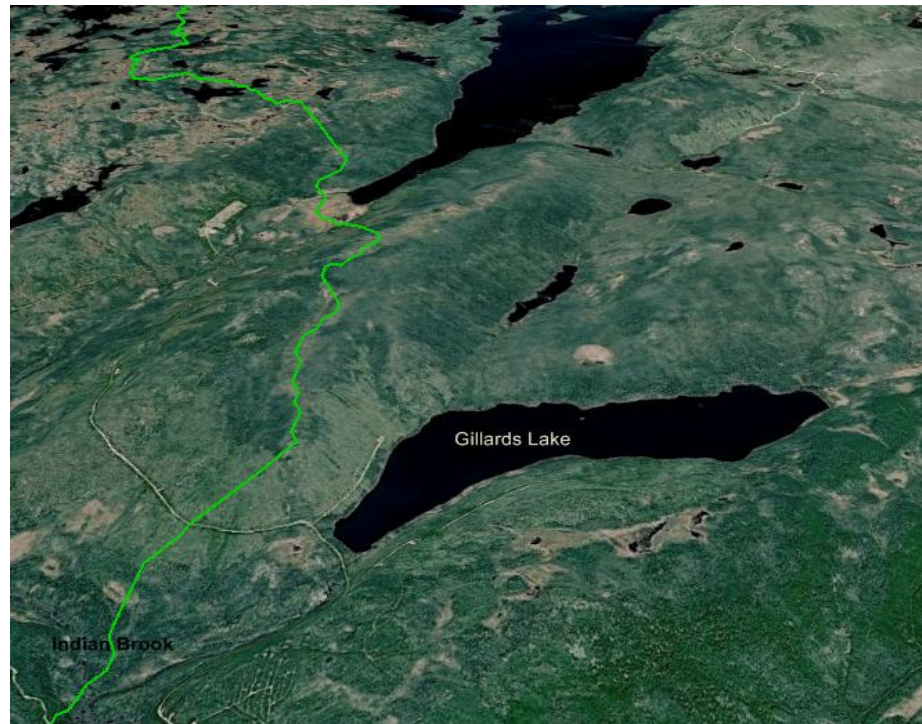


Figure 4.9: Watershed Delineation Errors near Indian Brook Diversion (Google Earth, 2013)

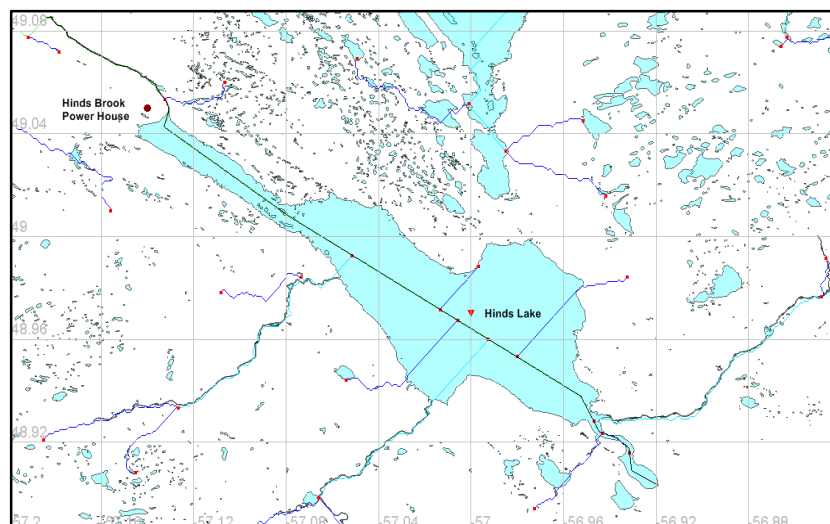
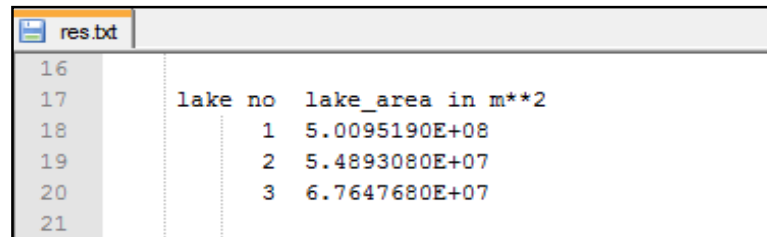


Figure 4.10: Channel Network Connections for Watershed Delineation

After adjusting the basin boundary, the areas of the lakes were checked to match the published lake areas. Figure 4.11 shows the areas of the lakes calculated by

WATFLOOD and written into the res.txt file in the RESULT folder. The areas shown here are areas of Grand Lake, Hinds Lake and Deer Lake respectively. These areas match closely with the actual lake areas.



The image shows a screenshot of a text editor window titled 'res.txt'. The window contains the following text:

```

16
17     lake no  lake_area in m**2
18         1  5.0095190E+08
19         2  5.4893080E+07
20         3  6.7647680E+07
21

```

Figure 4.11: Lake Areas Generated in WATFLOOD

4.10 Model Calibration and Validation

After obtaining a satisfactory model set-up, the model was calibrated with three different sets of data: (i) APC2 precipitation data and historical temperature data, (ii) uncorrected NARR precipitation and temperature data and (iii) CaPA precipitation and historical temperature data. October 1997 to December 2002 was selected as the calibration period for the model with APC2 and NARR precipitation as forcing data. January 2002 to December 2006 was the calibration period with CaPA as forcing data. The difference in the calibration period is due to the difference in the available data period. Eight stream gauge locations (all stream gauge locations except Indian Brook) were chosen for streamflow simulation. Section 3.3 contains the details of the stations including their location, drainage area and available data period. Indian Brook was not included in the calibration process.

The simulated results were compared with the observed streamflow at those eight gauge locations by using the Nash-Sutcliffe objective function. The Nash-Sutcliffe

coefficient (N_r) is a measure of statistical association, which indicates a percentage of the observed variance that is explained by the predicted data (MacLean, 2005). The representation of this statistical measure is given in Equation 4.7. N_r is commonly used in evaluating the performance of a model.

$$N_r = 1 - \frac{\sum_{i=1}^N (S_i - O_i)^2}{\sum_{i=1}^N (O_i - O_i^*)^2} \quad (4.7)$$

where S_i = Simulated streamflow (m^3/s),
 O_i = Observed streamflow (m^3/s),
 O_i^* = Average measured streamflow (m^3/s)
 N = Total number of values within the period of analysis.

The second term in Equation 4.7 represents the ratio between the mean square error and the variance of the observed data. N_r values can range from $-\infty$ to 1. $N_r = 0$ means that the model output is as accurate as the mean of the observed data. $N_r = 1$ corresponds to a perfect match of the modeled streamflow to the observed ones. $N_r < 0$ means the observed mean is a better predictor than the model.

The model was calibrated with three different sets of data and as a result three different parameter sets were found. Appendix A contains these calibrated parameter sets. The results of the calibration in terms of Nash-Sutcliffe and the simulated streamflow plots are given in Chapter 5 (Section 5.3).

There are two optimization routines available in WATFLOOD: (i) Pattern Search (PS) and (ii) Dynamically Dimensioned Search (DDS). PS incrementally changes the parameter values while DDS performs a random search of the parameter set. In this study the DDS optimization routine was performed, but as it is hard to get good results from

DDS, it was not possible to get a satisfactory result. Therefore, optimization was done manually by trying different values of parameters.

In this study, five land cover classes (vegetation, wetland, couples wetland, water and impervious) and three river classes were used. Optimized parameters fall into four categories: (i) global parameters, (ii) river and basin parameters, (iii) hydrological parameters and (iv) snowmelt parameters. These land cover classes are used to group parameters.

At first the river roughness parameter ($r2n$) was optimized so that the peaks of the computed hydrographs coincide with the peaks of the observed hydrographs. The base temperature ($tbase$) and melt factor (mf) showed a significant effect on the timing of the spring hydrograph and the rate of melt. These two parameters were set next. The base temperature affects the initial rise of the hydrograph while the melt factor has more effect on the peak flow.

The lower zone function (flz) and lower zone coefficient (pwr) were adjusted next. They showed a great effect on the recession limb of hydrographs and peak flow. flz controls the gradual depletion of baseflow between precipitation events. pwr controls the curvature of the recession limbs of the hydrographs (Carlaw, 2000).

As the study used couple wetland (another class coupling water and wetland), the wetland conductivity ($kcond$) and porosity ($theta$) were adjusted. The sublimation factor ($sublm_factor$) was adjusted to get the right amount of water in the melt hydrograph. $temp3$ (a coefficient) was adjusted to get the right amount of melt runoff in summer and fall.

The evapotranspiration parameters f_{pet} (Interception coefficient/evapotranspiration reduction coefficient) and f_{tall} (reduction in Potential evapotranspiration in tall vegetation) were adjusted next. Based on the type of land cover, precipitation and modeled runoff, these values were increased or decreased to match the observed hydrograph.

Other parameters adjusted were rec (interflow coefficient), ak_2 (recharge coefficient for bare ground), $retn$ (upper zone retention) and ak (infiltration coefficient for bare ground). All these parameters mentioned above are adjusted based on the observed fit of plotted hydrographs and the value of the objective function (N_r). After manual adjustments of the above parameters, the DDS optimization routine was run to fine tune the parameters. However, no better result was found with DDS. Therefore, the parameters found by manual fitting were used for model validation.

With APC2 and NARR precipitation data, WATFLOOD was validated with data for the period of January 2003 to December 2007. With CaPA, the validation period was January 2007 to December 2009. The difference in validation period is due to the difference in the available data period. The validation simulation gave similar results to the calibration simulations. The results found from the validation run are provided in Chapter 5 (Section 5.4). The streamflow station at Indian Brook was added to the validation simulation as it was not included in the calibration process. The N_r obtained for Indian Brook was 0.51, 0.34 and 0.36 with APC2, NARR and CaPA respectively, which was satisfactory. Figure 4.12 shows the streamflow plot with APC2 at Indian Brook for the validation period. Table 4.2 provides the optimized parameters for the model with

APC2, NARR and CaPA precipitation data. Total parameter sets are provided in Appendix A.

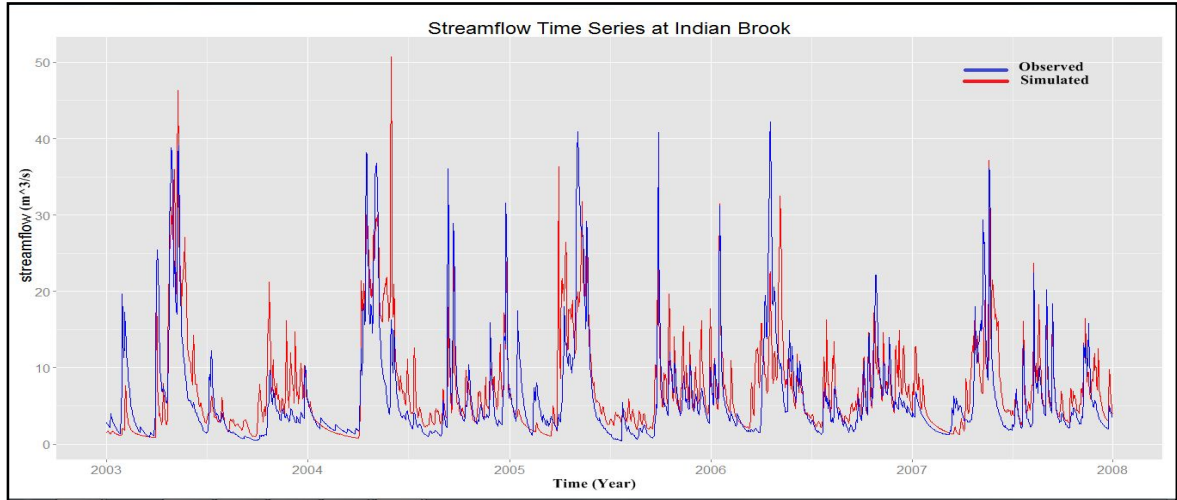


Figure 4.12: Streamflow Simulations at Indian Brook for Validation Period

Table 4.2: Optimized Parameter Sets

Parameter	APC2	NARR	CaPA
r2n	0.4, 0.04, 0.028	0.4, 0.04, 0.028	0.4, 0.04, 0.028
kcond	0.7, 0.2, 0.7	0.7, 0.2, 0.7	0.7, 0.2, 0.7
theta	0.263, 0.263, 0.263	0.263, 0.263, 0.263	0.263, 0.263, 0.263
tbase	-4.5, -4.5, -4.5, -4.5, 0	-4, -4, -4, -4, -4	-5, -5, -5, -5, -0.5
mf	0.08, 0.08, 0.08, 0.1, 0.15	0.06, 0.06, 0.06, 0.08, 0.1	0.06, 0.06, 0.06, 0.1, 0.15
Sublim	-0.1, -0.1, -0.1, -0.1, -0.1	-0.3, -1, -1, -1, -0.3	-0.3, -0.3, -0.3, -0.1, -0.1
temp3	500	1000	0
pwr	2.5, 2, 2.5	2, 1.5, 2	1.5, 2, 1.5
flz	10^{-6} , 10^{-6} , 10^{-6}	10^{-7} , 10^{-7} , 10^{-7}	10^{-6} , 10^{-6} , 10^{-6}
retn	70, 0.4, 0.4, 0.1, 0.1	70, 0.4, 0.4, 0.1, 0.1	300, 0.4, 0.4, 0.1, 0.1
rec	2, 0.9, 0.9, 0.1, 0.9	2, 0.9, 0.9, 0.1, 0.9	1, 1, 1, 0.1, 1
ak	12, 400, 400, -0.1, 10^{-11}	12, 400, 400, -0.1, 10^{-11}	12, 400, 400, -0.1, 10^{-11}
ak2	0.1, 0.02, 0.02, 0.001, 10^{-11}	0.1, 0.02, 0.02, 0.001, 10^{-11}	1, 0.2, 0.2, 0.01, 10^{-10}
fpet	2, 3, 3, 1, 1	2, 3, 3, 1, 1	2, 3, 3, 1, 1
ftall	0.7, 1, 1, 0, 1	0.7, 1, 1, 0, 1	0.7, 1, 1, 0, 1

No hydrological model can give a perfect picture of reality. It is important that the model represents well the main features of the hydrologic system relevant to the

particular study (Dibike and Coulibaly, 2007). In this case, the main interest was predicting streamflow. The validation results (Chapter 5) show that the calibration of the model managed to produce a good agreement between observed and simulated streamflow.

4.11 Model Initialization

It is crucial to have knowledge of initial conditions for modeling the basin responses at the storm event scale. For distributed parameter models, the spatial variability of the initial conditions must be specified over the entire domain. Use of spatial variability of soil moisture increases the runoff production relative to that produced by assuming an average soil moisture value (Noto *et al.*, 2007).

The APC2 dataset has a production lag with only data up to 2011 available. For forecasting purposes, up-to-date data is necessary. The selected methodology requires the model to run for the calibration period (1982-2011) with the best forcing data available, and then run with the up to date dataset (NARR/CaPA) from January 2012 to the present. For forecasting simulations, models are run for each forecast for only a year or two. For this reason, model initialization is needed to bring the result from the calibration period to the starting date of forecast simulation. The aim is to create resume files (Kouwen, 2011) that contain all the state variables at the time of program termination. With the option provided in WATFLOOD (Kouwen, 2011), the soil moisture and streamflow produced at the end of a simulation period 1982-2008 are carried over to resume the model and continue to run from 2009 to 2011 (up to the end of the study period). The results obtained with initialization runs are provided in the following chapter (Section 5.7).

Chapter 5 Results and Discussion

5.1 Streamflow Simulation at Gauge Locations

The WATFLOOD model described in Chapter 4 was initially calibrated with APC2 precipitation data and historical temperature data to ensure that the model set up was correct. The lake areas, modeled drainage areas at stream gauges and the generated hydrographs were used to ensure the accuracy of model calibration. Figure 5.1 shows the resulting hydrographs for the validation period (2003-2007) at the eight stream gauges.

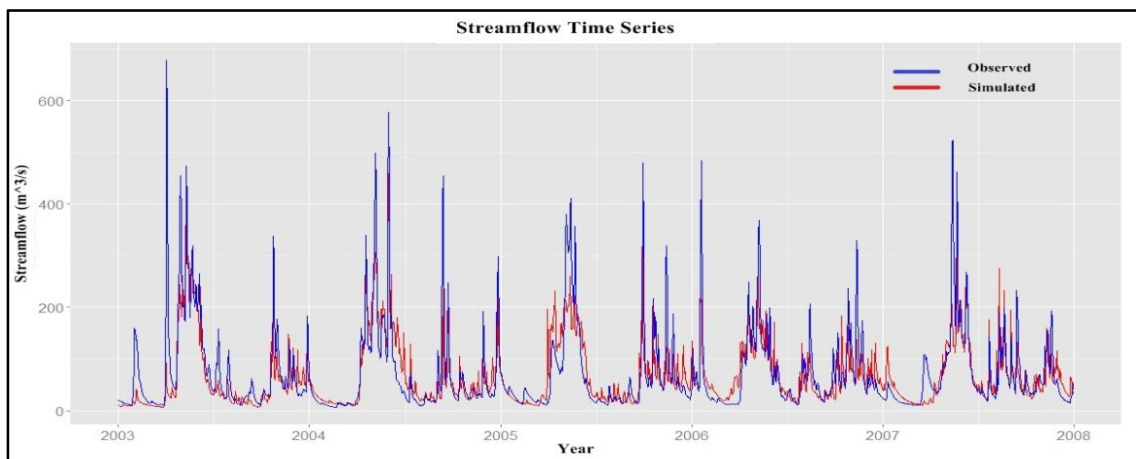


Figure 5.1(a): Streamflow Simulation at Reidville (2003-2007)

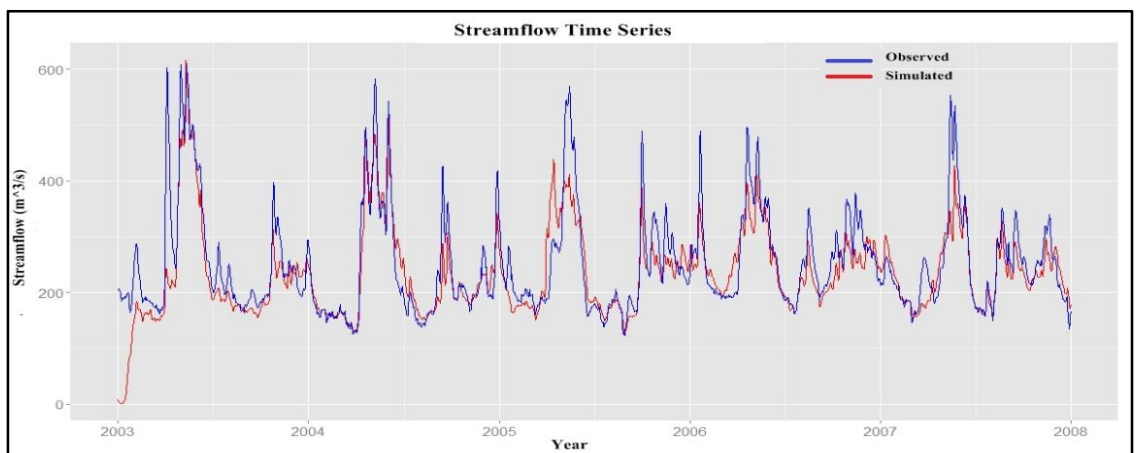


Figure 5.1(b): Streamflow Simulation at Humber River Village Bridge (2003-2007)

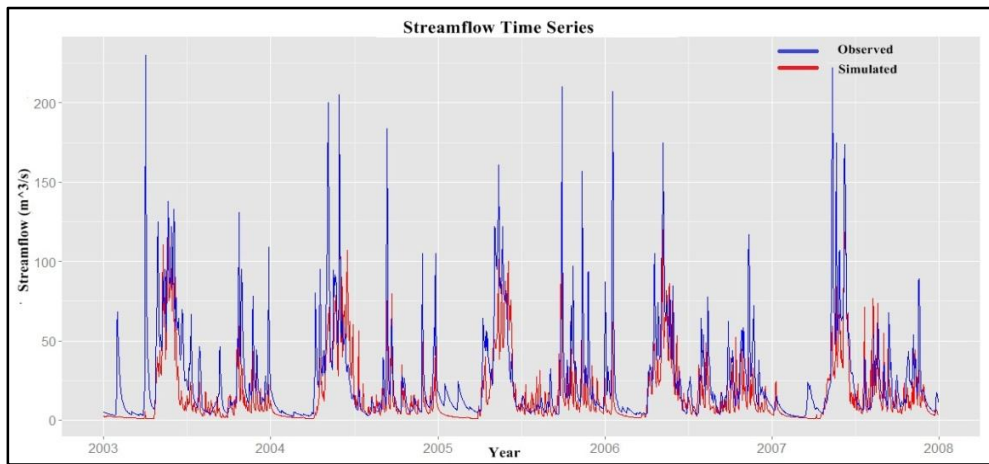


Figure 5.1(c): Streamflow Simulation at Black Brook (2003-2007)

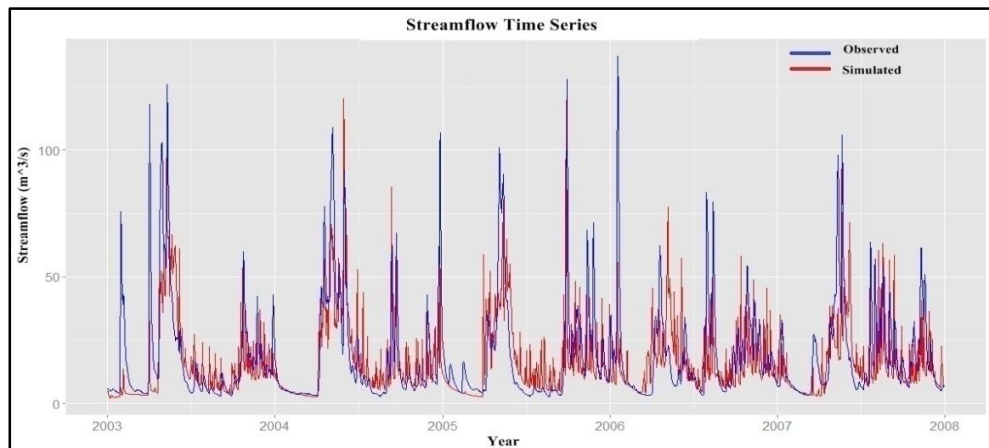


Figure 5.1(d): Streamflow Simulation at Lewasechjeech Brook (2003-2007)

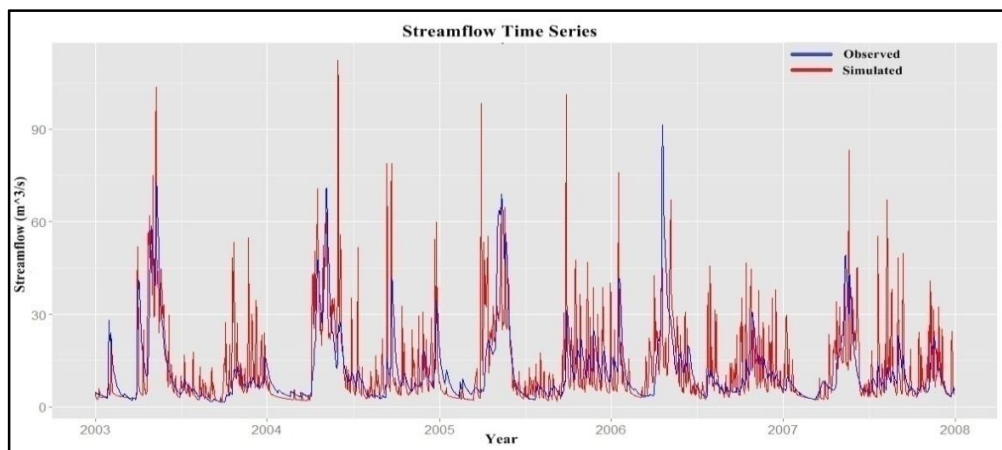


Figure 5.1(e): Streamflow Simulation at Sheffield Brook (2003-2007)

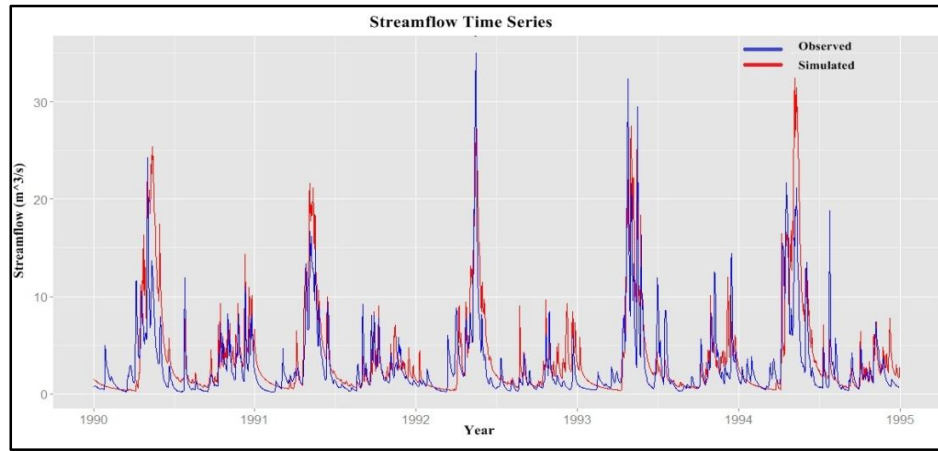


Figure 5.1(f): Streamflow Simulation at Glide Brook (2003-2007)

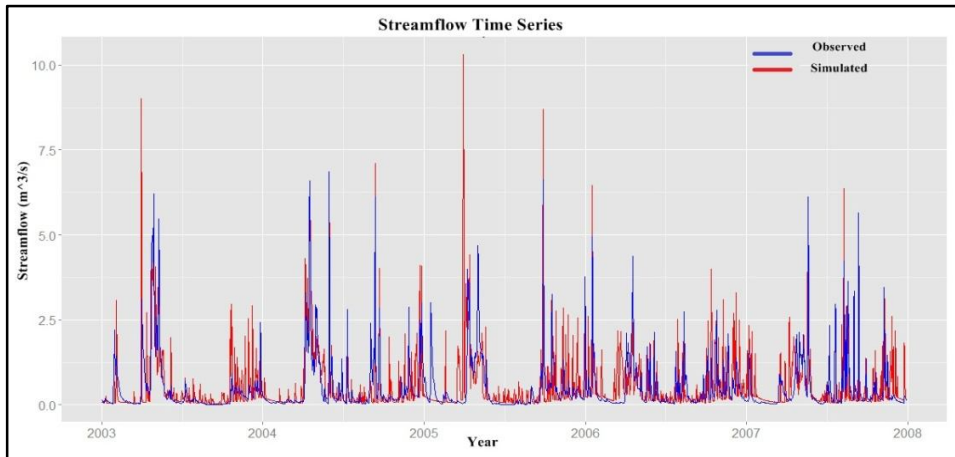


Figure 5.1(g): Streamflow Simulation at Boot Brook (2003-2007)

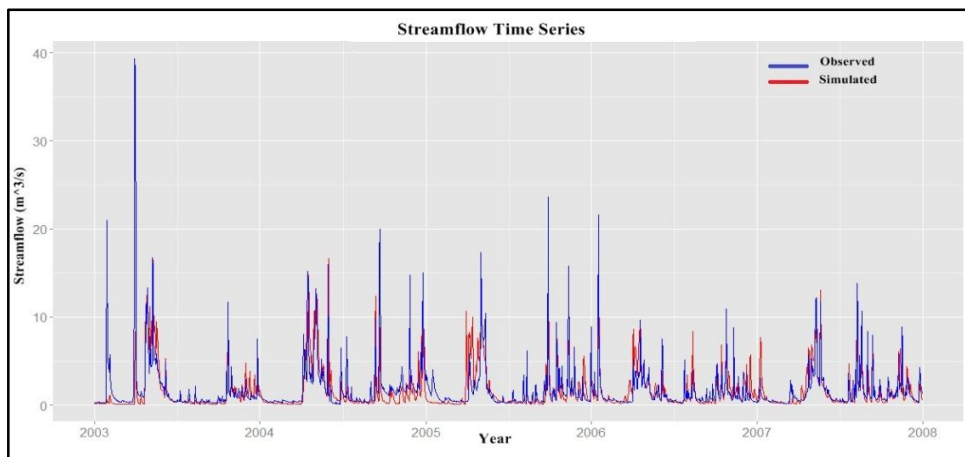


Figure 5.1(h): Streamflow Simulation at South Brook at Pasadena (2003-2007)

Figures 5(a) to 5(h) show that the model tends to underestimate streamflow. It is under-predicting streamflow for Reidville, Humber River at Village Bridge and Black Brook (Figures 5(a), 5(b) and 5(c)). The annual cycles of each hydrograph are better compared to the hydrographs at the rest of the gauge locations. The model over-predicts the peak flows at Sheffield Brook, Glide Brook and Boot Brook. The reason behind this might be highly adjusted gridded precipitation at those locations. Also, the Drainage area (DA) of Glide Brook outlet is 112 km² and the DA of Boot Brook outlet is only 20 km². Given that the grid size of the model is 5 km X 5 km (25 km²), it is difficult to capture the hydrology of small basins in hydrological models.

At each location, the bases of the simulated hydrographs seem to follow the bases of the measured hydrographs. The simulated hydrographs are too spiky in summer for all the stations. They are spiky over the entire year for Lewaseechjeech Brook, Sheffield Brook and Boot Brook. The DA of Sheffield Brook includes Sandy Lake. The lake effects might cause the spikes in hydrographs. The over-prediction of the simulated streamflows can be adjusted at these locations by adjusting the precipitation lapse rates. However, WATFLOOD allows for only one lapse rate value applicable to the entire basin. Varying the lapse rate improves the actual hydrographs in Sheffield Brook, Glide Brook and Boot Brook, but deteriorates the simulations at other locations.

As the study evolved, focus was shifted towards producing the best results for Reidville, Humber River at Village Bridge and Black Brook as streams in those locations are natural and flow is uncontrolled. Upper Humber River at Reidville (2110 km²) and Humber River at Black Brook (471 km²) have the largest DAs; together they consist of

one third of the basin area. Also, the gauge at Humber River at Village Bridge is the outlet for the entire Humber River basin. Therefore, the focus was to get the best possible results at those three locations. All the results will be discussed further based on the results obtained at Upper Humber River at Reidville.

5.2 Bias Correction for NARR Data

The base model was also calibrated later with NARR precipitation and temperature data. As described in Chapter 3, NARR precipitation was significantly lower than APC2 and a correction was made to check if the adjusted NARR data based on APC2 made any improvements in the simulated results. Two corrections were made on NARR precipitation data, linear and non-linear (details in Chapter 3). For both cases, the results obtained were poorer than the results obtained for the calibrated model with APC2 for the period 2003-2007. Table 5.1 shows the Nash values obtained for the model stations when calibrated with uncorrected, linear corrected and non-linear corrected NARR data.

Table 5.1: Comparison of Results Using Uncorrected and Corrected NARR Data

Station Name	NARR (Uncorrected)	NARR (Linear Corrected)	NARR (Non Linear Corrected)
Reidville	0.43	0.43	0.26
Humber River @ Village Bridge	0.48	0.52	0.33
Black Brook	0.37	0.37	0.10
Lewaseechjeech Brook	0.14	0.24	-0.13
Sheffield Brook	-0.03	0.01	-0.59
Boot Brook	-0.09	-0.27	-0.67
South Brook @ Pasadena	0.29	0.11	-0.30

In previous studies (Roberts *et al.*, 2011) the non-linear bias correction improved the results; however, in this study the expected result was not obtained. This may be due to the fact that the bias correction was made based on observed precipitation at Deer Lake only, ignoring the rest of the precipitation stations to avoid complexity. Though the station is the most representative station among all those available, it does not represent the actual precipitation over the entire basin. Also, the NARR data are 3 hourly accumulations, so the rainfall is distributed over the day. Linear corrected data were prepared for the same 3 hour accumulations. But the non-linear corrected NARR were daily precipitations (24 hour accumulations). So, all the rain water accumulates at a time during a day. The model fails to simulate correctly due to the sudden accumulation of the daily rain at a time.

Figure 5.2(a) and (b) shows the difference between the streamflow simulations obtained by using daily and hourly (using the ‘smearing’ option) precipitation accumulations with APC2 for the station at South Brook at Pasadena. The Nash-Sutcliffe values for daily and hourly accumulations are 0.24 and 0.37 respectively. The effects of rainfall distribution in 3-hour NARR are more comparable to the daily APC2. This is because; in APC2 the rain was generally smeared in the early 5 to 6 hours of day, but in NARR, rainfall is accumulated for each 3 hour of a day which makes NARR more distributed throughout the day. So, the results with NARR will be more affected, as we can see in Table 5.1.

A complex adjustment using more distributed precipitation gauges might improve the result, but due to time constraints, it was not possible to include in this study. As such

the remainder of the analysis was performed with the model calibrated with the uncorrected NARR data.

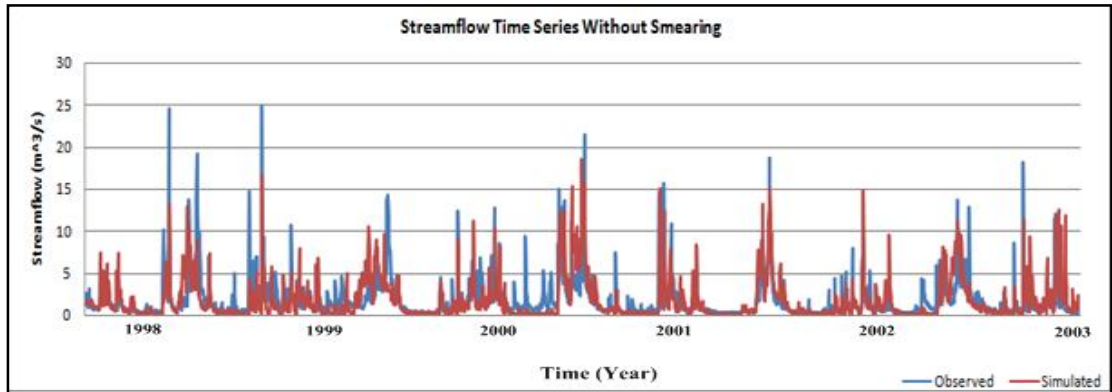


Figure 5.2(a): Streamflow Time Series at Pasadena without Smearing

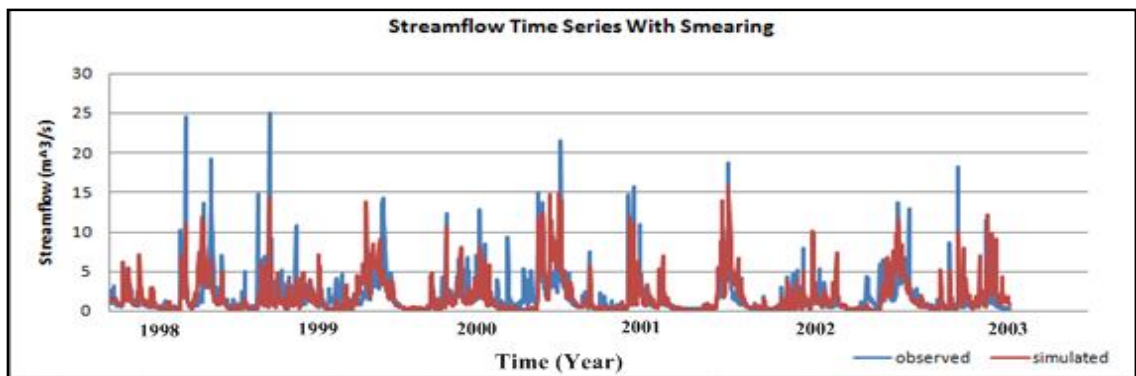


Figure 5.2(b): Streamflow Time Series at Pasadena with Smearing

5.3 Model Calibration Results with APC2, NARR and CaPA

The period of October 1997 to December 2002 was used for calibration with APC2 and NARR precipitation and January 2002 – December 2006 was used for calibration with CaPA. Once satisfied with the model set up, the model was calibrated with: (i) APC2 precipitation data and historical temperature data, (ii) uncorrected NARR precipitation and temperature data and (iii) CaPA precipitation and historical temperature

data. Table 5.2 summarizes the objective function scores (Nash-Sutcliffe) obtained with the three different datasets. For calculating the overall model performance, area weighted average Nash value was calculated to account for the effect of basin size, as small basins are hard to capture in the model.

According to Table 5.2, APC2 gives the best results for Reidville, Humber River at Village Bridge, Black Brook, Lewaseechjeech Brook and South Brook at Pasadena, but it fails to effectively model simulations at Sheffield Brook and Boot Brook. Though the overall basin average Nash value is highest with NARR data (0.56), it fails to capture the characteristics of the basin at these two locations. CaPA seems to be more spatially consistent in the calibration period compared to the other two datasets, producing positive Nash values at all the locations. However, the overall model performance is lower than the other two.

Table 5.2: Nash-Sutcliffe Values for Respective Calibration Period

Station Name	APC2	NARR	CaPA
Reidville	0.57	0.43	0.38
Humber River @ Village Bridge	0.71	0.48	0.41
Black Brook	0.45	0.37	0.31
Lewaseechjeech Brook	0.2	0.14	0.19
Sheffield Brook	-0.26	-0.03	0.2
Boot Brook	-0.15	-0.09	0.13
South Brook @ Pasadena	0.37	0.29	0.12
Weighted Average Nash-Sutcliffe	0.40	0.56	0.37

Considering our main study focus on the first three gauge locations, NARR data seems to work better than CaPA for the calibration period. Figures 5.3(a), (b) and (c) show the time series plots of streamflow with APC2, NARR and CaPA respectively for

the calibration period. For APC2 and NARR, the calibration period was October 1997-December 2002 and for CaPA, the calibration period is January 2002- December 2006.

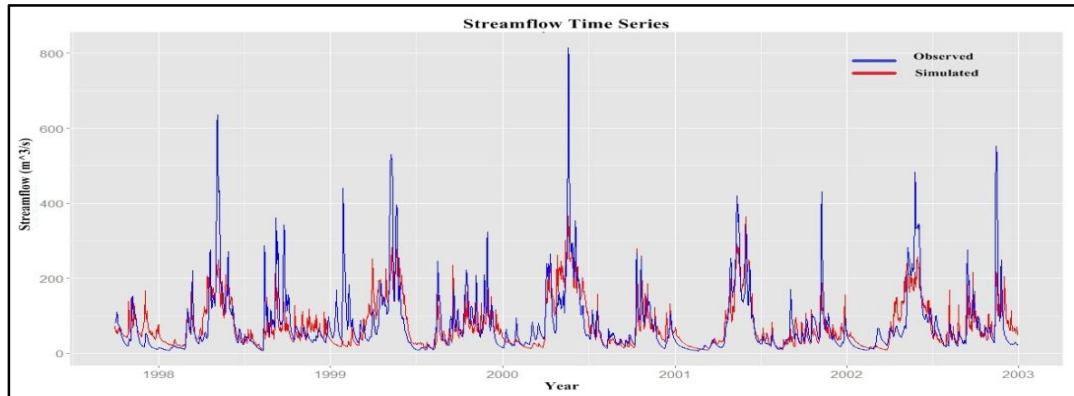


Figure 5.3(a): Streamflow Simulation at Reidville with APC2

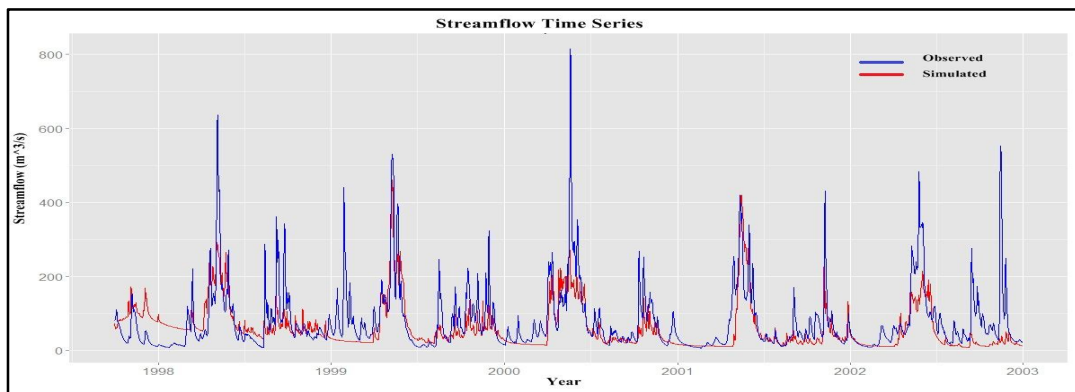


Figure 5.3(b): Streamflow Simulation at Reidville with NARR

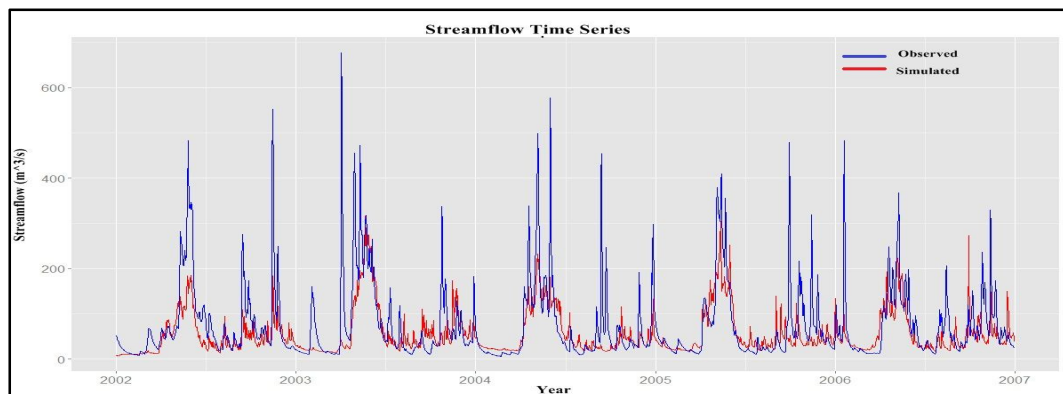


Figure 5.3(c): Streamflow Simulation at Reidville with CaPA

The base of the simulated hydrograph matches well with the actual one when APC2 is used (Figure 5.3(a)). NARR data could not capture the actual base, especially in the winter period (Figure 5.3(b)). This can be due to the higher snow cover as NARR estimates cooler winters (shown in Figure 3.7). Though CaPA did not perform as well as APC2, the base of the hydrograph is better than that using NARR (Figure 5.3(c)). In all three cases the volume of the simulated hydrograph is lower than the observed hydrograph. The differences in volume between observed and simulated hydrographs are 5.5%, 22.5% and 24.8% for APC2, NARR and CaPA respectively. Better results are possible for selected stations, however stations in the western portion of the basin deteriorate quickly when lapse rate adjustment is used in increase precipitation.

Figures 5.4(a), (b) and (c) represent the daily ensembles of streamflow at Reidville for the calibration period with APC2, NARR and CaPA respectively. Daily ensembles are the average values calculated for each days of a year. The daily ensemble plots (Figure 5.4) show that peaks of simulated hydrographs with APC2 and CaPA data match the peaks of observed hydrographs in time. NARR data fails to match peaks in time. With both NARR and CaPA, the hydrographs fall short in spring melt. This may be due to a low baseflow or melt factor.

Figures 5.5(a), (b) and (c) represent the monthly ensembles of streamflow at Reidville for the calibration period with APC2, NARR and CaPA respectively. Monthly ensembles are average values calculated for each months of a year. The monthly ensemble plots reveal that all three datasets produce hydrographs short in water

throughout the year. Both NARR and CaPA also produce hydrographs noticeably short in fall streamflow.

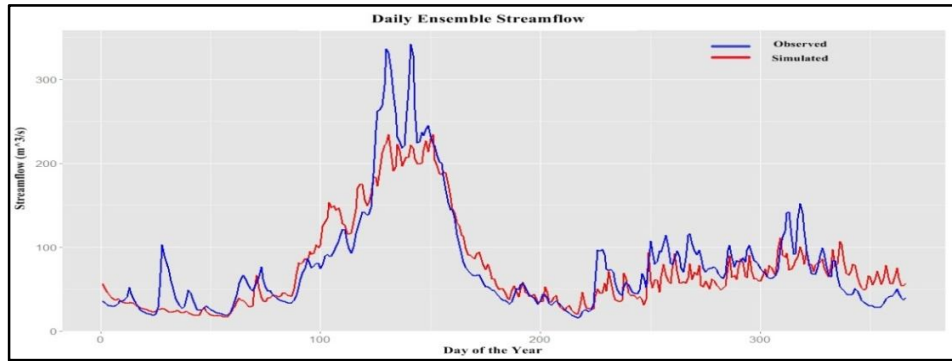


Figure 5.4(a): Daily Ensemble Plot at Reidville with APC2

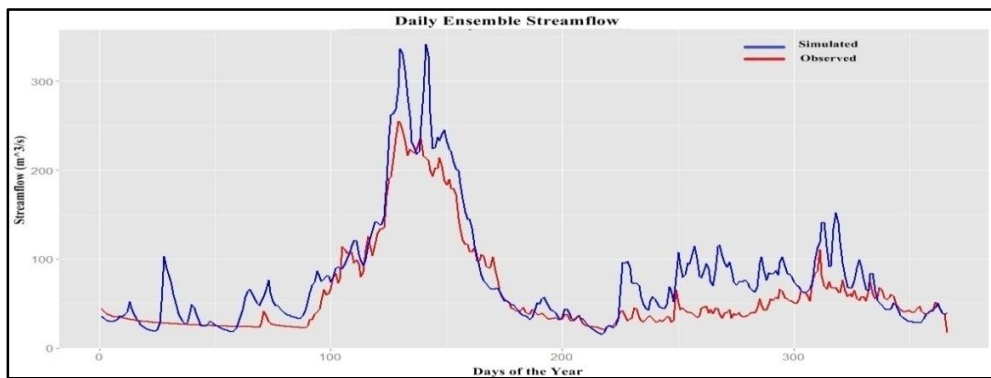


Figure 5.4(b): Daily Ensemble Plot at Reidville with NARR

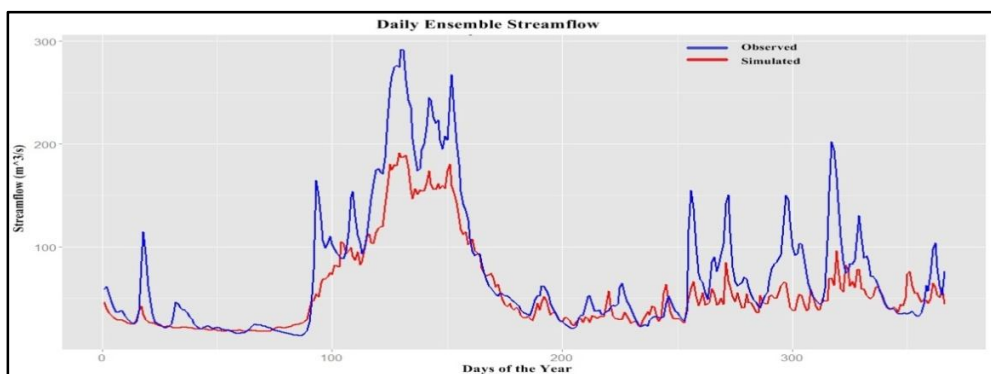


Figure 5.4(c): Daily Ensemble Plot at Reidville with CaPA

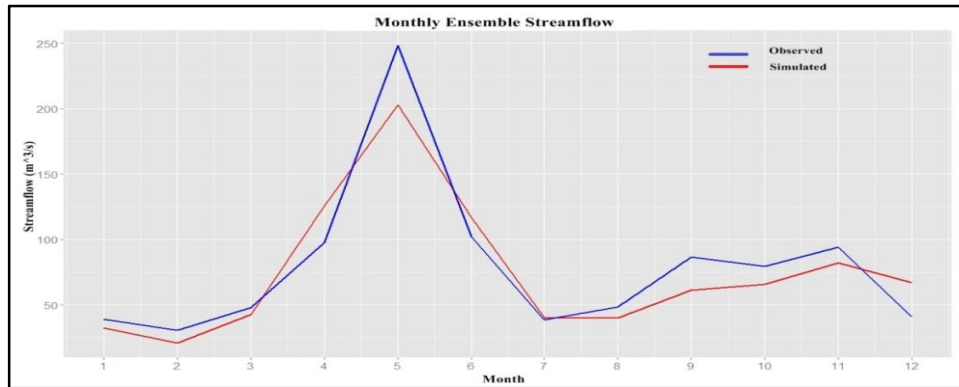


Figure 5.5(a): Monthly Ensemble Plot at Reidville with APC2

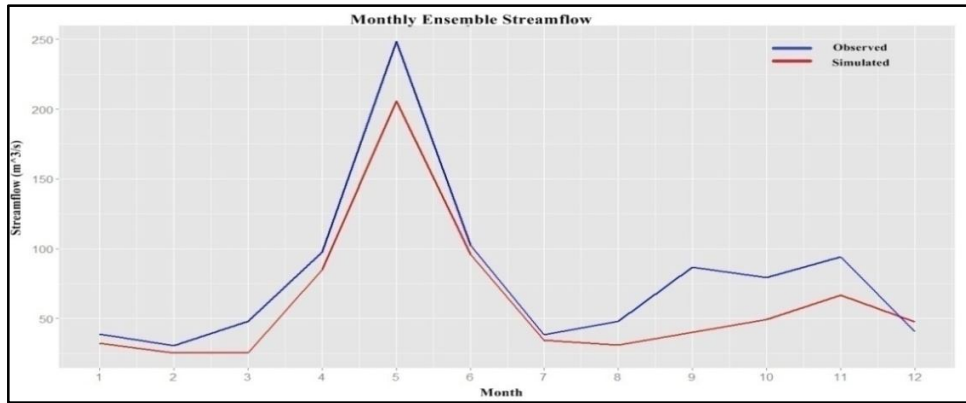


Figure 5.5(b): Monthly Ensemble Plot at Reidville with NARR

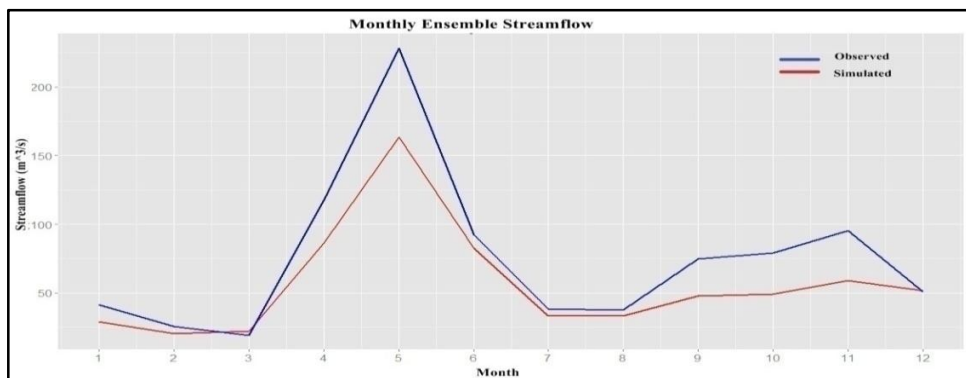


Figure 5.5(c): Monthly Ensemble Plot at Reidville with CaPA

5.4 Model Validation Results with APC2, NARR and CaPA

After obtaining satisfying model calibration results, the model was validated using (i) APC2 precipitation and historical temperature data (ii) uncorrected NARR precipitation and temperature data and (iii) CaPA precipitation and historical temperature data. The period of January 2003 to December 2007 was used for validation with APC2 and NARR precipitation and January 2007 to December 2009 was used for validation with CaPA. Table 5.3 summarizes the objective functions (Nash-Sutcliffe) obtained with the three different datasets. For calculating the overall model performance, area weighted average Nash values were calculated to negate the effect of basin sizes. A new streamflow station at Indian Brook was added for the validation run. This station was not used during calibration, so the results at Indian Brook can be tested to check the model performance.

Table 5.3: Nash-Sutcliffe Values for Respective Validation Period

Station Name	APC2	NARR	CaPA
Reidville	0.61	0.54	0.51
Humber River @ Village Bridge	0.69	0.54	0.38
Black Brook	0.44	0.41	0.43
Lewaseechjeech Brook	0.32	0.25	0.08
Sheffield Brook	0.04	0.09	0.16
Boot Brook	0.12	0.11	-0.03
South Brook @ Pasadena	0.41	0.26	0.05
Indian Brook	0.51	0.34	0.36
Weighted Average Nash-Sutcliffe	0.48	0.59	0.38

According to Table 5.3, APC2 gives the best results for Reidville, Humber River at Village Bridge, Black Brook, Lewasechjeech Brook, South Brook at Pasadena and Indian Brook. Though the overall basin average Nash value is highest with NARR data (0.59), it fails to capture the main characteristics of the basin at Sheffield Brook and Boot Brook. CaPA data works well for Reidville, Humber River village bridge, Black Brook and Indian Brook only. The overall model performance is lower than the model calibrated with APC2 and NARR. Considering our main study focus on the first three gauge locations, NARR data seems to work better than CaPA for the validation period. Figures 5.6(a), (b) and (c) show the time series plots of streamflow with APC2, NARR and CaPA respectively for their respective validation period.

The base of the simulated hydrograph matches well with observations when APC2 is used (Figure 5.6(a)). NARR data could not capture the actual base, especially in the winter period (Figure 5.6(b)). CaPA did not perform as well as APC2 and the base of the hydrograph is poorer compared to NARR (Figure 5.6(c)).

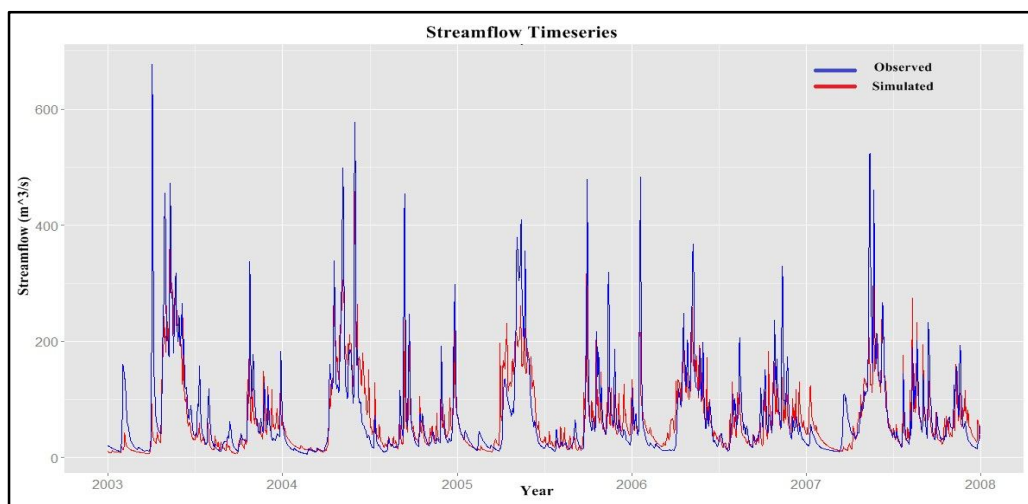


Figure 5.6(a): Streamflow Simulation at Reidville with APC2

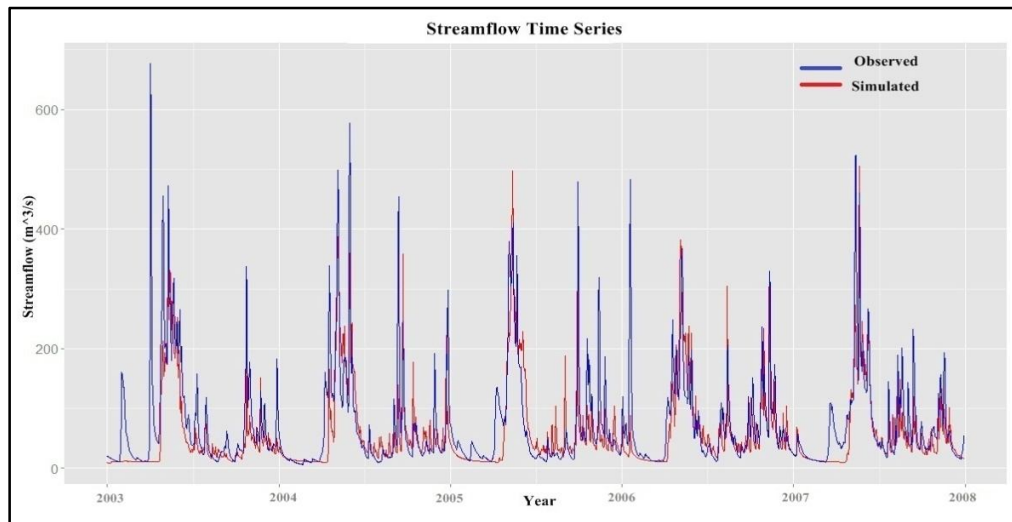


Figure 5.6(b): Streamflow Simulation at Reidville with NARR

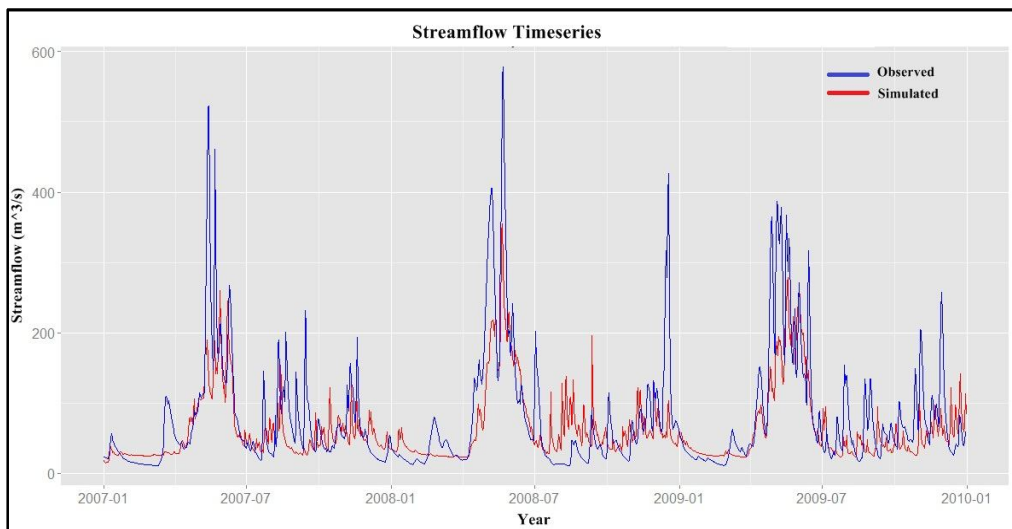


Figure 5.6(c): Streamflow Simulation at Reidville with CaPA

In all three cases the volume of the simulated hydrograph is lower than the observed volume. The differences in volume between observed and simulated hydrographs with APC2, NARR and CaPA are 9.3%, 21.1% and 19.9% respectively.

Figures 5.7(a), (b) and (c) represent the daily ensembles while Figures 5.8(a), (b) and (c) represent the monthly ensembles of streamflow at Reidville for the validation period with APC2, NARR and CaPA respectively.

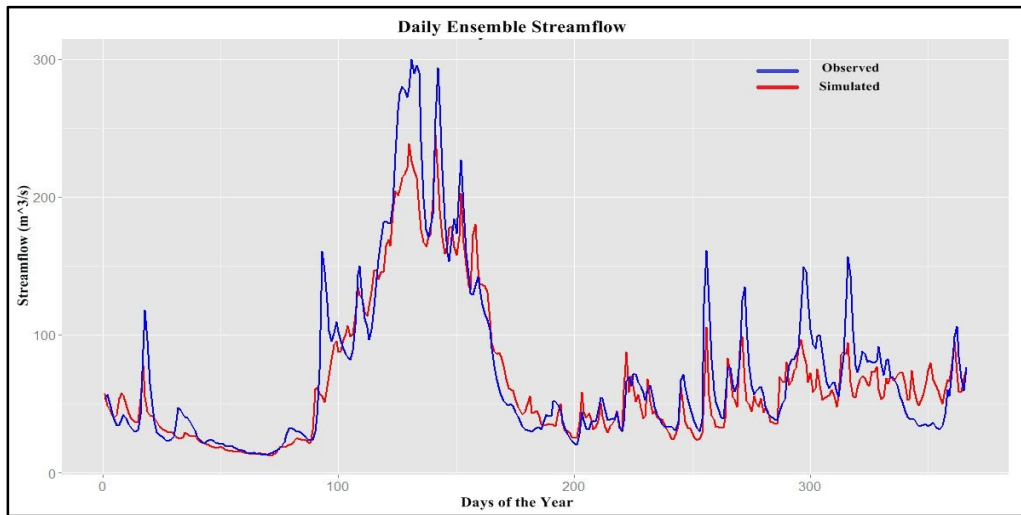


Figure 5.7(a): Daily Ensemble Plot at Reidville with APC2

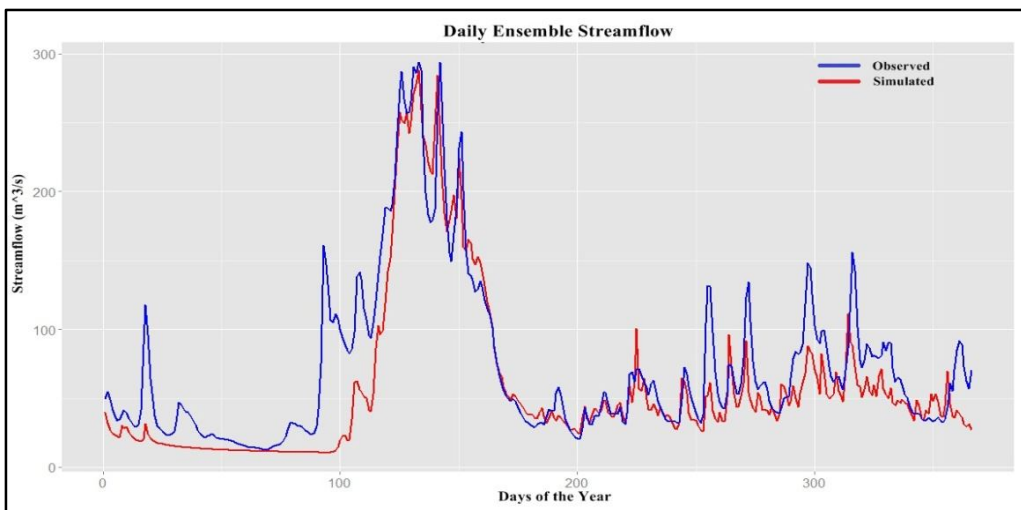


Figure 5.7(b): Daily Ensemble Plot at Reidville with NARR

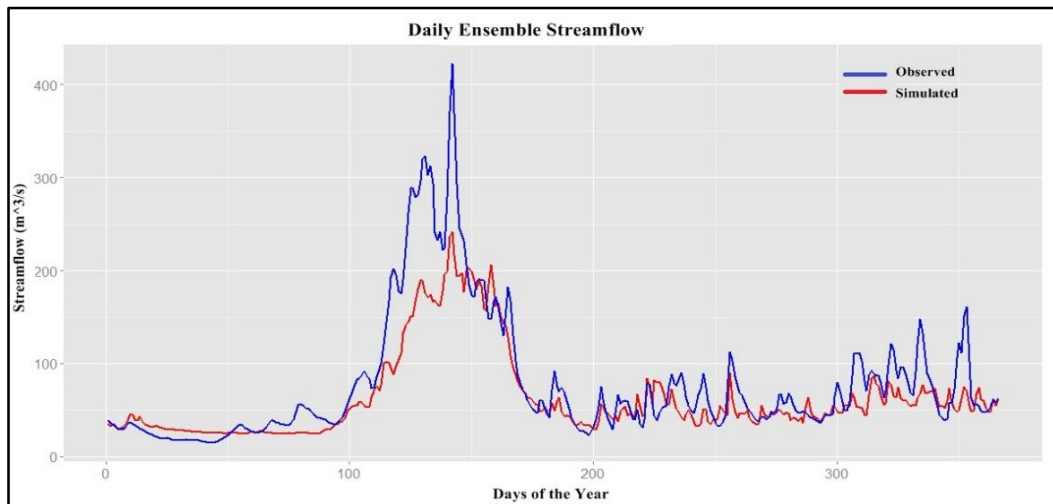


Figure 5.7(c): Daily Ensemble Plot at Reidville with CaPA

The daily ensemble plots (Figure 5.7) show that the timing of the spring peaks of simulated hydrographs with APC2, NARR and CaPA data matches those observed. NARR data fails to match peaks in time for winter periods. With both NARR and CaPA, the hydrographs are significantly short in winter melt. This may be due to low baseflow or melt factor.

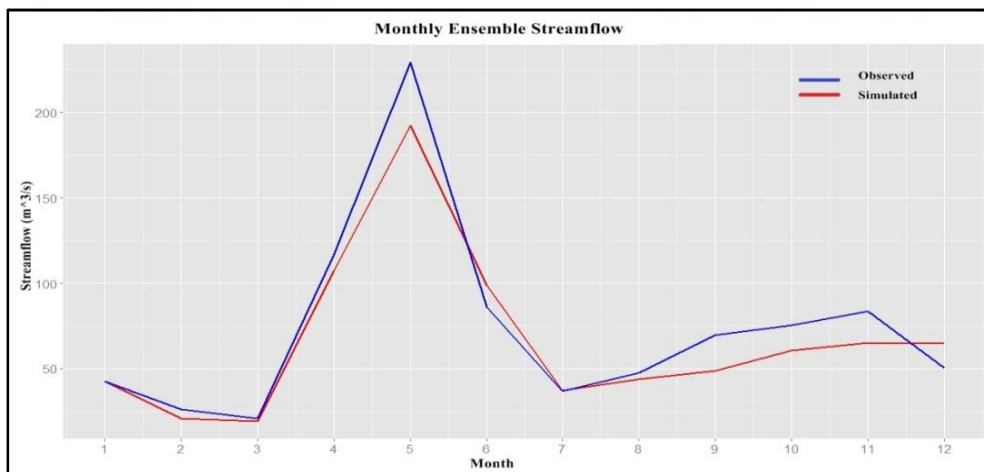


Figure 5.8(a): Monthly Ensemble Plot at Reidville with APC2

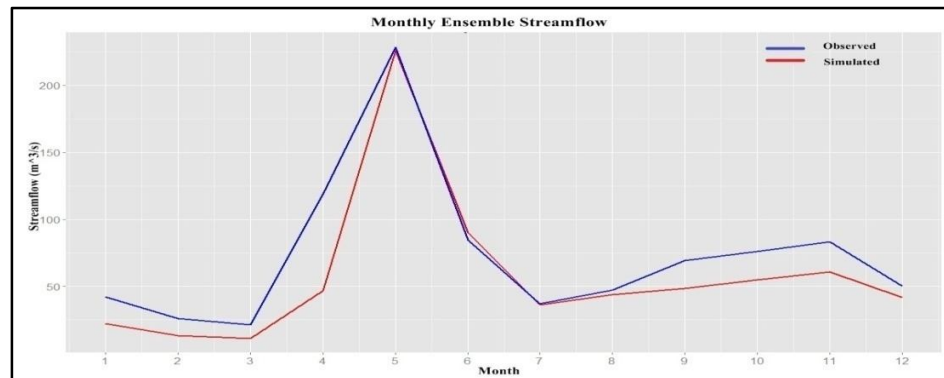


Figure 5.8(b): Monthly Ensemble Plot at Reidville with NARR

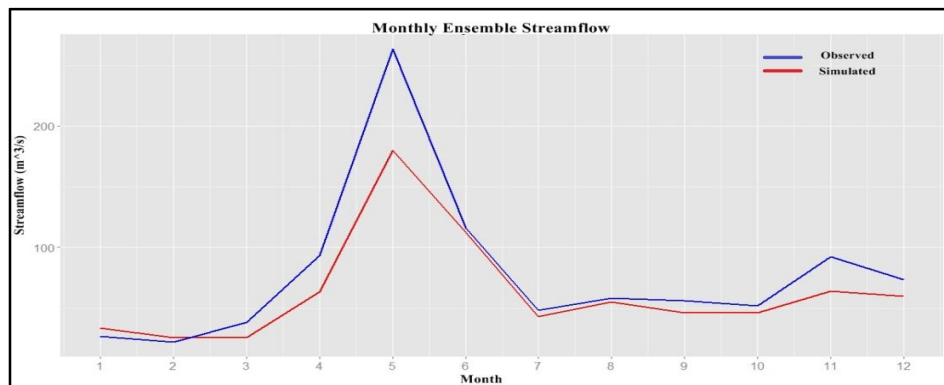


Figure 5.8(c): Monthly Ensemble Plot at Reidville with CaPA

The monthly ensemble plots reveal that all three datasets produce hydrographs short in water throughout the year, even though the timing of peak spring discharges matches.

5.5 Simulations for Entire Study Period

In this study, APC2, NARR precipitation and temperature data and historical temperature data were collected for a 30-year period (1982-2011). CaPA data was collected for a 10-year period (2002-2011). This section presents the time series plot of streamflows at Reidville and their daily and monthly ensembles using the three precipitation and temperature datasets previously specified (Section 5.3).

Figures 5.9(a), (b) and (c) present the simulations using APC2, NARR and CaPA precipitation with their respective temperature datasets. For better presentation, the 30 year simulations for APC2 (Figure 5.9(a)) and NARR (Figure 5.9(b)) have been broken down into 3 parts: (i) October 1982 – December 1991, (ii) January 1992 – December 2001, and (iii) January 2002 – December 2011.

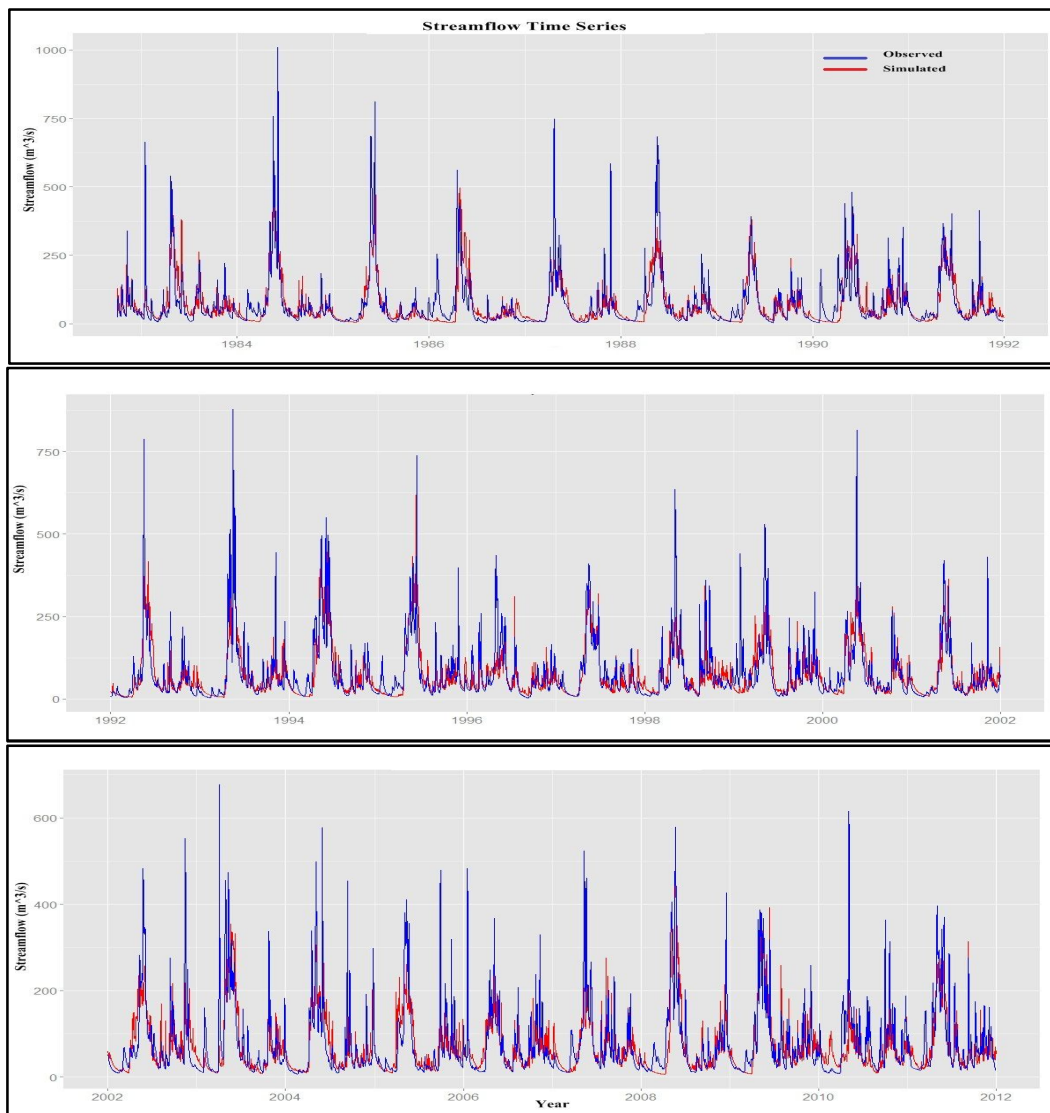


Figure 5.9(a): 30 Year Streamflow Simulation at Reidville with APC2

The 30-year long simulation shows the consistency of the model with time. The simulated hydrographs are similar throughout the study period. With APC2 (Figure 5.9(a)), the base of the observed and simulated hydrographs matches very well, while the peaks coincide in time. On average, the model is a little short on water for the entire study period (8%).

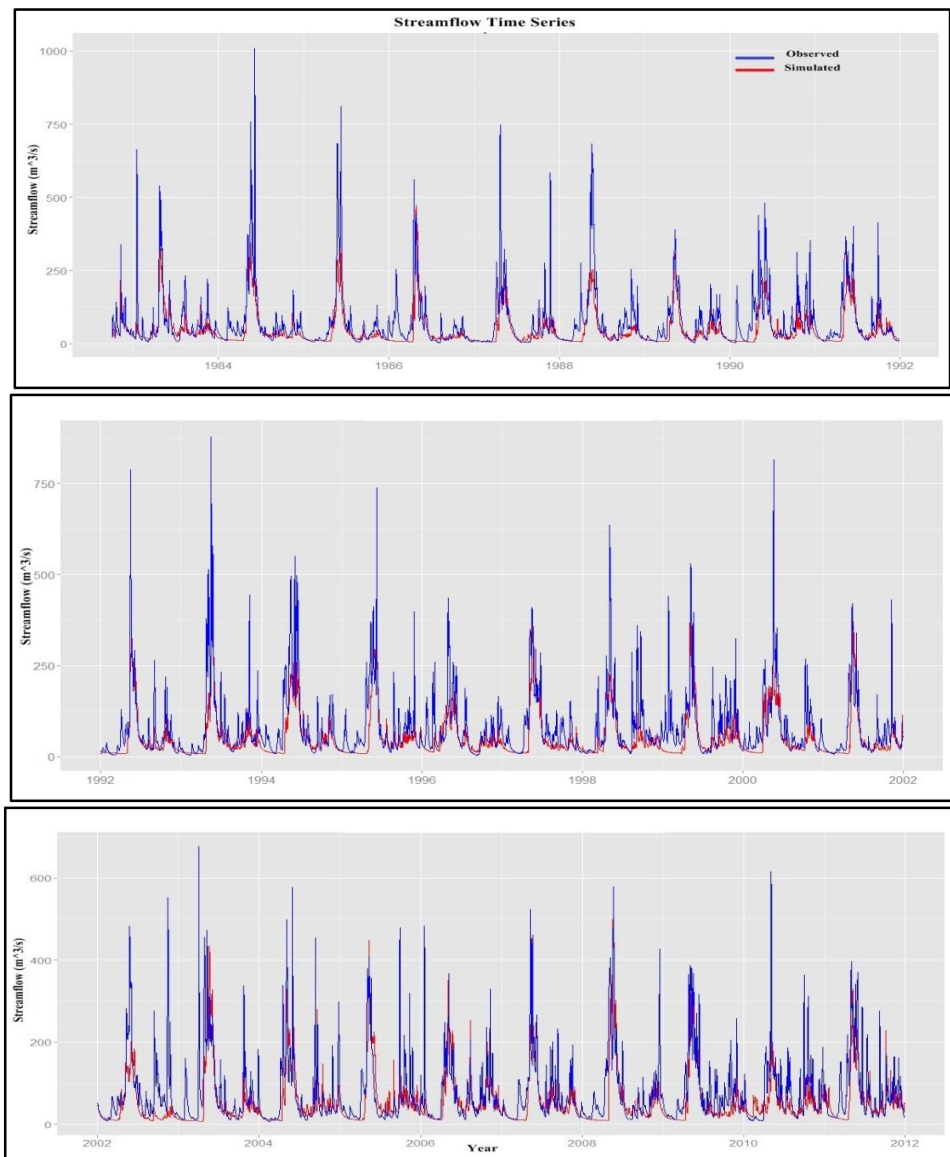


Figure 5.9(b): 30 Year Streamflow Simulation at Reidville with NARR

Figure 5.9(b) shows that NARR data fails to capture winter streamflows. The base of the simulated hydrograph matches poorly with the observed winter hydrograph. The consistency of the simulation stays the same with time. The entire simulation shows that the model is short on water throughout the study period by a substantial amount (34%).

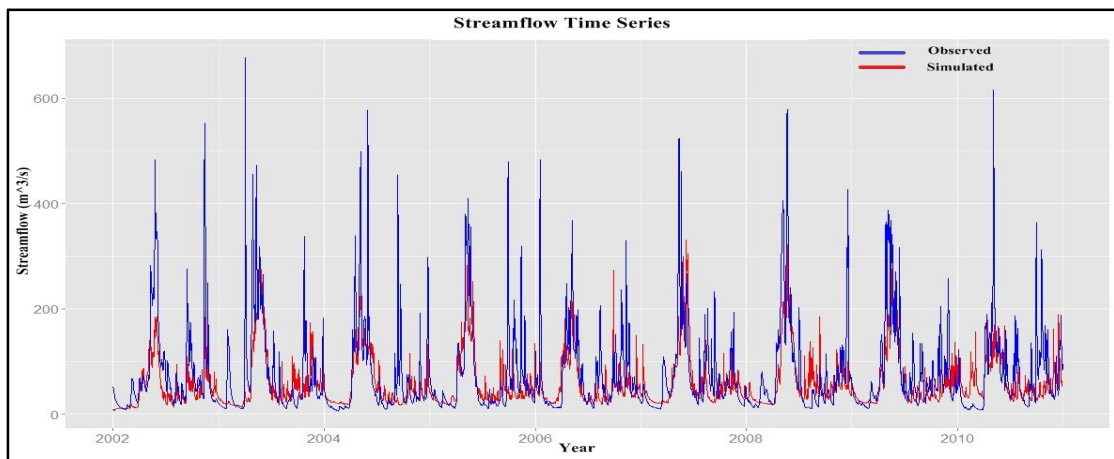


Figure 5.9(c): 10 year streamflow simulation at Reidville with CaPA

Figure 5.9(c) shows that CaPA data fails to capture the base flows, as the simulated hydrograph poorly matches observations. The consistency of the simulation stays the same with time. The entire simulation shows that the model is short on water throughout the study period (22%). Though the volume difference using CaPA is less than that obtained using NARR, the hydrographs do not match well.

The weighted average Nash-Sutcliffe values for the model with APC2, NARR and CaPA and their respective study periods are given in Table 5.3.

Figures 5.10 and 5.11 present scatter plots of daily and monthly ensembles of 30 year observed and simulated streamflows using APC2. The straight line represents the

line of perfect agreement. In both cases, low flows are in better agreement than high flows, as the simulated streamflows fall short during periods of higher flows.

Table 5.3: Nash-Sutcliffe Values for Respective Timeframes

Station	APC2	CaPA	NARR
Reidville	0.65	0.39	0.51
Humber River @ Village Bridge	0.63	0.26	0.39
Black Brook	0.47	0.31	0.41
Lewaseechjeech Brook	0.25	0.12	0.22
Sheffield Brook	0.01	0.14	0.23
Glide Brook	0.19	-	0.42
Boot Brook	0.04	0.04	0.07
South Brook @ Pasadena	0.32	0.09	0.20
Indian Brook	0.36	0.33	0.21
Weighted Average Nash-Sutcliffe	0.55	0.28	0.39

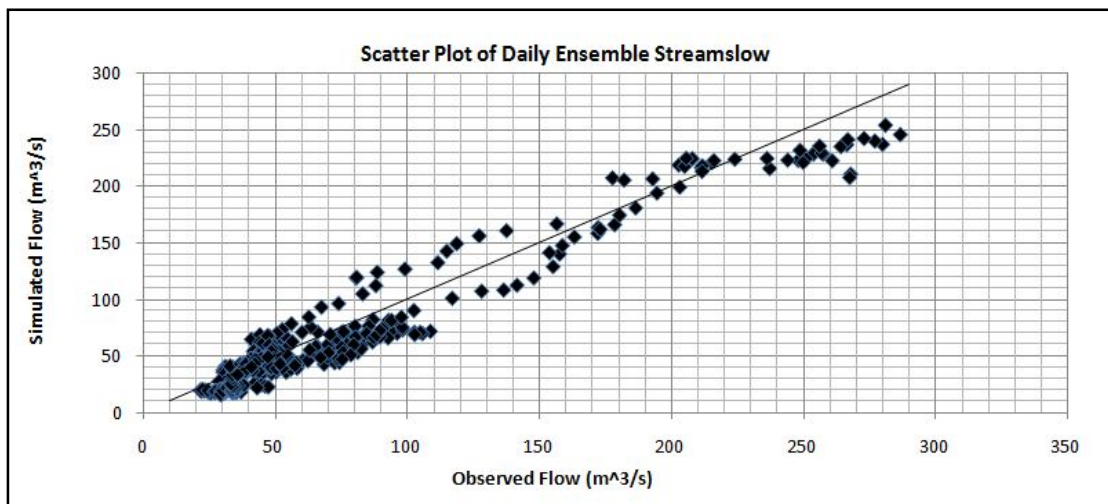


Figure 5.10: Daily Ensembles of Streamflow at Reidville Using APC2

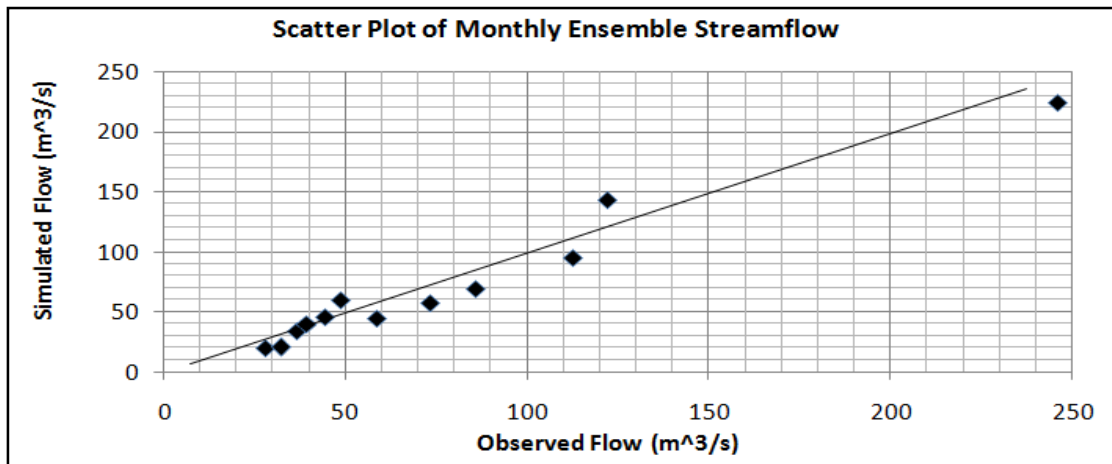


Figure 5.11: Monthly Ensembles of Streamflow at Reidville Using APC2

5.6 Comparison of Streamflow Results among Datasets

Tables 5.4(a) and (b) show the statistics for observed and simulated streamflows generated with APC2, NARR and CaPA for their respective timeframes.

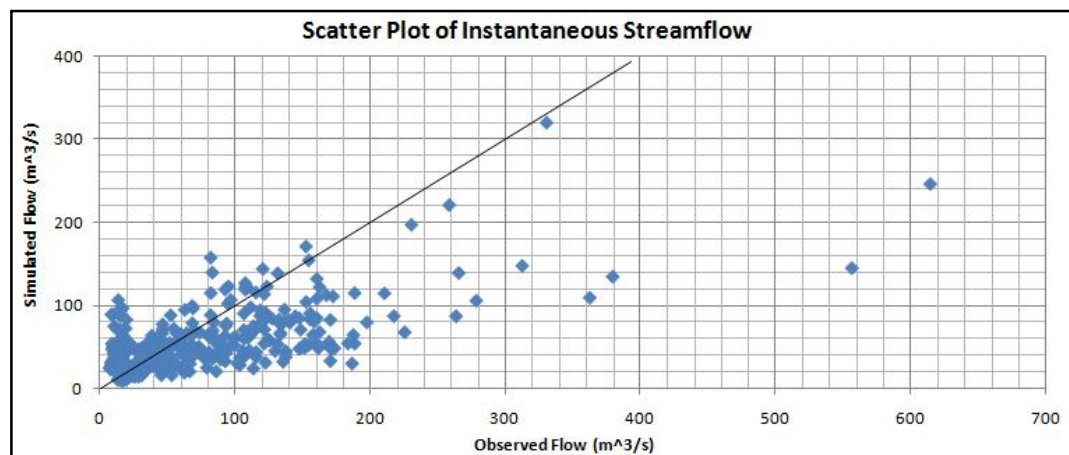
Table 5.4(a): Statistics for Streamflows with APC2 and NARR (1982-2011)

	Observed	APC2	NARR
Min (m ³ /s)	3.7	4.5	6.7
1st Quartile (m ³ /s)	23.0	24.0	13.4
Median (m ³ /s)	45.7	43.8	27.4
Mean (m ³ /s)	78.0	71.3	51.3
3rd Quartile (m ³ /s)	93.0	84.6	52.6
Max (m ³ /s)	1010.0	733.40	539.0
Standard Deviation (m ³ /s)	93.1	75.3	66.0
Skewness	2.9	2.1	2.8
Kurtosis	11.9	5.2	9.2

Table 5.4(b): Statistics for Streamflows with CaPA (2002-2011)

	Observed	CaPA
Min	6.4	7.5
1st Quartile	23.2	27.3
Median	46.3	41.7
Mean	76.6	59.6
3rd Quartile	96.9	71.65
Max	677.0	351.0
Standard Deviation	83.8	49.6
Skewness	2.5	2.0
Kurtosis	7.7	4.5

Figures 5.12(a), (b) and (c) represent the scatter plot of streamflows generated using APC2, NARR and CaPA respectively for the year 2010. From the plots, it is evident that the model is incapable of generating correct magnitude peak flows, especially with CaPA. Streamflow values are under-estimated in simulations using all three datasets.

**Figure 5.12(a): Scatter Plot Streamflows Using APC2 for 2010**

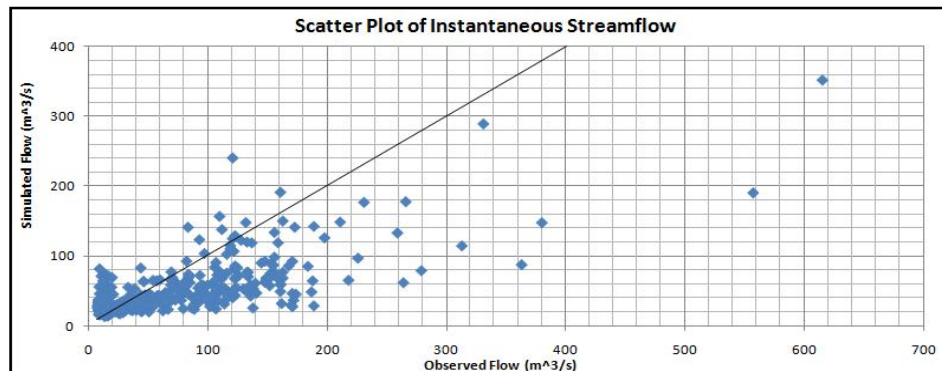


Figure 5.12(b): Scatter Plot Streamflows Using NARR for 2010

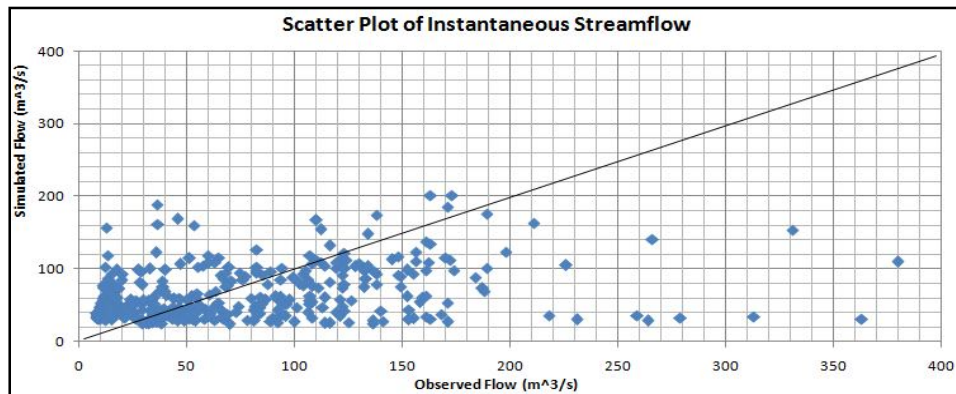


Figure 5.12(c): Scatter Plot Streamflows Using CaPA for 2010

Observed and simulated mean monthly streamflows for the period 2002-2010 are shown in Figure 5.13. The APC2 run over-estimates the winter streamflows and also the flow in June. The CaPA run shows better agreement for February, March, June and August. NARR data highly under-estimates the winter flow and over-estimates the flow in June. Comparing the three data types from bar plot; it is evident that APC2 works best for the model.

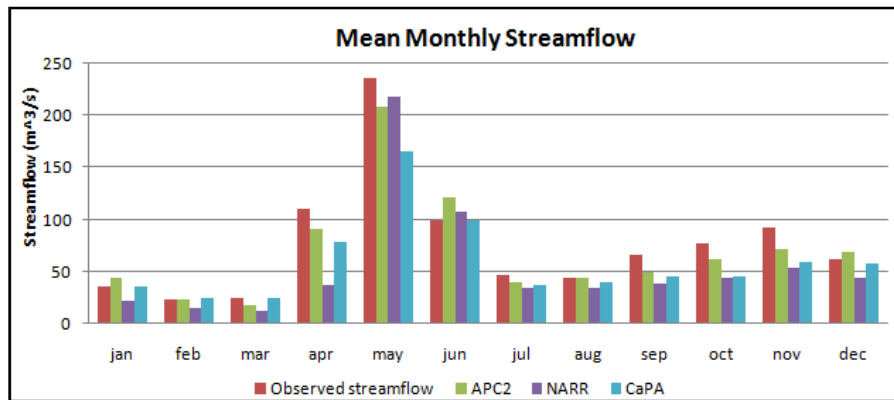


Figure 5.13: Bar Plot of Monthly Ensemble Streamflows (2002-2010)

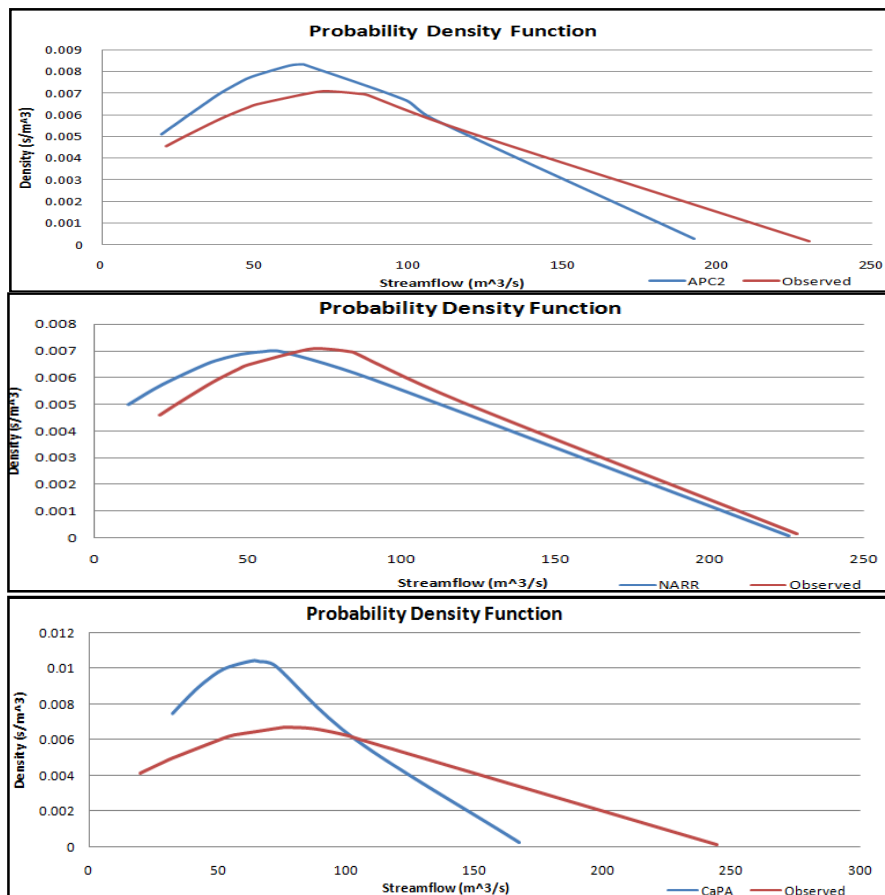


Figure 5.14: Probability Distribution Functions

Figure 5.14 shows the Probability Density Function (PDF) plots of monthly ensembles of observed and simulated streamflows with APC2, NARR and CaPA. A probability density function describes the relative likelihood for this random variable to take on a given value. The probability of the random variable falling within a particular range of values is given by the area under the density function above the horizontal axis and between the lowest and greatest values of the range. The probability density function is nonnegative everywhere, and its integral over the entire space is equal to one. Comparison with the PDF plot helps to identify the difference between the two datasets. The PDF plots show that there is good agreement between observed streamflow and NARR produced streamflow.

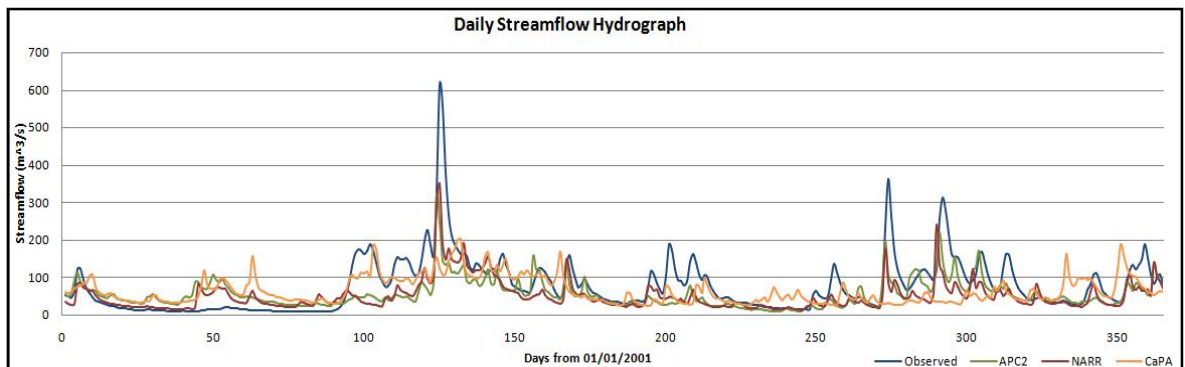


Figure 5.15: Comparison between Streamflows for 2011

Figure 5.15 shows observed and simulated daily streamflow hydrographs using APC2, NARR and CaPA for 2011. All the simulations are generally more or less effective in capturing the timing of spring melt and peak discharge. However, the hydrographs do not match well for the magnitude of summer and spring peaks. The hydrograph resulting from APC2 is most satisfactory. Both NARR and CaPA do not

perform well to simulate the correct magnitude of streamflows, but considering all the results discussed above NARR seems to provide a comparatively better result.

5.7 Model Initialization Results

As discussed in Chapter 4, model initialization was made with NARR and CaPA precipitation data. Results are compared with the initialization results alone from APC2 precipitation data and also with continuous model run results. At first, the total 30-year (1982-2011) simulation was generated with APC2. Then a model was run for the period 1982-2008 for which initial soil moisture, streamflow and lower zone storage were saved. The model was then initialized and run for the period 2009-2011 using APC2, NARR and CaPA. The resulted streamflow values were then compared with observations and also with simulated values obtained from the continuous run with APC2. Figure 5.16 shows the hydrographs generated from different datasets. Figure 5.17 shows the same plot but only for the first year (2009), for better observation of the differences in the hydrographs.

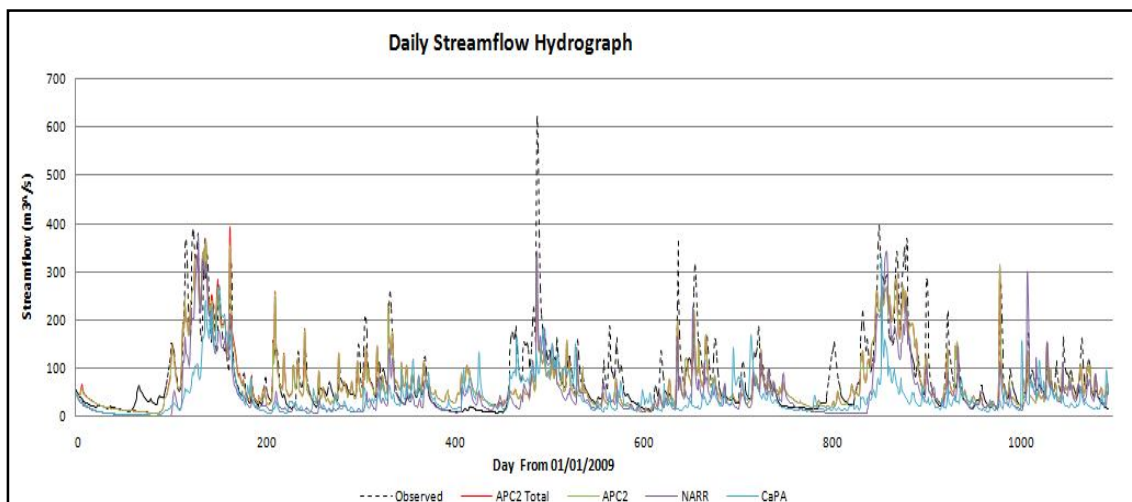


Figure 5.16: Hydrographs from Continuous Run and Initialization Runs (2009-2011)

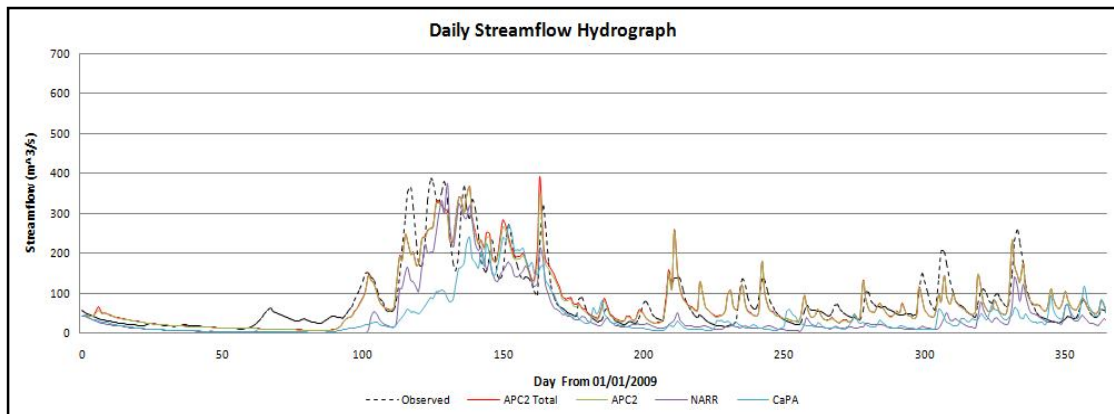


Figure 5.17: Hydrographs from Continuous Run and Initialization Runs (2009)

From the initialization runs, the differences between observed and simulated hydrographs generated using NARR and CaPA were calculated. The differences are plotted as a time series in Figure 5.18. It shows that the difference is higher in streamflows from the CaPA run. Also, the Nash-Sutcliffe for Reidville was found to be 0.44 and -0.01 with NARR and CaPA respectively (Table 5.5).

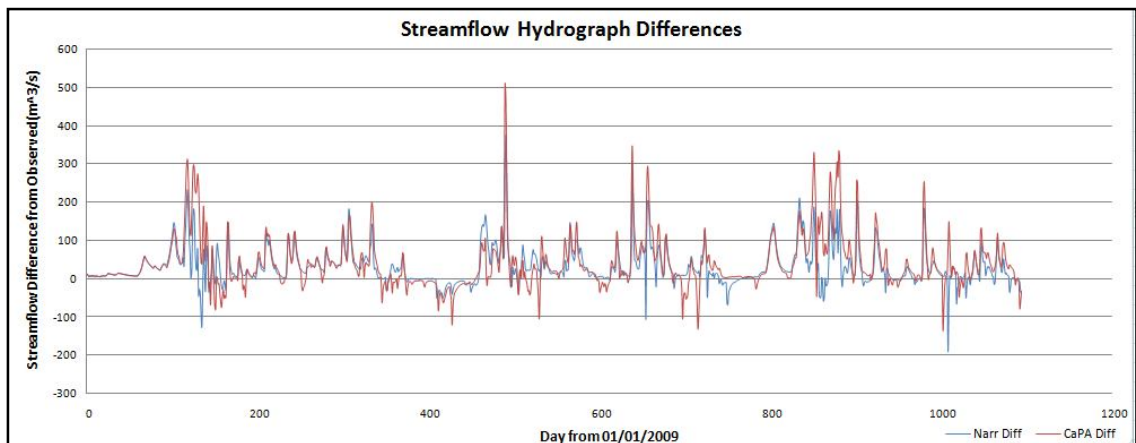


Figure 5.18: Simulation and Observation Hydrograph Differences Using NARR and CaPA

Table 5.5: Nash-Sutcliffe for Model Initialization with APC2, NARR and CaPA

Data	Nash-Sutcliffe
APC2(30 Year)	0.65
APC2 (3 Year)	0.61
NARR (3 Year)	0.44
CaPA (3 Year)	-0.01

It is difficult to comment on whether NARR or CaPA performs better. The performance of WATFLOOD when calibrated by these datasets is almost the same. However, comparing all the results discussed previously and judging by the streamflow simulations and Nash-Sutcliffe values, NARR can be recommended over CaPA as model forcing data for forecast simulations.

Chapter 6 Conclusions and Recommendations

The previous chapter discussed the results found from this study. It described the accuracy of the model set-up and compared APC2, NARR and CaPA in terms of the model objective function (N_r) and similarity in the patterns of observed and simulated streamflow hydrographs. This chapter presents the conclusions derived from the results and makes some recommendations for further study.

6.1 Conclusions

In this study the WATFLOOD model was set up as a base model for future flood forecasting studies in the Humber River basin (NL). The model was then calibrated with three different sets of precipitation and temperature data discussed in Chapter 3. The main findings of this study are provided below:

1. The initial model set up was checked with APC2 precipitation and historical temperature data. The simulated DA and lake areas were checked and matched. Reasonable streamflow simulations were obtained at nine selected stream gauge locations, which support the accuracy of the model set-up. The weighted average Nash-Sutcliffe efficiency was found to be 0.55 for the study period.

2. Satisfactory results were obtained at gauge locations at Reidville, Humber River at Village Bridge and Black Brook where discharges are important for flood forecasting. For Stations at Reidville, Humber River at Village Bridge and Upper Humber River at Black Brook, Nash-Sutcliffe values for the entire study period were found to be 0.65, 0.63 and 0.47 respectively.

3. DDS and PS optimization routines did not work well for this study. Due to time limitations, it was not possible to give more efforts in working out these optimization schemes. Therefore, manual adjustments were later done for model parameter optimization.

4. All three precipitation datasets were able to produce hydrographs that matched the observed hydrographs in the timing of peak discharges and base flows. NARR and CaPA failed to match the base of the hydrographs in winter periods. This is obvious, as a noticeably lower estimation of winter precipitation is observed in these datasets. However, this time is not critical for flood forecasting, so the model can be used for forecasting.

5. All the precipitation datasets underestimated the streamflow simulation in all the stations except Sheffield Brook and Lewaseechjeech Brook. A more accurate prediction could be achieved at the majority of the stations by increasing the lapse rate, but this resulted in over-estimation of flows in Sheffield Brook and Lewaseechjeech Brook. As the main focuses of the study were the Upper Humber near Reidville and Black Brook, lapse rate adjustments were made based mainly on the results simulated at these locations. Lower level of modeled results could be due to the underestimation of the precipitation that actually occurred at the measuring sites. Also, the use of higher channel roughness possibly reduced the simulated streamflow.

6. Both linear and non-linear bias corrections were made on the precipitation data and a linear bias correction was made on the temperature data. Unfortunately, the bias

corrected datasets failed to produce a better result. Therefore, uncorrected NARR data were used later for model calibration. The failure of NARR data in producing better result may be due to the facts that:

i) Meteorological data at Deer Lake alone were used for bias correction, which is not a perfect representation of the entire watershed;

ii) Corrections were made based on APC2 precipitation and historical temperature data, but rain gauges do not accurately predict the areal distribution of rainfall. APC2 itself is an adjusted dataset, which might not be very representative of the actual situation.

iii) Adjustment of a gridded 3-hourly dataset based on a gauge daily dataset might have destroyed the basic structure and efficiency of NARR data.

7. Among the three datasets, APC2 provided the best result ($N_r = 0.55$), followed by NARR and CaPA. It is difficult to comment on whether NARR or CaPA is more accurate, as they produced somewhat similar results. Based on N_r values and pattern of hydrographs, NARR seems to be better.

8. As APC2 has a production lag, one of the study objectives was to find an up-to-date dataset for flood forecasting analysis. NARR data is recommended for this purpose based on the results of this study.

6.2 Recommendations

This study developed a base model that can be further used for flood forecasting study in the Humber River basin. It also characterized a number of dataset that may be used as model forcing data. Due to the limited time, other possibilities of model performance enhancement could not be examined in this current study. Two of the

options among others can be: (i) lapse rate adjustment to increase the gridded precipitation and (ii) increasing the average NARR precipitation by a certain percentage of actual amounts. This research work could be extended by future researchers for the same watershed and other similar watersheds. Future work recommendations are discussed below.

1. The study was able to obtain a satisfactory model setup, and the initialization run also seems to be working well. The model should be tested for future simulation with forecast data from weather model as the next analysis step. For this purpose, GEM weather model data can be used.

2. Land cover changes have large effects on streamflow. In this study only four land cover types were used, including only one type of vegetation for the entire basin. More land cover types could be included to examine the effects of land cover in this region and to check whether model performance could be enhanced.

3. Model calibration is an essential first step in the application of WATFLOOD to a particular watershed. More works need to be done to improve the calibration of the model. The present calibration parameters should be reevaluated. Though no improvement in fitting the parameters were made from the DDS or PS routine in this research, they should be retried within the model. New parameters not optimized in this study could be optimized.

4. Bias correction should be made based on all the available station data within and closely around the basin. Bias correction for CaPA data should be done to check if it enhances model performance.

5. Precipitation bias correction for winter periods alone could be made to check the improvement in winter streamflow simulations.

6. Calibration was made based on streamflow alone. Streamflow is instantaneous result, where reservoir levels are cumulative results that tend to accumulate error over time. As a result, the error associated with model can be easily captured by running longer simulations. Therefore, calibration based on both streamflow and reservoir levels will be a better option over calibration with streamflow alone.

7. Though the WATFLOOD model seems to be working correctly in this study for simulation of streamflows, other hydrological processes (such as upper zone storage, evaporation, infiltration etc.) should also be checked. However, this would require field data that does not exist.

8. A more effective and accurate model initialization technique should be developed in future for initialization of the forecast model.

Bibliography

Abbot, M. B., et al. "An Introduction to European Hydrological System-"SHE"." *J. Journal of Hydrology* 87.1: History and Philosophy of a Physically Based Distributed Modeling System (1986): 45-59. Print.

Baxter, C. W., D. W. Smith, and S. J. Stanley. "A Comparison of Artificial Neural Networks and Multiple Regression Methods for the Analysis of Pilot-Scale Data." *J. Environmental Engineering and Science* 3(SI) (2004): S45-S58. Print.

Beven, K. "Changing Ideas in Hydrology- the Case of Physically-Based Models." *J. Journal of Hydrology* 105 (1989): 157-172. Print.

Bingeman, A. K., et al. "Validation of the Hydrological Processes in a Hydrological Model." *J. Journal of Hydrologic Engineering* 11(5) (2006): 451-463. Print.

Bostock, Hugh S. "Physiographic Subdivisions of Canada," Ottawa, ON, Canada: Geological Survey of Canada, Department of Energy, Mines and Resources, 1970. Print.

Brasnett, Bruce. "A Global Analysis of Sea Surface Temperature for Numerical Weather Prediction." *J. Atmospheric-Ocean Technology* 14 (1997): 925-937. Print.

Brasnett, Bruce. "A Global Analysis of Snow Depth for Numerical Weather Prediction." *J. Journal of Applied Meteorology* 38 (1999): 726-740. Print.

Cai, Haijie. "Flood Forecasting on the Humber River using an Artificial Neural Network Approach." Master of Engineering Memorial University of Newfoundland, 2010. Print.St. John's, NL, Canada.

Campolo, M., A. Soldati, and P. Andreussi. "Artificial Neural Network Approach to Flood Forecasting in the River Arno." *J. Hydrologic Sciences Journal* 48(3): 381-398. Print.

Carlaw, Shari M. "Soil Moisture Accounting in Distributed Hydrologic Modelling." Master of Applied Science in Civil Engineering University of Waterloo, 2000. Print. Waterloo, Ontario, Canada.

Carrera, Marco L., and Vincent Fortin. "The Canadian Precipitation Analysis (CaPA)-Description and Current Status". *North American Drought Monitor - International Workshop*. 15-17 April, Ottawa, Ontario. 2008. Print.

CBC News. "Flooding Warning Issued in Deer Lake." May 17 2013. Web. <<http://www.cbc.ca/news/canada/newfoundland-labrador/flooding-warning-issued-in-deer-lake-1.1371929>>.

Choi, W., A. Moore, and P. F. Rasmussen. "Evaluation of Temperature and Precipitation Data from NCEP-NCAR Global and Regional Reanalysis for Hydrological Modelling in Manitoba". *CSE 18th Hydrotechnical Conference on Challenges for Water Resources Engineering in a Changing World*. August 2009, Winnipeg, Manitoba. Canadian Society for Civil Engineers (CSCE) , 2007. 22-24. Print.

Choi, Woonsup, et al. "Use of the North American Regional Reanalysis for Hydrological Modelling in Manitoba." *J. Canadian Water Resources Journal* 34(1) (2009): 17-36. Print.

Cockburn, Cumming. *Hydrotechnical Study of the Steady Brook Area*. Main Report ed. St. John's, NL, Canada: Canada Newfoundland Flood Damage Reduction Program, 1984. Print.

Coltelli, M., et al. "SIR-C/X-SAR Multifrequency Multipass Interferometry: A New Tool for Geological Interpretation." *J. Journal of Geophysical Research* 101 (1996): 23127-48. Print.

Cranmer, A. J., N. Kouwen, and S. F. Mousavi. "Proving WATLOOD: Modelling the Nonlinearities of Hydrologic Response to Storm Intensities." *J. Canadian Journal of Civil Engineering* 28 (2001): 837-855. Print.

Danh, N. T., H. N. Phien, and A. D. Gupta. "Neural Networkmodels for River Flow Forecasting. Water SA," 25(1): 33-40. Print.

Davison, Bruce. *Canadian Precipitation Analysis (CaPA) Data, Environment Canada*. CaPA data for Humber River Basin (NL), Personal communication, 2013.

Dawson, C. W., et al. "Flood Estimation at Ungauged Sites using Artificial Neural Networks." *J. Journal of Hydrology* 319 (2006): 391-409. Print.

Department of Environment and Conservation. "Humber Water Level Information." September 17 2013. Web. Government of Newfoundland and Labrador, Canada. <<http://www.env.gov.nl.ca/env/waterres/flooding/humber.html>>.

Devine, K. A., and Eva Mekis. "Field Accuracy of Canadian Rain Measurements." *J. Atmospheric-Ocean* 46(2): 213-227. Print.

Dibike, Y. B., and P. Coulibaly. "Validation of Hydrological Models for Climate Scenarios Simulation: The Case of Saguenay Watershed in Quebec." *J. Hydrological Processes* 21 (2007): 3132-3135. Print.

Ding, Y., et al. "Effects of Bias Correction on Precipitation Trend Over China." *J. Geophys. Res.* 112 (2007)Print.

Donald, J. R. "Snowcover Depletion Curves and Satellite Snowcover Estimates for Snowmelt Runoff Modelling." Ph. D. Thesis University of Waterloo, 1992. Print.ON, Canada: .

Ensor, L. A., and S. M. Robenson. "Statistical Characteristics of Daily Precipitation: Comparisons of Gridded and Point Datasets." *J. Journal of Applied Meteorology and Climatology* 47(9) (2008): 2468-2476. Print.

Fortin, Vincent. "Using GEM, CaPA and MESH to Predict Great Lakes Net Basin Supplies". *IUGLS Hydroclimate TWG Workshop*. May 18-19, Ottawa, ON, Canada. 2011. Print.

Franke, R. "Smooth Interpolation of Scatter Data by Local Thin Plate Splines." *J. Comp. and Maths. with Appls* 8 (1982): 237-281. Print.

Gamache, M. "Free and Low Cost Datasets for International Mountain Cartography." (2004)Print.

"Global Energy Observatory." 2012-03-06 2012.Web.
<<http://globalenergyobservatory.org/geoid/42944>>.

Goodison, B. E. *Canadian Geographer*. Ed. M. K. Woo. 29 Vol. , 1985. Print. Snow in Focus: Hydrology of Snow and Ice .

Goodrich, Robert L. *Applied Statistical Forecasting*. Belmont, MA: Business Forecast Systems Inc., 1989. Print.

Google Earth V 7.1.1.1888 (June 21, 2012). Gillards Lake, Island of Newfoundland, 49°25' 33" N, 56°37' 19.04" W, Eye alt 8.4km. SIO, NOAA, U.S Navy, NGA, GEBCO. DigitalGlobe 2013. <http://www.earth.google.com> [September 4, 2013].

Gourrion, J. *Ku-Band Wind Speed Model Functions Via Neural Network Methods.*, 2000. Print. Technical Report DOS, French Research Institute for Exploitation of the Sea, Vol. 2000-02.

Harberlandt, U., and G. W. Kite. "Estimaton of Daily Space-Time Precipitation Series for Macroscale Hydrologic Modelling." *J. Hydrological Processes* 12(9) (1998): 1419-1432. Print.

Hargreaves, G. H., and Z. A. Samani. "Estimating Potential Evapotranspiration." *ASCE, J. Irrigation and Drainage Division* 108(3) (1982): 225-263. Print.

Hutchinson, M. F., and T. I. Dowling. "A Continental Hydrological Assessment of a New Grid-Based Digital Elevation Model of Australia." *J. Hydrological Processes* 5 (1991): 45-58. Print.

Hutchinson, M. F. "A New Procedure for Gridding Elevation and Stream Line Data with Automatic Removal of Spurious Pits." *J. Journal of Hydrology* 106 (1989): 211-232. Print.

Andrew, J. *Flooding-Canada Water Book*. 1993rd ed. Ottawa, ON, Canada: Environment Canada, 1993. Print.

Jarvis, A., et al. "Hole-Filled SRTM for the Globe, Version 4." 2008.Web. CGIAR-CSI.

Johanson, R. C., et al. *User's Manual for Hydrologic Simulation Program-Fortran (HSPS)*. 70th ed. Athens, Georgia: U.S. Environmental Protection Agency, 1981. Print.

Joon, Kim Sung. "Evaluation of Surface Climate Data from the North American Regional Reanalysis for Hydrological Applications in Central Canada." Doctor of Philosophy, University of Manitoba, 2012. Print. Winnipeg, Canada: .

Devine, K. A. and Eva Mekis. "Field Accuracy of Canadian Rain Measurements." *J. Atmospheric-Ocean* 46(2) (2008): 213-227. Print.

Kalnay, E., et al. "The NCEP-NCAR Reanalysis Project." *Bulletin of the American Meteorological Society* 77(3) (1996): 437-471. Print.

Kite, G. W. "The Development of a Hydrologic Model for Resource Planning." *Proc. Canadian Hydrology Symposium* 92 (1992): 330-348. Print.

Kittel, T. G. F., et al. "VEMAP Phase 2 Bioclimate Database I. Grodden Historical (20th Century) Climate for Modelling Ecosystem Dynamics Across the Conterminous USA." *J. Climate Research* 27 (2004): 151-170. Print.

Kouwen, N., et al. "Case Study: Watershed Modelling with Distributed Weather Model Data." *J. Journal of Hydrologic Engineering* 10(1) (2005): 23-38. Print.

Kouwen, N., et al. "Grouped Response Units for Distributed Hydrologic Modelling." *J. Journal of Water Resources Planning and Management* 119(3) (1993): 289-305. Print.

Kouwen, Nicholas. *WATFLOOD/WATROUTE: Hydrological Model Routing & Flow Forecasting System (Manual)*., 2011. Print.

Kouwen, Nicholas. "WATFLOOD: A Micro-Computer Based Flood Forecasting System Based on Real-Time Weather Radar." *J. Canadian Water Resources Journal* 13 (1988): 62-77. Print.

Lawford, R. G., et al. "Hydrometeorological Aspects of Flood Hazards in Canada." *J. Atmospheric-Ocean* 33:2 (1995): 303-328. Print.

Leander, Robert, and T. Adri Buishand. "Resampling of Regional Climate Model Output for the Simulation of Extreme River Flows." *J. Journal of Hydrology* 332 (2007): 487-496. Print.

Li, X., D. W. Smith, and E. E. Prepas. "Artificial Neural Network Modelling of Nitrogen in Streams: With Emphasis on Accessible Database". *CSCE 2008 Annual Conference*. Quebec, Canada. 2008. Print.

Mahfouf, Jean-Francois, Bruce Brasnett, and Stephanie Gagnon. "A Canadian Precipitation Analysis (CaPA) Project: Description and Preliminary Results." *J. Atmospheric-Ocean* 45:1 (2007): 1-17. Print.

McBratney, A. B., and R. Webster. "Choosing Functions for Semi-Variograms of Soil Properties and Fitting them to Sampling Estimates." *J. Journal of Soil Science* 37 (1986): 617-639. Print.

Mekis, Eva. Second Generation Adjusted Precipitation Dataset for Newfoundland, Personal Communication, 2013.

Mekis, Eva, and R. Brown. "Derivation of an Adjustment Factor Map for the Estimation Equivalent of Snowfall from Ruler Measurements in Canada." *J. Atmospheric-Ocean* 48(4) (2010): 284-293. Print.

Mekis, Eva, and W. D. Hogg. "Rehabilitation and Analysis of Canadian Daily Precipitation Time Series." *J. Atmospheric-Ocean* 37(1) (1999): 53-85. Print.

Mekis, Eva, and Lucie A. Vincent. "An Overview of the Second Generation Adjusted Daily Precipitation Dataset for Trend Analysis in Canada." *Atmospheric -Ocean*, 49 (2011): 163-177. Print.

Mesinger, Fedor, et al. "North American Regional Reanalysis." *Bulletin of the American Meteorological Society* 87(3) (2006): 343-360. Print.

Mitas, L., and H. Mitasova. "General Variational Approach to the Interpolation Problem." *J. Comput. Math. Applic* 16 (1988): 983-992. Print.

Moore, I., R. Grayson, and A. Ladson. "Digital Terrain Modelling: A Review of Hydrological, Geomorphological, and Biological Applications." *Hydrological Processes* 5: 3-30. Print.

"NHN Work Units, Geobase." 2009-04-13, 2009. Web. <<http://www.geobase.ca/geobase/en/data/nhn/units.html>>.

Nigam, S., and A. Ruiz-Barradas. "Seasonal Hydroclimate Variability Over North American Global and Regional Reanalysis and AMIP Simulations: Varied Representation." *J. Journal of Climate* 19(5) (2006): 815-837. Print.

Noto, Leonardo V., et al. "Effects of Initialization on Response of a Fully-Distributed Hydrologic Model." *J. Journal of Hydrology* 352 (2007): 107-125. Print.

Philip, J. R. "An Infiltration Equation with Physical Significance." *J. Soil Science* 77(1) (1954): 153-157. Print.

Picco, Robert C. "A Comparative Study of Flow Forecasting in the Humber River Basin using a Deterministic Hydrologic Model and a Dynamic Regression Statistical Model." Master of Engineering Memorial University of Newfoundland, 1997. Print. St. John's, NL, Canada.

Reuter, H. I., A. Nelson, and A. Jarvis. "An Evaluation of Void Filling Interpolation Methods for SRTM." *J. International Journal of Geographical Information Science* 21(9) (2007): 983-1008. Print.

Roberts, Jonas, Amy Pryse-Phillips, and Ken Snelgrove. "Modeling the Potential Impacts of Climate Change on a Small Watershed in Labrador, Canada." *J. Canadian Water Resources Journal* 37(3) (2012): 231-251. Print.

Savelieva, E. "Automatic Spatial Prediction with General Regression Neural Network (GRNN)." *Nuclear Safety Institute (IBRAE) of Russian Academy of Science*. 1(2) (2004) Print.

Shrestha, Rajesh R., Yonas B. Dibiye, and Terry D. Prowse. "Modelling of Climate-Induced Hydrologic Changes in the Lake Winnipeg Watershed." *J. Journal of Great Lakes Research* (2011) Print.

Singh, Vijay P., ed. *Hydrologic Systems: Watershed Modelling*. 2 Vol. New Jersey: Prentice - Hall, Inc. Division of Simon & Schuster Englewood Cliffs, 1989. Print.

Solaiman, Tarana A., and Slobodan P. Simonovic. "National Centers for Environmental Prediction- National Center for Atmospheric Research (NCEP-NCAR) Reanalysis Data

for Hydrologic Modelling on a Basin Scale." *J. Canadian Journal of Civil Engineering* 37 (2010): 611-623. Print.

"SRTM Data Processing Methodology." *The CGIAR Consortium for Special Information (CGIAR-CSI)*. 2004. Web.

<<http://srtm.csi.cgiar.org/SRTMdataProcessingMethodology.asp>>.

Stadnyk, T. "International Workshop on the Application of Isotope Techniques in Hydrological and Environmental Studies, UNESCO." *Validation of Hydrological Models Using Stable Isotope Tracers*. Paris, France. 2004. Print.

Statistics Canada. *Community Profile - Corner Brook, Newfoundland and Labrador.*, 2006. Print.

Tang, P. W., and J. G. Lockhart. *Technology Transfer Workshop, Technical Workshop Series No. 5, Inland Water Directorate, Environment Canada*. Ottawa, ON, Canada. 1983. Print.

Terink, W., et al. "Bias Correction of Temperature and Precipitation Data for Regional Climate Model Application to the Rhine Basin." *J. Hydrology and Earth System Sciences* (2009): 5377-5413. Print.

W. E., Watt, and Nozdryn-Plotnicki M. J. "Hydrology of Floods in Canada- A Guide to Planning and Design." *J. National Research Council of Canada* (1989): 245. Print.

Ward System Group, Inc. *Neuroshell 2, Release 4.0.*, 2000. Print.

Watson, D. F., and G. M. Philip. "A Refinement of Inverse Distance Weighted Interpolation." *J. Geo-Processing* 2 (1985): 75-79. Print.

Western, A. W., R. B. Grayson, and T. R. Green. "The Tarrawarra Project: High Resolution Spatial Measurement, Modelling and Analysis of Soil Moisture and Hydrological Response." *Hydrological Processes* 13: 633-652. Print.

Williams, Mark. "Hydrological Modeling, Guggenheim Kesda Lab." 2004. Web. <http://snobear.colorado.edu/Markw/geog5321_webpage_04.html>.

Woo, M. K., and R. Thorne. "Snowmelt Contribution to Discharge from a Large Mountainous Catchment in Subarctic Canada." *J. Hydrological Processes* 20 (10) (2006): 2129-2139. Print.

Zhang, X., et al. "Temperature and Precipitation Trends in Canada during the 20th Century." *J. Atmospheric-Ocean* 38 (2000): 395-429. Print.

Appendix A: Parameter File for APC2

:FileType	WatfloodParameter	10.1	# parameter file version number			
:CreationDate	#####					
:GlobalParameters						
:iopt	1	# debug level				
:itype	0	# channel type - floodplain/no				
:itrace	4	# Tracer choice				
:a1	1	# ice cover weighting factor				
:a2	1	# Manning's correction for instream lake				
:a3	0.05	# error penalty coefficient				
:a4	0.03	# error penalty threshold				
:a5	0.985	# API coefficient				
:a6	900	# Minimum routing time step in seconds				
:a7	0.9	# weighting - old vs. new sca value				
:a8	0.1	# min temperature time offset				
:a9	0.333	# max heat deficit /swe ratio				
:a10	2	# exponent on uz discharge function				
:a11	0.01	# bare ground equiv. veg height for ev				
:a12	0.001	# min precip rate for smearing				
:fmadjust	0	# snowmelt ripening rate				
:fmalow	0	# min melt factor multiplier				
:fmahigh	0	# max melt factor multiplier				
:gladjust	0	# glacier melt factor multiplier				
:rlapse	0	# precip lapse rate mm/km				
:tlapse	-0.0065	# temperature lapse rate dC/km				

:elvref	0	# reference elevation		
:rainsnowtemp	0	# rain/snow temperature		
:radiusinflce	300	# radius of influence km		
:smoothdist	35	# smoothing distance km		
:flgevp2	2	# 1=pan;2=Hargreaves;3= Priestley-Taylor		
:albe	0.11	# albedo????		
:tempa2	500	#		
:tempa3	500	#		
:tton	0	#		
:lat	50	# latitude		
:chnl(1)	1	# manning's n multiplier		
:chnl(2)	0.9	# manning's n multiplier		
:chnl(3)	0.7	# manning's n multiplier		
:chnl(4)	0.7	# manning's n multiplier		
:chnl(5)	0.6	# manning's n multiplier		
:EndGlobalParameters				
#				
:RoutingParameters				
:RiverClasses	3			
:RiverClassName	class1	class2	class3	
:flz	1.00E-06	1.00E-06	1.00E-06	# lower zone coefficient
:pwr	2.5	2	2.5	# lower zone exponent
:r1n	0.12	0.12	0.12	# overbank Manning's n
:r2n	0.4	4.00E-02	2.80E-02	# channel Manning's n
:mndr	1	1	1	# meander channel length multiplier
:aa2	1.1	1.1	1.1	# channel area intercept = min channel xsect area
:aa3	1.00E-02	1.00E-02	1.00E-02	# channel area coefficient

:fratio	1	1	1	1	1	# int. capacity multiplier
:EndHydrologicalParameters						
#						
:SnowParameters						
:fm	0.08	0.08	0.08	0.1	0.15	# melt factor mm/dC/hour
:base	-4.5	-4.5	-4.5	-4.5	0	# base temperature dC
:fmn	0.1	0.1	0.1	0.1	0.1	# -ve melt factor
:uadj	0	0	0	0	0	# not used
:tipm	0.1	0.1	0.1	0.1	0.1	# coefficient for ati
:rho	0.333	0.333	0.333	0.333	0.333	# snow density
:whcl	0.035	0.035	0.035	0.035	0.035	# fraction of swe as water in ripe snow
:alb	0.11	0.11	0.11	0.11	0.11	# albedo
:sublim_factor	-0.1	-0.1	-0.1	-0.1	-0.1	# sublimation factor ratio
:idump	2	4	4	5	6	# receiving class for snow redistribution
:snocap	-600	-600	-600	-600	-600	# max swe before redistribution
:nsdc	2	2	2	2	2	# no of points on scd curve - only 1 allowed
:sdcscsca	1	1	1	1	1	# snow covered area - ratio=1.0
:sdccl	200	150	150	1	100	# swe for 100% snow covered area
:EndSnowParameters						
#						
:InterceptionCapacityTable						
:IntCap_Jan	1.2	0.65	0.65	0.11	0.01	# interception capacity jan mm
:IntCap_Feb	1.2	0.65	0.65	0.11	0.01	# interception capacity feb mm
:IntCap_Mar	1.2	0.65	0.65	0.11	0.01	# interception capacity mar mm
:IntCap_Apr	1.2	0.65	0.65	0.11	0.01	# interception capacity apr mm
:IntCap_May	1.6	1.06	0.85	0.11	0.01	# interception capacity may mm
:IntCap_Jun	1.9	1.56	1	0.11	0.01	# interception capacity jun mm

:IntCap_Jul	1.9	1.56	1	0.11	0.01	# interception capacity jul mm
:IntCap_Aug	1.9	1.56	1	0.11	0.01	# interception capacity aug mm
:IntCap_Sep	1.9	1	1	0.11	0.01	# interception capacity sep mm
:IntCap_Oct	1.2	0.65	0.65	0.11	0.01	# interception capacity oct mm
:IntCap_Nov	1.2	0.65	0.65	0.11	0.01	# interception capacity nov mm
:IntCap_Dec	1.2	0.65	0.65	0.11	0.01	# interception capacity dec mm
:EndInterceptionCapacityTable						
#						
:MonthlyEvapotranspirationTable						
:Montly_ET_Jan	0	0	0	0	0	# monthly evapotranspiration jan mm
:Montly_ET_Feb	0	0	0	0	0	# monthly evapotranspiration feb mm
:Montly_ET_Mar	0	0	0	0	0	# monthly evapotranspiration mar mm
:Montly_ET_Apr	0	0	0	0	0	# monthly evapotranspiration apr mm
:Montly_ET_May	0	0	0	0	0	# monthly evapotranspiration may mm
:Montly_ET_Jun	0	0	0	0	0	# monthly evapotranspiration jun mm
:Montly_ET_Jul	0	0	0	0	0	# monthly evapotranspiration jul mm
:Montly_ET_Aug	0	0	0	0	0	# monthly evapotranspiration aug mm
:Montly_ET_Sep	0	0	0	0	0	# monthly evapotranspiration sep mm
:Montly_ET_Oct	0	0	0	0	0	# monthly evapotranspiration oct mm
:Montly_ET_Nov	0	0	0	0	0	# monthly evapotranspiration nov mm
:Montly_ET_Dec	0	0	0	0	0	# monthly evapotranspiration dec mm
:EndMonthlyEvapotranspirationTable						
#						
:OptimizationSwitches						
:numa	0	# PS optimization 1=yes 0=no				
:nper	1	# opt 1=delta 0=absolute				
:kc	2	# no of times delta halved				

:maxn	10	# max no of trials				
:ddsflg	0	# 0=single run 1=DDS				
:errflg	7	# 1=wMSE 2=SSE 3=wSSE 4=VOL				
:EndOptimizationSwitches						
#						
:APILimits						
:a5dlt	-1.00E-03					
:a5low	0.98					
:a5hgh	0.999					
:EndAPILimits						
#						
:HydrologicalParLimits						
:ClassName	vegetation	wetland	wetland	water	impervious	
# infiltration coefficient bare ground						
:akdlt	-0.02	-0.02	-0.02	-0.02	-0.02	
:aklow	0.4	0.004	0.004	0.04	0.04	
:akhgh	50	0.05	0.05	5	5	
# infiltration coefficient snow covered ground						
:akfsdlt	-0.02	-0.02	-0.02	-0.02	-0.02	
:akfslow	0.04	0.04	0.04	0.04	0.04	
:akfshgh	20	5	5	5	5	
# interflow coefficient						
:recdlt	-2.00E-02	-2.00E-02	-2.00E-02	-2.00E-02	-2.00E-02	
:reclow	5.00E-04	5.00E-04	5.00E-04	5.00E-04	5.00E-04	
:rechgh	0.1	0.1	0.1	0.1	0.1	
# overland flow roughness coeff bare ground						
:r3dlt	-2.00E-02	-2.00E-02	-2.00E-02	-2.00E-02	-2.00E-02	

:r3low	1	1	1	1	1	
:r3hgh	10	10	10	10	10	
# interception evaporation factor * pet						
:fpetdlt	-2.00E-02	-2.00E-02	-2.00E-02	-2.00E-02	-2.00E-02	
:fpetlow	5.00E-02	5.00E-02	5.00E-02	5.00E-02	5.00E-02	
:fpehgh	3	3	3	3	3	
# reduction in PET for tall vegetation						
:ftalldlt	-1	-1	-1	-1	-1	
:ftalllow	0.1	0.1	0.1	0.1	0.1	
:ftalhgh	10	10	10	10	10	
# multiplier for interception capacity						
:fratiodlt	-1	-1	-1	-1	-1	
:fratiolow	0.1	0.1	0.1	0.1	0.1	
:fratiohgh	10	10	10	10	10	
# upper zone retention mm						
:retndlt	-2.00E-02	-2.00E-02	-2.00E-02	-2.00E-02	-2.00E-02	
:retnlow	1.00E-02	1.00E-02	1.00E-02	1.00E-02	1.00E-02	
:retnhgh	0.3	0.3	0.3	0.3	0.3	
# recharge coefficient bare ground						
:ak2dlt	-2.00E-02	-2.00E-02	-2.00E-02	-2.00E-02	-2.00E-02	
:ak2low	1.00E-04	1.00E-04	1.00E-04	1.00E-04	1.00E-04	
:ak2hgh	0.1	0.1	0.1	0.1	0.1	
# recharge coefficient snow covered ground						
:ak2fsdlt	-2.00E-02	-2.00E-02	-2.00E-02	-2.00E-02	-2.00E-02	
:ak2fslow	0	0	0	0	0	
:ak2fshgh	0.1	0.1	0.1	0.1	0.1	
:EndHydrologicalParLimits						

#						
:GlobalSnowParLimits						
# snowmelt ripening rate						
:fmadjustdlt	-1					
:fmadjustlow	0.1					
:fmadjusthgh	1					
# min melt factor multiplier						
:fmalowdlt	-0.1					
:fmalowlow	0					
:fmalowhgh	0.75					
# max melt factor multiplier						
:fmahighdlt	-0.1					
:fmahighlow	0.75					
:fmahighhgh	1.5					
# glacier melt factor multiplier						
:gladjustdlt	-0.1					
:gladjustlow	0.5					
:gladjusthgh	1.5					
:EndGlobalSnowParLimits						
#						
:SnowParLimits						
:ClassName	vegetation	wetland	wetland	water	impervious	
# melt factor mm/dC/hour						
:fmdlt	5.00E-02	5.00E-02	5.00E-02	5.00E-02	5.00E-02	
:fmlow	5.00E-02	5.00E-02	5.00E-02	5.00E-02	5.00E-02	
:fmhgh	0.5	0.55	0.55	0.55	0.55	
# base temperature dC						

:basedlt	2.00E-03	2.00E-03	2.00E-03	2.00E-03	2.00E-03	
:baselow	-5	-5	-5	-5	-5	
:basehgh	5	5	5	5	5	
# sublimation factor OR ratio						
:subdlt	1.00E-03	1.00E-03	1.00E-03	1.00E-03	1.00E-03	
:sublow	-5.00E-02	-5.00E-02	-5.00E-02	-5.00E-02	-5.00E-02	
:subhgh	0.5	0.5	0.5	0.5	0.5	
:EndSnowParLimits						
#						
:RoutingParLimits						
:RiverClassName	class1	class2	class3			
# lower zone coefficient						
:flzdlt	2.00E-02	2.00E-02	2.00E-02			
:flzlow	1.00E-07	1.00E-07	1.00E-07			
:flzhgh	1.00E-04	1.00E-04	1.00E-04			
# lower zone exponent						
:pwrdlt	2.00E-02	2.00E-02	2.00E-02			
:pwrlow	0.3	0.3	0.3			
:pwrhgh	4	4	4			
# channel Manning's n						
:r2ndlt	-2.00E-02	-2.00E-02	-2.00E-02			
:r2nlow	1.00E-02	1.00E-02	1.00E-02			
:r2nhgh	0.5	0.5	0.5			
# wetland or bank porosity						
:thetadlt	2.00E-02	2.00E-02	2.00E-02			
:thetalow	0.1	0.1	0.1			
:thetahgh	0.6	0.6	0.6			

# wetland/bank lateral conductivity					
:kcondlft	2.00E-02	2.00E-02	2.00E-02		
:kcondlow	0.1	0.1	0.1		
:kcondhgh	0.9	0.9	0.9		
# in channel lake retardation coefficient					
:rlakedlft	-0.1	-0.1	-0.1		
:rlakelow	0	0	0		
:rlakehgh	3	3	3		
:EndRoutingParLimits					
#					
:GlobalParLimits					
# precip lapse rate					
:rlapsedlft	0				
:rlapselow	0				
:rlapsehgh	0				
# temperature lapse rate					
:tlapsedlft	0				
:tlapselow	0				
:tlapsehgh	0				
# radius of influence					
:radinflft	0				
:radinflw	0				
:radinflhgh	0				
# smoothing distance					
:smoothdislft	0				
:smoothdislow	0				
:smoothdishgh	0				

:EndGlobalParLimits						
#						

Appendix B: Parameter File for NARR

:FileType	WatfloodParameter	10.1	# parameter file version number		
:CreationDate	#####				
:GlobalParameters					
:iopt	1	# debug level			
:itype	0	# channel type - floodplain/no			
:itrace	4	# Tracer choice			
:a1	1	# ice cover weighting factor			
:a2	1	# Manning's correction for instream lake			
:a3	0.05	# error penalty coefficient			
:a4	0.03	# error penalty threshold			
:a5	0.985	# API coefficient			
:a6	900	# Minimum routing time step in seconds			
:a7	0.9	# weighting - old vs. new sca value			
:a8	0.1	# min temperature time offset			
:a9	0.333	# max heat deficit /swe ratio			
:a10	2	# exponent on uz discharge function			
:a11	0.01	# bare ground equiv. veg height for ev			
:a12	0.001	# min precip rate for smearing			
:fmadjust	0	# snowmelt ripening rate			
:fmalow	0	# min melt factor multiplier			
:fmahigh	0	# max melt factor multiplier			
:gladjust	0	# glacier melt factor multiplier			
:rlapse	0.0002	# precip lapse rate mm/km			
:tlapse	-0.0065	# temperature lapse rate dC/km			
:elvref	0	# reference elevation			

:rainsnowtemp	0	# rain/snow temperature				
:radiusinflce	300	# radius of influence km				
:smoothdist	35	# smoothing distance km				
:flgevp2	2	# 1=pan;2=Hargreaves;3= Priestley-Taylor				
:albe	0.11	# albedo????				
:tempa2	1000	#				
:tempa3	1000	#				
:tton	0	#				
:lat	50	# latitude				
:chnl(1)	1	# manning's n multiplier				
:chnl(2)	0.9	# manning's n multiplier				
:chnl(3)	0.7	# manning's n multiplier				
:chnl(4)	0.7	# manning's n multiplier				
:chnl(5)	0.6	# manning's n multiplier				
:EndGlobalParameters						
#						
:RoutingParameters						
:RiverClasses	3					
:RiverClassName	class1	class2	class3			
:flz	1.00E-07	1.00E-07	1.00E-07	# lower zone coefficient		
:pwr	2	1.5	2	# lower zone exponent		
:r1n	0.12	0.12	0.12	# overbank Manning's n		
:r2n	0.4	4.00E-02	2.80E-02	# channel Manning's n		
:mndr	1	1	1	# meander channel length multiplier		
:aa2	1.1	1.1	1.1	# channel area intercept = min channel xsect area		
:aa3	1.00E-02	1.00E-02	1.00E-02	# channel area coefficient		
:aa4	1	1	1	# channel area exponent		

:theta	0.263	0.263	0.263	# wetland or bank porosity		
:widep	30	30	30	# channel width to depth ratio		
:kcond	7.00E-01	2.00E-01	7.00E-01	# wetland/bank lateral conductivity		
:pool	0	0	0	# average area of zero flow pools		
:rlake	0	0	0	# in channel lake retardation coefficient		
:EndRoutingParameters						
#						
:HydrologicalParameters						
:LandCoverClasses	5					
:ClassName	vegetation	wetland	wetland	water	impervious	# class name
:ds	10	1.00E+0 9	1.00E+09	0	1	# depression storage bare ground mm
:dsfs	10	1.00E+0 9	1.00E+09	0	1	# depression storage snow covered area mm
:rec	2	0.9	0.9	0.1	0.9	# interflow coefficient
:ak	12	400	400	-0.1	1.00E-11	# infiltration coefficient bare ground
:akfs	1.2	400	400	-0.1	1.00E-11	# infiltration coefficient snow covered ground
:retn	70	0.4	0.4	0.1	0.1	# upper zone retention mm
:ak2	0.1	2.00E-02	2.00E-02	1.00E-03	1.00E-11	# recharge coefficient bare ground
:ak2fs	0.1	2.00E-02	2.00E-02	1.00E-03	1.00E-11	# recharge coefficient snow covered ground
:r3	8.48E-02	8.98E-02	8.98E-02	4.00E-02	4	# overland flow roughness coeff bare ground
:r3fs	0.1	0.1	0.1	4.00E-02	4	# overland flow roughness coeff snow covered
:r4	10	10	10	10	10	# overland flow roughness coeff impervious
:fpet	2	3	3	1	1	# interception evaporation factor * pet
:ftall	0.7	1	1	0	1	# reduction in PET for tall vegetation
:flint	1	1	1	1	1	# interception flag 1=on <1=off

:fcap	0.15	0.15	0.15	0.15	0.15	# not used - replaced by retn (retention)
:ffcap	0.1	0.1	0.1	0.1	0.1	# wilting point - mm of water in uzs
:spore	0.33	0.33	0.33	0.33	0.33	# soil porosity
:fratio	1	1	1	1	1	# int. capacity multiplier
:EndHydrologicalParameters						
#						
:SnowParameters						
:fm	0.06	0.06	0.06	0.08	0.1	# melt factor mm/dC/hour
:base	-4	-4	-4	-4	1	# base temperature dC
:fmn	0.1	0.1	0.1	0.1	0.1	# -ve melt factor
:uadj	0	0	0	0	0	# not used
:tipm	0.1	0.1	0.1	0.1	0.1	# coefficient for ati
:rho	0.333	0.333	0.333	0.333	0.333	# snow density
:whcl	0.035	0.035	0.035	0.035	0.035	# fraction of swe as water in ripe snow
:alb	0.11	0.11	0.11	0.11	0.11	# albedo
:sublim_factor	-0.3	-1	-1	-1	-0.3	# sublimation factor ratio
:idump	2	4	4	5	6	# receiving class for snow redistribution
:snocap	-600	-600	-600	-600	-600	# max swe before redistribution
:nsdc	2	2	2	2	2	# no of points on scd curve - only 1 allowed
:sdcsca	1	1	1	1	1	# snow covered area - ratio=1.0
:sdcd	200	150	150	1	100	# swe for 100% snow covered area
:EndSnowParameters						
#						
:InterceptionCapacityTable						
:IntCap_jan	1.2	0.65	0.65	0.11	0.01	# interception capacity jan mm

:IntCap_Feb	1.2	0.65	0.65	0.11	0.01	# interception capacity feb mm
:IntCap_Mar	1.2	0.65	0.65	0.11	0.01	# interception capacity mar mm
:IntCap_Apr	1.2	0.65	0.65	0.11	0.01	# interception capacity apr mm
:IntCap_May	1.6	1.06	0.85	0.11	0.01	# interception capacity may mm
:IntCap_Jun	1.9	1.56	1	0.11	0.01	# interception capacity jun mm
:IntCap_Jul	1.9	1.56	1	0.11	0.01	# interception capacity jul mm
:IntCap_Aug	1.9	1.56	1	0.11	0.01	# interception capacity aug mm
:IntCap_Sep	1.9	1	1	0.11	0.01	# interception capacity sep mm
:IntCap_Oct	1.2	0.65	0.65	0.11	0.01	# interception capacity oct mm
:IntCap_Nov	1.2	0.65	0.65	0.11	0.01	# interception capacity nov mm
:IntCap_Dec	1.2	0.65	0.65	0.11	0.01	# interception capacity dec mm
:EndInterceptionCapacityTable						
#						
:MonthlyEvapotranspirationTable						
:Montly_ET_Jan	0	0	0	0	0	# monthly evapotranspiration jan mm
:Montly_ET_Feb	0	0	0	0	0	# monthly evapotranspiration feb mm
:Montly_ET_Mar	0	0	0	0	0	# monthly evapotranspiration mar mm
:Montly_ET_Apr	0	0	0	0	0	# monthly evapotranspiration apr mm
:Montly_ET_May	0	0	0	0	0	# monthly evapotranspiration may mm
:Montly_ET_Jun	0	0	0	0	0	# monthly evapotranspiration jun mm
:Montly_ET_Jul	0	0	0	0	0	# monthly evapotranspiration jul mm
:Montly_ET_Aug	0	0	0	0	0	# monthly evapotranspiration aug mm
:Montly_ET_Sep	0	0	0	0	0	# monthly evapotranspiration sep mm
:Montly_ET_Oct	0	0	0	0	0	# monthly evapotranspiration oct mm
:Montly_ET_Nov	0	0	0	0	0	# monthly evapotranspiration nov mm
:Montly_ET_Dec	0	0	0	0	0	# monthly evapotranspiration dec mm
:EndMonthlyEvapotranspirationTable						

#						
:OptimizationSwitches						
:numa	0	# PS optimization 1=yes 0=no				
:nper	1	# opt 1=delta 0=absolute				
:kc	2	# no of times delta halved				
:maxn	10	# max no of trials				
:ddsflg	0	# 0=single run 1=DDS				
:errflg	7	# 1=wMSE 2=SSE 3=wSSE 4=VOL				
:EndOptimizationSwitches						
#						
:APILimits						
:a5dlt	-1.00E-03					
:a5low	0.98					
:a5hgh	0.999					
:EndAPILimits						
#						
:HydrologicalParLimits						
:ClassName	vegetation	wetland	wetland	water	impervious	# class name
# infiltration coefficient bare ground						
:akdlt	-0.02	-0.02	-0.02	-0.02	-0.02	
:aklow	0.4	0.004	0.004	0.04	0.04	
:akhgh	50	0.05	0.05	5	5	
# infiltration coefficient snow covered ground						
:akfsdlt	-0.02	-0.02	-0.02	-0.02	-0.02	
:akfslow	0.04	0.04	0.04	0.04	0.04	
:akfshgh	20	5	5	5	5	
# interflow coefficient						

:recdlf	-2.00E-02	-2.00E-02	-2.00E-02	-2.00E-02	-2.00E-02	
:reclow	5.00E-04	5.00E-04	5.00E-04	5.00E-04	5.00E-04	
:rechgh	0.1	0.1	0.1	0.1	0.1	
# overland flow roughness coeff bare ground						
:r3dlf	-2.00E-02	-2.00E-02	-2.00E-02	-2.00E-02	-2.00E-02	
:r3low	1	1	1	1	1	
:r3hgh	10	10	10	10	10	
# interception evaporation factor * pet						
:fpetdlf	-2.00E-02	-2.00E-02	-2.00E-02	-2.00E-02	-2.00E-02	
:fpetlow	5.00E-02	5.00E-02	5.00E-02	5.00E-02	5.00E-02	
:fpethgh	3	3	3	3	3	
# reduction in PET for tall vegetation						
:ftalldf	-1	-1	-1	-1	-1	
:ftallow	0.1	0.1	0.1	0.1	0.1	
:ftalhgh	10	10	10	10	10	
# multiplier for interception capacity						
:fratiodf	-1	-1	-1	-1	-1	
:fratiolow	0.1	0.1	0.1	0.1	0.1	
:fratiohgh	10	10	10	10	10	
# upper zone retention mm						
:retnddf	-2.00E-02	-2.00E-02	-2.00E-02	-2.00E-02	-2.00E-02	
:retnlow	1.00E-02	1.00E-02	1.00E-02	1.00E-02	1.00E-02	
:retnhgh	0.3	0.3	0.3	0.3	0.3	
# recharge coefficient bare ground						
:ak2ddf	-2.00E-02	-2.00E-02	-2.00E-02	-2.00E-02	-2.00E-02	
:ak2low	1.00E-04	1.00E-04	1.00E-04	1.00E-04	1.00E-04	
:ak2hgh	0.1	0.1	0.1	0.1	0.1	

# recharge coefficient snow covered ground						
:ak2fsdlt	-2.00E-02	-2.00E-02	-2.00E-02	-2.00E-02	-2.00E-02	
:ak2fslow	0	0	0	0	0	
:ak2fshgh	0.1	0.1	0.1	0.1	0.1	
:EndHydrologicalParLimits						
#						
:GlobalSnowParLimits						
# snowmelt ripening rate						
:fmadjustdlt	-1					
:fmadjustlow	0.1					
:fmadjusthgh	1					
# min melt factor multiplier						
:fmalowdlt	-0.1					
:fmalowlow	0					
:fmalowhgh	0.75					
# max melt factor multiplier						
:fmahighdlt	-0.1					
:fmahighlow	0.75					
:fmahighhgh	1.5					
# glacier melt factor multiplier						
:gladjustdlt	-0.1					
:gladjustlow	0.5					
:gladjusthgh	1.5					
:EndGlobalSnowParLimits						
#						
:SnowParLimits						
:ClassName	vegetation	wetland	wetland	water	impervious	# class name

# melt factor mm/dC/hour						
:fmdlt	5.00E-02	5.00E-02	5.00E-02	5.00E-02	5.00E-02	
:fmlow	5.00E-02	5.00E-02	5.00E-02	5.00E-02	5.00E-02	
:fmhgh	0.5	0.55	0.55	0.55	0.55	
# base temperature dC						
:basedlt	2.00E-03	2.00E-03	2.00E-03	2.00E-03	2.00E-03	
:baselow	-5	-5	-5	-5	-5	
:basehgh	5	5	5	5	5	
# sublimation factor OR ratio						
:subdlt	1.00E-03	1.00E-03	1.00E-03	1.00E-03	1.00E-03	
:sublow	-5.00E-02	-5.00E-02	-5.00E-02	-5.00E-02	-5.00E-02	
:subhgh	0.5	0.5	0.5	0.5	0.5	
:EndSnowParLimits						
#						
:RoutingParLimits						
:RiverClassName	class1	class2	class3			
# lower zone coefficient						
:flzdlt	2.00E-02	2.00E-02	2.00E-02			
:flzlow	1.00E-07	1.00E-07	1.00E-07			
:flzhgh	1.00E-04	1.00E-04	1.00E-04			
# lower zone exponent						
:pwrldt	2.00E-02	2.00E-02	2.00E-02			
:pwrlow	0.3	0.3	0.3			
:pwrhgh	4	4	4			
# channel Manning's n						
:r2ndlt	-2.00E-02	-2.00E-02	-2.00E-02			
:r2nlow	1.00E-02	1.00E-02	1.00E-02			

:r2nhgh	0.5	0.5	0.5			
# wetland or bank porosity						
:thetadlt	2.00E-02	2.00E-02	2.00E-02			
:thetalow	0.1	0.1	0.1			
:thetahgh	0.6	0.6	0.6			
# wetland/bank lateral conductivity						
:kcondltd	2.00E-02	2.00E-02	2.00E-02			
:kcondlow	0.1	0.1	0.1			
:kcondhgh	0.9	0.9	0.9			
# in channel lake retardation coefficient						
:rlakedlt	-0.1	-0.1	-0.1			
:rlakelow	0	0	0			
:rlakehgh	3	3	3			
:EndRoutingParLimits						
#						
:GlobalParLimits						
# precip lapse rate						
:rlapsedlt	0					
:rlapselow	0					
:rlapsehgh	0					
# temperature lapse rate						
:tlapsedlt	0					
:tlapselow	0					
:tlapsehgh	0					
# radius of influence						
:radinfdlt	0					
:radinflow	0					

:radinflgh	0				
# smoothing distance					
:smoothdislt	0				
:smoothislow	0				
:smoothishgh	0				
:EndGlobalParLimits					
#					

Appendix C: Parameter File for CaPA

:FileType	WatfloodParameter	10.1	# parameter file version number		
:CreationDate	#####				
:GlobalParameters					
:iopt	1	# debug level			
:itype	0	# channel type - floodplain/no			
:itrace	4	# Tracer choice			
:a1	1	# ice cover weighting factor			
:a2	1	# Manning's correction for instream lake			
:a3	0.05	# error penalty coefficient			
:a4	0.03	# error penalty threshold			
:a5	0.985	# API coefficient			
:a6	900	# Minimum routing time step in seconds			
:a7	0.9	# weighting - old vs. new sca value			
:a8	0.1	# min temperature time offset			
:a9	0.333	# max heat deficit /swe ratio			
:a10	2	# exponent on uz discharge function			
:a11	0.01	# bare ground equiv. veg height for ev			
:a12	1	# min precip rate for smearing			
:fmadjust	0	# snowmelt ripening rate			
:fmalow	0	# min melt factor multiplier			
:fmahigh	0	# max melt factor multiplier			
:gladjust	0	# glacier melt factor multiplier			
:rlapse	0.0005	# precip lapse rate mm/km			
:tlapse	-0.0065	# temperature lapse rate dC/km			
:elvref	0	# reference elevation			

:rainsnowtemp	0	# rain/snow temperature			
:radiusinflce	300	# radius of influence km			
:smoothdist	35	# smoothing diatance km			
:flgevp2	2	# 1=pan;2=Hargreaves;3= Priestley-Taylor			
:albe	0.11	# albedo????			
:tempa2	500	#			
:tempa3	0	#			
:tton	0	#			
:lat	50	# latitude			
:chnl(1)	1	# manning's n multiplier			
:chnl(2)	0.9	# manning's n multiplier			
:chnl(3)	0.7	# manning's n multiplier			
:chnl(4)	0.7	# manning's n multiplier			
:chnl(5)	0.6	# manning's n multiplier			
:EndGlobalParameters					
#					
:RoutingParameters					
:RiverClasses	3				
:RiverClassName	class1	class2	class3		
:flz	1.00E-06	1.00E-06	1.00E-06	# lower zone oefficient	
:pwr	1.5	2	1.5	# lower zone exponent	
:r1n	0.12	0.12	0.12	# overbank Manning's n	
:r2n	0.4	4.00E-02	2.80E-02	# channel Manning's n	
:mndr	1	1	1	# meander channel length multiplier	
:aa2	1.1	1.1	1.1	# channel area intercept = min channel xsect area	
:aa3	1.00E-02	1.00E-02	1.00E-02	# channel area coefficient	
:aa4	1	1	1	# channel area exponent	

:fratio	1	1	1	1	1	# int. capacity multiplier
:EndHydrologicalParameters						
#						
:SnowParameters						
:fm	0.06	0.06	0.06	0.1	0.15	# melt factor mm/dC/hour
:base	-5	-5	-5	-5	-0.5	# base temperature dC
:fmn	0.1	0.1	0.1	0.1	0.1	# -ve melt factor
:uadj	0	0	0	0	0	# not used
:tipm	0.1	0.1	0.1	0.1	0.1	# coefficient for ati
:rho	0.333	0.333	0.333	0.333	0.333	# snow density
:whcl	0.035	0.035	0.035	0.035	0.035	# fraction of swe as water in ripe snow
:alb	0.11	0.11	0.11	0.11	0.11	# albedo
:sublim_factor	-0.3	-0.3	-0.3	-0.1	-0.1	# sublimation factor ratio
:idump	2	4	4	5	6	# receiving class for snow redistribution
:snocap	-600	-600	-600	-600	-600	# max swe before redistribution
:nsdc	2	2	2	2	2	# no of points on scd curve - only 1 allowed
:sdcsca	1	1	1	1	1	# snow covered area - ratio=1.0
:sdcd	200	150	150	1	100	# swe for 100% snow covered area
:EndSnowParameters						
#						
:InterceptionCapacityTable						
:IntCap_Jan	1.2	0.65	0.65	0.11	0.01	# interception capacity jan mm
:IntCap_Feb	1.2	0.65	0.65	0.11	0.01	# interception capacity feb mm
:IntCap_Mar	1.2	0.65	0.65	0.11	0.01	# interception capacity mar mm
:IntCap_Apr	1.2	0.65	0.65	0.11	0.01	# interception capacity apr mm
:IntCap_May	1.6	1.06	0.85	0.11	0.01	# interception capacity may mm
:IntCap_Jun	1.9	1.56	1	0.11	0.01	# interception capacity jun mm

:IntCap_Jul	1.9	1.56	1	0.11	0.01	# interception capacity jul mm
:IntCap_Aug	1.9	1.56	1	0.11	0.01	# interception capacity aug mm
:IntCap_Sep	1.9	1	1	0.11	0.01	# interception capacity sep mm
:IntCap_Oct	1.2	0.65	0.65	0.11	0.01	# interception capacity oct mm
:IntCap_Nov	1.2	0.65	0.65	0.11	0.01	# interception capacity nov mm
:IntCap_Dec	1.2	0.65	0.65	0.11	0.01	# interception capacity dec mm
:EndInterceptionCapacityTable						
#						
:MonthlyEvapotranspirationTable						
:Montly_ET_Jan	0	0	0	0	0	# monthly evapotranspiration jan mm
:Montly_ET_Feb	0	0	0	0	0	# monthly evapotranspiration feb mm
:Montly_ET_Mar	0	0	0	0	0	# monthly evapotranspiration mar mm
:Montly_ET_Apr	0	0	0	0	0	# monthly evapotranspiration apr mm
:Montly_ET_May	0	0	0	0	0	# monthly evapotranspiration may mm
:Montly_ET_Jun	0	0	0	0	0	# monthly evapotranspiration jun mm
:Montly_ET_Jul	0	0	0	0	0	# monthly evapotranspiration jul mm
:Montly_ET_Aug	0	0	0	0	0	# monthly evapotranspiration aug mm
:Montly_ET_Sep	0	0	0	0	0	# monthly evapotranspiration sep mm
:Montly_ET_Oct	0	0	0	0	0	# monthly evapotranspiration oct mm
:Montly_ET_Nov	0	0	0	0	0	# monthly evapotranspiration nov mm
:Montly_ET_Dec	0	0	0	0	0	# monthly evapotranspiration dec mm
:EndMonthlyEvapotranspirationTable						
#						
:OptimizationSwitches						
:numa	0	# PS optimization 1=yes 0=no				
:nper	1	# opt 1=delta 0=absolute				
:kc	2	# no of times delta halved				

:maxn	10	# max no of trials				
:ddsflg	0	# 0=single run 1=DDS				
:errflg	7	# 1=wMSE 2=SSE 3=wSSE 4=VOL				
:EndOptimizationSwitches						
#						
:APILimits						
:a5dlt	-1.00E-03					
:a5low	0.98					
:a5hgh	0.999					
:EndAPILimits						
#						
:HydrologicalParLimits						
:ClassName	vegetation	wetland	wetland	water	impervious	# class name
# infiltration coefficient bare ground						
:akdlt	-0.02	-0.02	-0.02	-0.02	-0.02	
:aklow	0.4	0.004	0.004	0.04	0.04	
:akhgh	50	0.05	0.05	5	5	
# infiltration coefficient snow covered ground						
:akfsdlt	-0.02	-0.02	-0.02	-0.02	-0.02	
:akfslow	0.04	0.04	0.04	0.04	0.04	
:akfshgh	20	5	5	5	5	
# interflow coefficient						
:recdlt	-2.00E-02	-2.00E-02	-2.00E-02	-2.00E-02	-2.00E-02	
:reclow	5.00E-04	5.00E-04	5.00E-04	5.00E-04	5.00E-04	
:rechgh	0.1	0.1	0.1	0.1	0.1	
# overland flow roughness coeff bare ground						
:r3dlt	-2.00E-02	-2.00E-02	-2.00E-02	-2.00E-02	-2.00E-02	

:r3low	1	1	1	1	1	
:r3hgh	10	10	10	10	10	
# interception evaporation factor * pet						
:fpetdlt	-2.00E-02	-2.00E-02	-2.00E-02	-2.00E-02	-2.00E-02	
:fpetlow	5.00E-02	5.00E-02	5.00E-02	5.00E-02	5.00E-02	
:fpethgh	3	3	3	3	3	
# reduction in PET for tall vegetation						
:ftalldlt	-1	-1	-1	-1	-1	
:ftallow	0.1	0.1	0.1	0.1	0.1	
:ftalhgh	10	10	10	10	10	
# multiplier for interception capacity						
:fratiodlt	-1	-1	-1	-1	-1	
:fratiolow	0.1	0.1	0.1	0.1	0.1	
:fratiohgh	10	10	10	10	10	
# upper zone retention mm						
:retndlt	-2.00E-02	-2.00E-02	-2.00E-02	-2.00E-02	-2.00E-02	
:retnlow	1.00E-02	1.00E-02	1.00E-02	1.00E-02	1.00E-02	
:retnhgh	0.3	0.3	0.3	0.3	0.3	
# recharge coefficient bare ground						
:ak2dlt	-2.00E-02	-2.00E-02	-2.00E-02	-2.00E-02	-2.00E-02	
:ak2low	1.00E-04	1.00E-04	1.00E-04	1.00E-04	1.00E-04	
:ak2hgh	0.1	0.1	0.1	0.1	0.1	
# recharge coefficient snow covered ground						
:ak2fsdlt	-2.00E-02	-2.00E-02	-2.00E-02	-2.00E-02	-2.00E-02	
:ak2fslow	0	0	0	0	0	
:ak2fshgh	0.1	0.1	0.1	0.1	0.1	
:EndHydrologicalParLimits						

#						
:GlobalSnowParLimits						
# snowmelt ripening rate						
:fmadjustdlt	-1					
:fmadjustlow	0.1					
:fmadjusthgh	1					
# min melt factor multiplier						
:fmalowdlt	-0.1					
:fmalowlow	0					
:fmalowhgh	0.75					
# max melt factor multiplier						
:fmahighdlt	-0.1					
:fmahighlow	0.75					
:fmahighhgh	1.5					
# glacier melt factor multiplier						
:gladjustdlt	-0.1					
:gladjustlow	0.5					
:gladjusthgh	1.5					
:EndGlobalSnowParLimits						
#						
:SnowParLimits						
:ClassName	vegetation	wetland	wetland	water	impervious	# class name
# melt factor mm/dC/hour						
:fmdlt	5.00E-02	5.00E-02	5.00E-02	5.00E-02	5.00E-02	
:fmlow	5.00E-02	5.00E-02	5.00E-02	5.00E-02	5.00E-02	
:fmhgh	0.5	0.55	0.55	0.55	0.55	
# base temperature dC						

:basedlt	2.00E-03	2.00E-03	2.00E-03	2.00E-03	2.00E-03	
:baselow	-5	-5	-5	-5	-5	
:basehgh	5	5	5	5	5	
# sublimation factor OR ratio						
:subdlt	1.00E-03	1.00E-03	1.00E-03	1.00E-03	1.00E-03	
:sublow	-5.00E-02	-5.00E-02	-5.00E-02	-5.00E-02	-5.00E-02	
:subhgh	0.5	0.5	0.5	0.5	0.5	
:EndSnowParLimits						
#						
:RoutingParLimits						
:RiverClassName	class1	class2	class3			
# lower zone coefficient						
:flzdl	2.00E-02	2.00E-02	2.00E-02			
:flzlow	1.00E-07	1.00E-07	1.00E-07			
:flzhgh	1.00E-04	1.00E-04	1.00E-04			
# lower zone exponent						
:pwrdl	2.00E-02	2.00E-02	2.00E-02			
:pwrlow	0.3	0.3	0.3			
:pwrhgh	4	4	4			
# channel Manning's n						
:r2ndl	-2.00E-02	-2.00E-02	-2.00E-02			
:r2nlw	1.00E-02	1.00E-02	1.00E-02			
:r2nhgh	0.5	0.5	0.5			
# wetland or bank porosity						
:thetadl	2.00E-02	2.00E-02	2.00E-02			
:thetalow	0.1	0.1	0.1			
:thetahgh	0.6	0.6	0.6			

# wetland/bank lateral conductivity						
:kcondlt	2.00E-02	2.00E-02	2.00E-02			
:kcondlow	0.1	0.1	0.1			
:kcondhgh	0.9	0.9	0.9			
# in channel lake retardation coefficient						
:rlakedlt	-0.1	-0.1	-0.1			
:rlakelow	0	0	0			
:rlakehgh	3	3	3			
:EndRoutingParLimits						
#						
:GlobalParLimits						
# precip lapse rate						
:rlapsedlt	0					
:rlapselow	0					
:rlapsehgh	0					
# temperature lapse rate						
:tlapsedlt	0					
:tlapselow	0					
:tlapsehgh	0					
# radius of influence						
:radinfdlt	0					
:radinfllow	0					
:radinflhgh	0					
# smoothing distance						
:smoothdisdlt	0					
:smoothdislow	0					
:smoothdishgh	0					

:EndGlobalParLimits				
---------------------	--	--	--	--

